

PREDICTION OF DIOXIN EMISSION FROM MUNICIPAL SOLID WASTE INCINERATION BY  
ARTIFICIAL NEURAL NETWORK AND ADSORPTION MODEL OF DIOXIN DERIVATIVES



Miss Sond Bunsan

จุฬาลงกรณ์มหาวิทยาลัย

CHULALONGKORN UNIVERSITY

บทคัดย่อและแฟ้มข้อมูลฉบับเต็มของวิทยานิพนธ์ตั้งแต่ปีการศึกษา 2554 ที่ให้บริการในคลังปัญญาจุฬาฯ (CUIR)  
เป็นแฟ้มข้อมูลของนิสิตเจ้าของวิทยานิพนธ์ ที่ส่งผ่านทางบัณฑิตวิทยาลัย

The abstract and full text of theses from the academic year 2011 in Chulalongkorn University Intellectual Repository (CUIR)  
are the thesis authors' files submitted through the University Graduate School.

A Dissertation Submitted in Partial Fulfillment of the Requirements  
for the Degree of Doctor of Philosophy Program in Environmental Management  
(Interdisciplinary Program)  
Graduate School  
Chulalongkorn University  
Academic Year 2014

Copyright of Chulalongkorn University

การทำนายการปลดปล่อยไดออกซินจากระบบเตาเผาขยะชุมชนโดยใช้โครงข่ายประสาทเทียม  
และแบบจำลองการดูดซับของสารอนุพันธ์ไดออกซิน



วิทยานิพนธ์นี้เป็นส่วนหนึ่งของการศึกษาตามหลักสูตรปริญญาวิทยาศาสตรดุษฎีบัณฑิต  
สาขาวิชาการจัดการสิ่งแวดล้อม (สหสาขาวิชา)  
บัณฑิตวิทยาลัย จุฬาลงกรณ์มหาวิทยาลัย  
ปีการศึกษา 2557  
ลิขสิทธิ์ของจุฬาลงกรณ์มหาวิทยาลัย

Thesis Title	PREDICTION OF DIOXIN EMISSION FROM MUNICIPAL SOLID WASTE INCINERATION BY ARTIFICIAL NEURAL NETWORK AND ADSORPTION MODEL OF DIOXIN DERIVATIVES
By	Miss Sond Bunsan
Field of Study	Environmental Management
Thesis Advisor	Associate Professor Nurak Grisdanurak, Ph.D.
Thesis Co-Advisor	Professor Ho-wen Chen, Ph.D.

---

Accepted by the Graduate School, Chulalongkorn University in Partial Fulfillment of the Requirements for the Doctoral Degree

.....Dean of the Graduate School  
(Associate Professor Sunait Chutintaranond, Ph.D.)

THESIS COMMITTEE

.....Chairman  
(Assistant Professor Chantra Tongcumpou, Ph.D.)

.....Thesis Advisor  
(Associate Professor Nurak Grisdanurak, Ph.D.)

.....Thesis Co-Advisor  
(Professor Ho-wen Chen, Ph.D.)

.....Examiner  
(Associate Professor Sirima Panyametheekul, Ph.D.)

.....Examiner  
(On-anong Larpparisudthi, Ph.D.)

.....Examiner  
(Pichet Chaiwiwatworakul, Ph.D.)

.....External Examiner  
(Daisy Morknoy, Ph.D.)

สนธิ์ บุญสุวรรค์ : การทำนายการปลดปล่อยไดออกซินจากระบบเตาเผาขยะชุมชนโดยใช้โครงข่ายประสาทเทียมและแบบจำลองการดูดซับของสารอนุพันธ์ไดออกซิน (PREDICTION OF DIOXIN EMISSION FROM MUNICIPAL SOLID WASTE INCINERATION BY ARTIFICIAL NEURAL NETWORK AND ADSORPTION MODEL OF DIOXIN DERIVATIVES) อ.ที่ปรึกษาวิทยานิพนธ์  
 หลัก: รศ. ดร.นุรักษ์ กฤษดานุรักษ์, อ.ที่ปรึกษาวิทยานิพนธ์ร่วม: ศ. ดร.โหว-เหวิน เฉิน, 113 หน้า.

การปลดปล่อยไดออกซิน (Dioxin) จากระบบเตาเผาถูกทำนายโดยใช้โครงข่ายประสาทเทียม (ANN) อาศัยข้อมูลต่อเนื่อง 4 ปี ของระบบเตาเผาต้นแบบที่รองรับปริมาณขยะ 90 ตันต่อวันในประเทศไต้หวัน ผลการศึกษาบ่งชี้ว่า แบบจำลองอาศัยหลักการเทคนิคเครือข่ายงานระบบประสาทแบบป้อนกลับ ที่อาศัยข้อมูลเชิงซ้อนและไม่เป็นเชิงเส้น การทำนายนี้จะใช้หลักสถิติในการเลือกตัวแปรที่มีประโยชน์ในแต่ละแบบจำลอง ซึ่งประกอบด้วย 5 กลุ่มตัวแปรอินพุต (Input), 3 ชั้นพื้นฐาน (Basic layer) ที่มี 8 โหนดแฝง (Hidden node) ผลการวิเคราะห์พบว่า ตัวแปรที่สำคัญในการปล่อยไดออกซินคือ; ปริมาณและความถี่ในการฉีดผงถ่านกัมมันต์, ความเข้มข้นของไฮโดรเจนคลอไรด์ (HCl) ในก๊าซทิ้งที่ปล่อยสู่อากาศ, อุณหภูมิที่ห้องผสม (Mixing chamber), และ อุณหภูมิของก๊าซทิ้งที่ปล่อยทิ้ง (Flue gas) ผลการเปรียบเทียบค่าแฟคเตอร์สัมพันธภาพ ( $R^2$ ) มีค่าเท่ากับ 0.998 ทั้งในขั้นตอนการฝึกฝน (Training) และการทดสอบ (Testing) ความถี่ในการฉีดผงถ่านกัมมันต์เข้าสู่ระบบถูกพบว่าเป็นตัวแปรที่มีความไว (Sensitive) ต่อการเกิดและปล่อยไดออกซิน การกำจัดสารที่เป็นอนุพันธ์ของไดออกซินโดยถ่านกัมมันต์ได้ถูกทดลองในระดับห้องปฏิบัติการ Benzene, Chlorobenzene, Dichlorobenzene, และ O-chlorophenol ถูกใช้เป็นสารถูกดูดซับ (Adsorbate) โดยทดสอบผ่านถ่านกัมมันต์ 4 ชนิด การทดลองผ่านหอปฏิกรณ์แบบเบดคงที่ (Fixed-bed reactor) ที่อัตราการไหลเชิงปริมาตรเท่ากับ 1.2 ลูกบาศก์เมตรต่อกิโลกรัมต่อชั่วโมง พบว่าค่า Bed capacity ที่สูงที่สุดในทุกการทดลองเป็นของถ่านกัมมันต์ที่ได้มาจากกะลามะพร้าว พฤติกรรมการดูดซับถูกศึกษาโดย การวิเคราะห์การสูญเสียน้ำหนักเมื่อได้รับความร้อน (Thermal gravimetric analysis) พบว่า ค่าพลังงานกระตุ้นคายซับ (Activation energy for desorption) ที่มีค่าสูงที่สุดเป็นของ O-chlorophenol เท่ากับ 107 กิโลจูลต่อโมลแสดงถึงพฤติกรรมการดูดซับเป็นแบบเคมี การดูดซับสารที่เป็นอนุพันธ์ของไดออกซินโดยใช้ถ่านกัมมันต์จากกะลามะพร้าวจึงถูกเลือกเพื่อจำลองพฤติกรรมการดูดซับ (Breakthrough curve) พบว่า ค่าคงที่ไอโซเทอม (Isotherm parameters) สำหรับสารที่เป็นอนุพันธ์ของไดออกซินมีลักษณะเป็น;  $q_e = (IP_1 P_i) / (1 + IP_2 P_i)$  เมื่อ  $q_e$  คือ ปริมาณที่ดูดซับต่อน้ำหนักตัวดูดซับ (มิลลิกรัมของตัวถูกดูดซับต่อกรัมตัวดูดซับ) และ  $P_i$  คือ ความเข้มข้นที่สมดุล (มิลลิกรัมของตัวถูกดูดซับต่อลิตร) และมีค่าคงที่ของสารแต่ละตัวดังนี้ Benzene:  $IP_1 = 204$  มิลลิกรัมต่อกรัมตัวดูดซับ,  $IP_2 = 1.20$  ลิตรต่อมิลลิกรัม, Chlorobenzene:  $IP_1 = 358$  มิลลิกรัมต่อกรัมตัวดูดซับ,  $IP_2 = 1.46$  ลิตรต่อมิลลิกรัม, Dichlorobenzene:  $IP_1 = 349$  มิลลิกรัมต่อกรัมตัวดูดซับ,  $IP_2 = 1.51$  ลิตรต่อมิลลิกรัม, และ O-chlorophenol:  $IP_1 = 603$  มิลลิกรัมต่อกรัมตัวดูดซับ,  $IP_2 = 1.28$  ลิตรต่อมิลลิกรัม

สาขาวิชา การจัดการสิ่งแวดล้อม

ปีการศึกษา 2557

ลายมือชื่อนิสิต .....

ลายมือชื่อ อ.ที่ปรึกษาหลัก .....

ลายมือชื่อ อ.ที่ปรึกษาร่วม .....

# # 5287854620 : MAJOR ENVIRONMENTAL MANAGEMENT

KEYWORDS: DIOXIN / ARTIFICIAL NEURAL NETWORK / INCINERATION / ADSORPTION / ASPEN

SOND BUNSAN: PREDICTION OF DIOXIN EMISSION FROM MUNICIPAL SOLID WASTE INCINERATION BY ARTIFICIAL NEURAL NETWORK AND ADSORPTION MODEL OF DIOXIN DERIVATIVES. ADVISOR: ASSOC. PROF. NURAK GRISDANURAK, Ph.D., CO-ADVISOR: PROF. HO-WEN CHEN, Ph.D., 113 pp.

Dioxin (PCDDs) emission from incineration was predicted by an artificial neural network (ANN). The prediction was based on four-year monitoring data received from an incineration in Taiwan under a capacity of 90 tons a day. The result indicated that the prediction using model based on a back-propagation neural network, a promising method to deal with a complex and non-linear data with statistical analyses in the selection of useful variables for modeling was satisfied. The suitable architecture of an ANN for using in the dioxin prediction consisted of 5 input factors, 3 basic layers with 8 hidden nodes. Five important variables included amount and frequency of activated carbon injection, concentration of hydrogen chloride in the flue gas at the stack emission, temperature at the mixing chamber, and temperature of final fuel gas emission. The correlation factor ( $R^2$ ) was approximately equal to 0.998 in both training and testing steps. Activated carbon injection frequency was found as the most sensitive factor for PCDDs formation and emission. Laboratory experiment was carried out to remove the derivatives of dioxin compounds using activated carbon (AC). Benzene, chlorobenzene, dichlorobenzene, and O-chlorophenol were used as adsorbates. These chemicals were adsorbed onto four types of ACs. The adsorption experiments were carried out in a fixed-bed reactor with WHSV equal to  $1.2 \text{ m}^3/\text{kg}\cdot\text{hr}$ . The highest bed capacities in all experiments were obtained from AC derived from coconut shell (ACC). The adsorption behaviors were examined by thermal gravimetric analysis (TGA). O-chlorophenol showed the highest activation energy for desorption, 107 kJ/mol, implying chemisorption behavior. The adsorptions of the derivatives of dioxin compounds onto ACC were selected for the modeling of breakthrough curves. Isotherm parameters for selected chemicals can be listed as  $q_e = (IP_1 P_i) / (1 + IP_2 P_i)$  where  $q_e$  is equilibrium adsorption (mg adsorbate/g adsorbent), and  $P_i$  is equilibrium concentration (mg adsorbate/L); Benzene:  $IP_1 = 204 \text{ mg/g adsorbent}$ ,  $IP_2 = 1.20 \text{ L/ml}$ , Chlorobenzene  $IP_1 = 358 \text{ mg/g adsorbent}$ ,  $IP_2 = 1.46 \text{ L/ml}$ , Dichlorobenzene  $IP_1 = 349 \text{ mg/g adsorbent}$ ,  $IP_2 = 1.51 \text{ L/ml}$ , and O-chlorophenol  $IP_1 = 603 \text{ mg/g adsorbent}$ ,  $IP_2 = 1.28 \text{ L/ml}$ .

Field of Study: Environmental Management

Student's Signature .....

Academic Year: 2014

Advisor's Signature .....

Co-Advisor's Signature .....

## ACKNOWLEDGEMENTS

First and foremost, I would like to express my sincere appreciation to my advisor Assoc.Prof.Nurak Grisdanurak, for his guidance, encouragement and continued support. Without him I would have had no chance to come this far. His patience and thoughtfulness are remarkable. And I would like to express my appreciation also to Dr.Som-O for her support and guidance in getting my graduate career.

I particularly grateful to Professor Ho-Wen Chen and his coworkers at Tunghai University, for not only giving me the opportunity to work in his laboratories but also being a great mentor. I am extremely grateful to Professor Wei-Yea Chen, the thesis would not have come to a successful completion, without your guide in statistical analyses.

I would also like to thank the committee members for their guidance in my research. Furthermore I would also like to acknowledge the grant from the Center of Excellence on Hazardous Substance Management Program, Thailand. I would like to thank the Faculty of Chemical Engineering, Thammasat university, Thailand for allow me to use the laboratory facilities during this research.

Special gratitude and acknowledgment are extended to my parents who have presented me the opportunity of an education from the best institutions and help throughout my life. I would also like to express my gratitude to my family for their financial support. Above all, I would like to express my deepest appreciation to my best partner for his great patience at all times. I couldn't be able to finish my dissertation without the support from him. Thank you for being at your very best.

## CONTENTS

	Page
THAI ABSTRACT .....	iv
ACKNOWLEDGEMENTS .....	vi
CONTENTS .....	vii
LIST OF TABLES .....	x
LIST OF FIGURES .....	xii
Chapter I Introduction .....	1
1.1 Research Reasonable .....	1
1.2 Objectives .....	4
1.3 Scopes of work .....	4
1.4 Hypotheses .....	5
Chapter II Background and Literature Review .....	6
2.1 Incineration system .....	6
2.2 Dioxin .....	12
2.3 Dioxins Formation in Combustion process .....	17
2.4 Dioxins in Thailand .....	22
2.5 An estimation of Dioxin formation by mathematical analysis .....	23
2.6 Dioxin Removal by activated carbon adsorption .....	27
2.7 Modeling of breakthrough curve in adsorption process .....	30
2.8 Aspen Gas Adsorption Simulation Program .....	31
Chapter III Methodology: An estimation of Dioxin formation by ANN .....	38
3.1 Data Collection .....	38
3.2 Data pre-treatment .....	42

	Page
3.3 Statistical analyses .....	42
3.4 Prediction the PCDDs emission by ANNs.....	45
Chapter IV Result and Discussion: An Estimation of Dioxin Emission by ANN .....	47
4.1 Basic statistical analysis and variable selection.....	47
4.2 The estimation of dioxin emission using ANN.....	53
4.3 Sensitivity analysis .....	57
Chapter V Experimental procedures: Adsorption of dioxin derivatives .....	58
5.1 Chemicals and Materials .....	58
5.2 Adsorption Experimental.....	59
5.3 Derivatives of Dioxin Compounds Calibration.....	61
5.4 Adsorption Behavior .....	63
5.5 Activated Carbon Characterization by N <sub>2</sub> Adsorption Isotherms and BET Surface Area.....	63
5.6 Aspen Gas Adsorption Simulation Program.....	63
5.7 General function in Aspen.....	71
Chapter VI Results and discussion: Adsorption of dioxin derivatives .....	74
6.1 Characterization of Activated Carbon.....	74
6.2 Adsorption of the derivatives of dioxin compounds.....	77
6.3 Adsorption Behavior .....	83
6.4 Modeling of the breakthrough curves by Aspen Gas simulation Program.....	86
Chapter VII Conclusions and recommendations.....	91
REFERENCES .....	93
APPENDIX A Sensitivity Analysis.....	99



	Page
APPENDIX B Calculation to convert volume to concentration.....	104
APPENDIX C Breakthrough curve data.....	105
VITA.....	113



## LIST OF TABLES

Table		Page
Table 2.1	PCDDs and PCDFs congeners.....	14
Table 2.2	The 2005 World Health Organization re-evaluation of human and mammalian toxic equivalency factors for dioxins and dioxin-like compounds.....	15
Table 2.3	Standard Value of PCDDs/PCDFs Emission from Waste Incineration .....	16
Table 2.4	Review of literature data on ANNs-based model application as predicting tool.....	26
Table 2.5	Review of literature data for the removal of PCDD/Fs and dioxin-like compounds using activated carbon in fixed-bed adsorption reactor .....	29
Table 3.1	Basic statistical characteristic of variables .....	41
Table 4.1	Selected variables for building artificial neural network by correlation analysis.....	48
Table 4.2	Selected variables for building artificial neural network by principal component analysis .....	50
Table 4.3	Properties of the ANN model for the Dioxin emission prediction .....	54
Table 5.1	Chemical properties. ....	58
Table 5.2	Liner equation and $R^2$ of the derivatives of dioxin compounds.....	62
Table 5.3	Required information in Aspen Gas Adsorption Simulation Program.....	67
Table 5.4	Required information in Aspen Gas Adsorption Simulation Program (Continue).....	68
Table 5.5	Required information in Aspen Gas Adsorption Simulation Program (Continue).....	69
Table 5.6	Required information in Aspen Gas Adsorption Simulation Program (Continue).....	70
Table 6.1	Porous structure of activated carbons.....	77
Table 6.2	Bed capacity of derivatives of dioxin compounds adsorbed onto various activated carbons at $WHSV=1.2 \text{ m}^3/\text{kg-hr}$ .....	80
Table 6.3	Assumptions for the simulation in Aspen Gas Adsorption Program.....	86
Table 6.4	Isotherm parameters obtained by Aspen Gas Adsorption Simulation program.....	90
Table C.1	Breakthrough curve for benzene.....	105

	<b>Page</b>
Table C.2 Breakthrough curve for benzene (continue).....	106
Table C.3 Breakthrough curve for chlorobenzene .....	107
Table C.4 Breakthrough curve for chlorobenzene (continue).....	108
Table C.5 Breakthrough curve for dichlorobenzene.....	109
Table C.6 Breakthrough curve for dichlorobenzene (continue).....	110
Table C.7 Breakthrough curve for O-chlorophenol.....	111
Table C.8 Breakthrough curve for O-chlorophenol (continue).....	112



## LIST OF FIGURES

Figure	Page
Figure 2.1 Schematic of incineration process .....	7
Figure 2.2 Rotary kiln incinerator .....	8
Figure 2.3 Moving grate incinerator or stoker-type incinerator .....	9
Figure 2. 4 Fluidized bed-type incinerator.....	10
Figure 2. 5 Chemical Structures of PCDD, PCDF, and PCB.....	12
Figure 2.6 Formation route of PCDD from 2,4,6-trichlorophenols.....	19
Figure 2.7 Formation route of PCDD/F from chlorobenzenes and chlorophenols .....	20
Figure 2.8 Formation route of PCDD/F from by De novo synthesis .....	21
Figure 2.9 Schematic description of experimental procedure.....	32
Figure 3.1 The Schematic of Taichung city refuses incineration plant .....	39
Figure 3.2 Flow chart of the artificial neural network approach for predicting the dioxin emission .....	40
Figure 4.1 Scree Plot for determine the principal components (PC).....	49
Figure 4.2 The structure of ANN model for the Dioxin emission prediction .....	54
Figure 4.3 The dioxin emission predicted value versus target value (a) training step .....	55
Figure 4.4 The result of sensitivity analysis from weights method.....	57
Figure 6.1 The classification of adsorption isotherms defined by IUPAC.....	75
Figure 6.2 N <sub>2</sub> adsorption/desorption isotherms of the adsorbents.....	75
Figure 6.3 Breakthrough curve for Benzene adsorption by various activated carbons .....	81
Figure 6.4 Breakthrough curve for Chlorobenzene adsorption by various activated carbons.....	81
Figure 6.5 Breakthrough curve for Di-chlorobenzene adsorption by various activated carbons.....	82

	<b>Page</b>
Figure 6.6	Breakthrough curve for O- chlorophenol adsorption by various activated carbons .. 82
Figure 6.7	TPD profiles of dioxin derivatives from activated carbon derived from coconut shell at various heating rates..... 84
Figure 6.8	Plot of $2\ln T_m - \ln B$ value as a function of $1000/T_m$ of the derivatives of dioxin compounds adsorb onto activated carbon derived from coconut shell ..... 85
Figure 6.9	The comparison between the simulations (strength line) and experimental (points) for O-chlorophenol adsorbed onto ACC ..... 88
Figure 6.10	The comparison between the simulations (strength line) and experimental (points) for Dichlorobenzene adsorbed onto ACC ..... 88
Figure 6.11	The comparison between the simulations (strength line) and experimental (points) for Chlorobenzene adsorbed onto ACC ..... 89
Figure 6.12	The comparison between the simulations (strength line) and experimental (points) for Benzene adsorbed onto ACC..... 89
Figure A. 1	The structure of ANN model for the Dioxin emission prediction..... 100

## Chapter I

### Introduction

#### 1.1 Research Reasonable

Dioxins are released as an undesired by-product from the combustion process of waste incineration. With the health concern, the formation of dioxins in the combustion process has been extensively investigated (Altwicker, 1996; Cunliffe & Williams, 2009). Because dioxins can be rapidly accumulated in the fatty tissue of animals and result in immune system damage of human beings (Yoshida, Ikeda, & Nakanishi, 2000), governments in many countries launch various guidelines to regulate the dioxins emissions. In addition, the U.S. Environmental Protection Agency (EPA) has set up an emission standard for PCDDs/Fs from a stack gas at  $0.5 \text{ ng TEQ/Nm}^3$  for an incinerator with a handling capacity of municipal solid waste (MSW) not exceed 50 tons per day.

Given this fact, many researches have revealed that combustion conditions may affect the formation of dioxin emission in an incinerator. Several dioxin reduction technologies based on combustion control have been established so far (Buekens & Huang, 1998; Y.-M. Chang, Hun, Che, Chan, & Chen, 2009; Milosavljevic & Pullumbi, 2000). However, it is worth noting that effective PCDDs emission control strategies should be supported by the accurate prediction of the pollutants (Y.-H. Chang, Chen, & Chang, 1998). Thus, the estimation of PCDDs/Fs emission and their conditions by which the pollutant was form are needed to be taken into consideration.

In 2007, Choi et al., investigated the concentrations of PCDD/DF from selected seven incinerators in Korea using mathematical approach called multi-regression analysis. Note that, the concentration of PCDD/DF in this study was modeled only at the wet scrubber unit using the correlation between dust concentrations and change of temperatures. The study also suggested that these parameters were marked as predominant parameters for the PCDD/DF formation cause by memory effect in wet scrubber. However, it is important to point out here, that, the concentration of dioxins and furans emission in incineration process is influenced by many factors

including the presence of precursors (chlorinated phenols, chlorinated benzenes, and PCBs), MSW waste components provide a source of chlorine, temperature at chambers, and activated carbon injection unit (Hsi, Wang, & Yu, 2007; McKay, 2002). Thus, the prediction which based on empirical data in the study area operation unit within incinerators might not consistently estimate the levels of PCDD/DF in different incineration plants. Accordingly, it is clear that the comprehensive mathematical approach for the estimation of dioxins and furans must be included with various parameters of the operation system in the incineration process.

For the existing treatment, scrubbing system is the major component in incinerator plant to control the particulate emission in flue gas from combustion process. The reduction of polychlorinated dibenzo-*p*-dioxins and polychlorinated dibenzofurans (PCDD/Fs) emission was using activated carbon injection unit. It is certain that activated carbon is a promising approach in treatment facilities among contaminated air, sediment, and water (Hale et al., 2012). The comparative adsorption studies on waste-polymer-based, activated carbon, and carbon nanotube to remove of hydrophobic organic compounds (Lian et al., 2012). The article further states that activated carbon was found to be superior adsorption to other adsorbents due to high surface area, microporous structure, and narrow pore size distribution. Furthermore, efficiency and performance of activated carbon can be illustrated by adsorption breakthrough curves, which show the relationship between the ratio of outlet inlet concentration and the function of operating conditions (Cheng, Jiang, Zhang, & Liu, 2004; Pan et al., 2005). Consequently, it is important to reliable on how activated carbon adsorbs a specific substance incorporate with operational and system parameters with regard to scale-up the process as well.

Mostly, the activated carbon injection plays an important factor on PCDD emission. Due to the highly toxic of PCDD, the incineration plant must be effectively regulated in order to minimize the level of PCDD in fuel gas before discharged into the atmosphere. Several incinerators have been employed the activated carbon injection devices coupled with fixed-bed or moving bed adsorption (Hung, Lo, Chi, Chang, & Chang, 2011).

The main drawback of activated carbon injection, however, is the removal efficiency of contaminants might be inefficient when the adsorption operation is not reaching the maximum capacity of adsorbent (Karademir, Bakoglu, Taspinar, & Ayberk, 2004). Activated carbon is injected

semi-continuously into the system; therefore, an entire adsorption capability of activated carbon has not been reached. In this manner, the residues from the combustion process can be increased with the excess amount of activated carbon injection. Additionally, spent activated carbon from incineration plant is a hazardous waste because it uses as adsorbent to remove contaminants and impurities from fuel gas (Bonte, Fritsky, Plinke, & Wilken, 2002; Zhou, Zhong, Jin, Huang, & Xiao, 2005). Chen et al., (2012) reported that a large amount of poisonous material from spent activated carbon generated each year in Taiwan is at least 5000 tons. Thus, improving the design of adsorption system and the performance of adsorbents is an effective way to reduce the generation of hazardous waste. Note that, the volume requirement for landfill disposal can be reduced in this regard.

The empirical data has been identified as major contributing factors to simulate dynamic behavior for the full-scale design in adsorption process (Burkert, Barbosa, Mazutti, & Mauger, 2011). A number of studies have been reported on the adsorption modeling of various pollutants on several adsorbent materials. Normally, the characteristic between adsorbent and adsorbate is representing in terms of breakthrough curve. Therefore, the breakthrough curve is widely used in the most case of adsorption simulation models to predict the adsorption behavior. From previous works, it can be stated that the simulation model can be constructed base on a small-scale experiment and the isotherm parameters and mass transfer models are the crucial factors that should be taken in considered (Richard, Delgado Núñez, & Schweich, 2010; Sansalone & Ma, 2011). According to the previous literatures (Chuang, Chuang, & Chang, 2003; Sperlich et al., 2005; Xiu & Li, 2000), the required important factors for simulation program can be described in case of material balance, momentum balance, kinetic model, and energy balance.

In brief, this work will be carried out for two main parts; first part was highlighted to build an accurate prediction model for dioxin emission control, and develops a series of procedures for planning a long-term effectiveness policy in an incinerator, in which an integrated statistical approach composed of correlation analysis and principal component analysis was used to screen out the key variables from massive observed and control variables, and then a feed-forward ANN is established after training and testing steps. Moreover, sensitivity analysis was utilized to find the key contributor to dioxin emission control.



In the second part, the main objective is to investigate the adsorption behavior of the derivatives of dioxin compounds onto activated carbons in a continuous system. Four-type derivatives of dioxin compounds were adsorbed onto granular activated carbon derived from different raw materials. Additionally this study proposed the kinetic study of the derivatives of dioxin compounds adsorption on the activated carbon. The adsorption kinetics will be applied in an attempt to predict the adsorption behavior which could describe the removal of the derivatives of dioxin compounds from gas stream pass through activated carbon bed.

## 1.2 Objectives

### 1.2.1 First part: Estimation of dioxin (PCDDs) emission from municipal solid waste incineration

- To build an accurate prediction model for PCDDs emission.
- To investigate the key contributors to PCDDs emission control in the incinerator.

### 1.2.2 Second part: The dioxin derivatives compounds removal by activated carbons

- To propose a reliable adsorption model for representing the adsorption dioxin derivatives in a fixed-bed column.

## 1.3 Scopes of work

### 1.3.1 First part: Estimation of dioxin (PCDDs) emission from municipal solid waste incineration

- Taichung MSW incineration plant was selected as a case study.
- Taichung MSW incineration plant operated with an average waste daily loading of 900 tons.
- Samples in various conditions were analyzed by Taiwan's EPA laboratory, Executive Yuan (ROC.).

- Artificial neural network (ANN-based) prediction modeling was built using the four-year monitoring data.
- Back-propagation algorithm was used in the training step.
- Twenty-four 24 operating condition parameters were considered as predominant factors.
- A sensitivity analysis was performed to determine the relative importance among various input factors on dioxin emission.

### 1.3.2 Second Part: The dioxin derivatives compounds removal by activated carbons

- Adsorbents: four types of granular activated carbons.
- Adsorbates: four dioxin derivatives including Chlorobenzene ( $C_6H_5Cl$ ), Ortho-dichlorobenzene ( $C_6H_4Cl_2$ ), Ortho-chlorophenol ( $C_6H_5ClO$ ), and Benzene ( $C_6H_6$ ).
- Initial concentration of chlorinated aromatic compounds was fixed at 1,800 ppm and the experiments were carried out in a continuous fixed-bed flow reactor.

## 1.4 Hypotheses

- A neural network prediction model could provide an accurate estimation of dioxin emission.
- Breakthrough curves for the adsorptions dioxin derivatives adsorbed onto activated carbon can be further foreseen precisely by Aspen Adsorption Simulation Program.

## Chapter II

### Background and Literature Review

This chapter provides the fundamental information that involves in this study. The content is divided into five parts including: incineration system, dioxin properties and formation, prediction model of dioxin generated during the combustion, mitigation of dioxin by adsorption, and an introduction of Simulation Program (Aspen Gas Adsorption). In brief, this chapter is summarized and reviewed the related articles so finally the previous knowledge will be applied in this study.

#### 2.1 Incineration system

An incineration system is one of the appropriate options for waste disposal in the country which available land is limited. The advantages of using incineration could be listed as follows;

- It requires a small area for the plant construction,
- Waste volume could be reduced approximately 90% of the initial amount within a short time, and
- Exhausted energy released from the process can be utilized for power plant (Hartenstein & Horvay, 1996).
- By products of bottom ash and leftover materials from the burning process can be utilized in the road construction (Olsson, Kärrman, & Gustafsson, 2006).

A main feature of incineration system is shown in Fig 2.1. Normally, incineration plant consists of three main parts (Kim, Song, Seok, Ko, & Hunsinger, 2013):

- Waste storage and feeding
- Waste burning and heat recovery, and
- Exhaust gas treatment

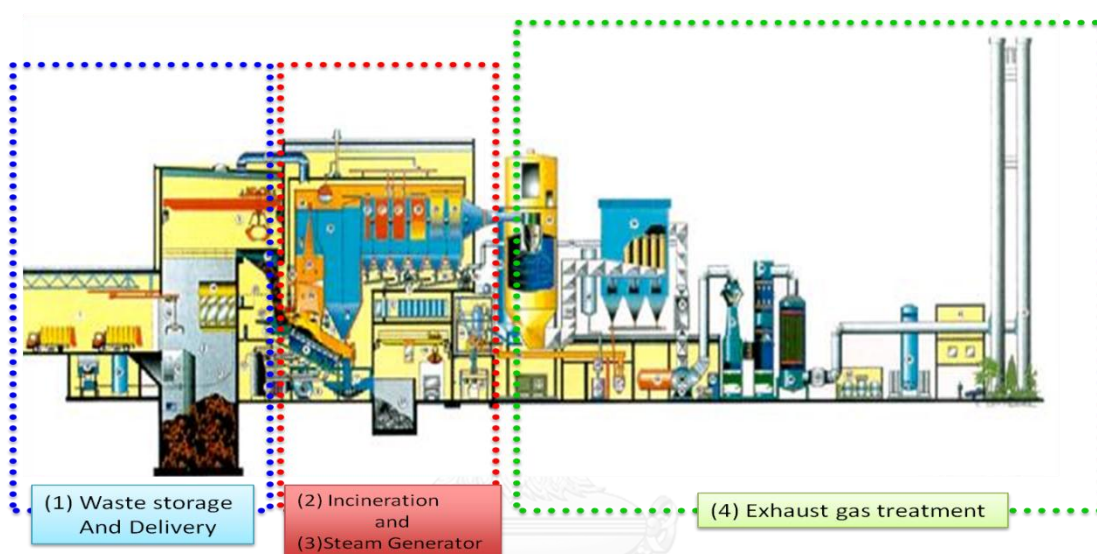


Figure 2.1 Schematic of incineration process

### (2.1.1) Waste storage and feeding

In particular, the waste-presorting unit is necessary to be carried out before sending waste to the other parts of incineration. In this unit, the recyclable materials and ferrous metals are sorted from the waste stream to ensure higher efficient burning performance (Y.-H. Chang et al., 1998). The treated waste after the pretreatment method is delivered via collection vehicles and dumped in the bunker.

### (2.1.2) Waste burning and heat recovery

A hydraulic crane system is used for transportation waste into the primary combustion chamber in which the most of waste volume can be reduced. Typically, most incinerators supply oxygen pass from below the incineration hearth with less than stoichiometric to provide the full combustion. The heat from the burning process in the primary combustion chamber is transferred to the boiler and piped to the steam turbine generator to generate electricity in the heat recovery unit. Meanwhile, the incomplete combustion materials from the primary chamber are flew pass through the secondary combustion chamber by the air blower. In order to ensure the complete combustion, the excess air is added in the secondary combustion chamber.

Technically, there are three different patterns of furnace in modern incineration plant, as displayed in Figure 2.2-2.4. Each furnace feature relied on waste composition, operation location, and investment requirement. They are rotary kiln, moving grate, and fluidized bed.

#### (a) Rotary kiln incinerator

This type of incinerator is widely used in a large scale of waste stream, including hazardous, municipal, and industrial processes. Pre-treatment of the raw waste by crushing or shredding into the appropriate size for the combustion is necessary. This kind of incinerator designed with the rotary cylindrical cement kiln and placed slightly angle with the horizontal (Hartenstein & Horvay, 1996; Y. Yang, Reuter, & Hartman, 2003). The waste stream with variety of compositions, materials, or calorific values is suitable for rotary kiln incineration.

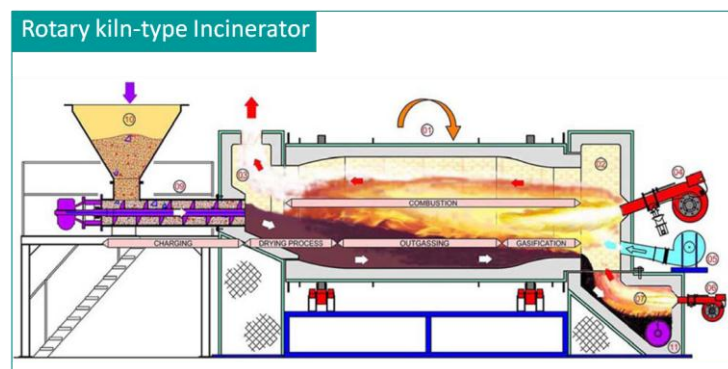


Figure 2.2 Rotary kiln incinerator

b) **Moving grate incinerator or stoker-type incinerator**

The other type of combustion technique is a moving grate furnace. It is known as municipal solid waste incinerator. Waste is fed on the top of furnace and waste stream is directly burned on the series of grates, which located in flat or sloping style. The waste stream is delivered and agitated on the grates that are continuously moving forward and backward through the furnace (Y. B. Yang, Sharifi, & Swithenbank, 2007). The advantages of moving grate incinerator are: this type of this incinerator allows operating with no pretreatment required, capable to combust a high amount of MSW (1,200 tons per day), and provide 85% of thermal efficiently (Nixon, Wright, Dey, Ghosh, & Davies, 2013; Vandecasteele, Wauters, Arickx, Jaspers, & Van Gerven, 2007). The disadvantage is the cost of the construction is high.

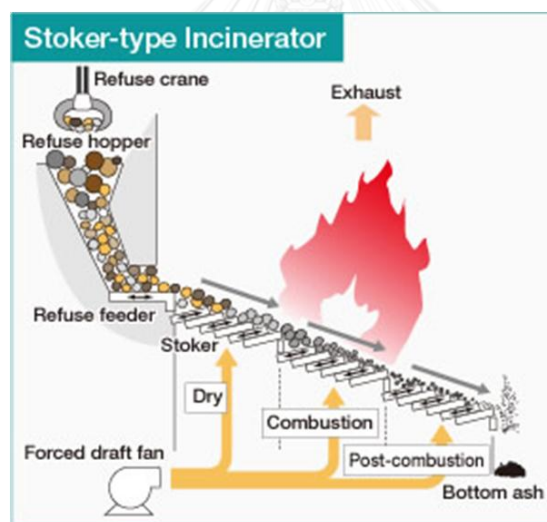


Figure 2.3 Moving grate incinerator or stoker-type incinerator

### c) Fluidized bed incinerator

For this furnace type, the combustion chamber contains bed of sand or limestone and air distribution system. Air is fed into the bed through the nozzles with the proper velocity and temperature, the bed is fluidized and circulated (Caneghem et al., 2012; C. K. Chen, Lin, Wang, & Chang-Chien, 2006). Therefore, the system should provide high heat transfer and excellent mixing between combustible materials and fluidized bed to promote the combustion in the furnace (Ishikawa, Buekens, Huang, & Watanabe, 1997). The complete combustion condition involves with the turbulent mixing among gases, fuel and waste stream burning in the adequate combustion time (1-2 seconds) and the temperature must be provided in high temperature range of  $1000^{\circ}\text{C}$ , or higher (Y.-H. Chang et al., 1998).

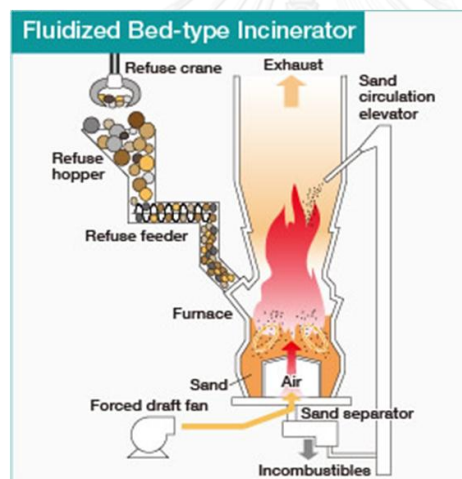


Figure 2. 4 Fluidized bed-type incinerator

### (2.1.3) Exhaust gas treatment

Hazardous materials such as heavy metal compounds, CO, HCl, HF, HBr, HI, NO<sub>x</sub>, SO<sub>2</sub>, VOCs, and the most harmful hazardous chemicals like dioxins-polychlorinated dibenzo dioxins and polychlorinated dibenzofurans (PCDDs/Fs) are partly destroyed in a secondary combustion chamber. After that, the exhausted gases from the high temperature combustion zone of the furnace are immediately cooled in the post combustion zone to reduce the dioxin formation. Finally, contaminated gas produced from the burning process must be essentially treated and cleaned by air pollution control devices before released to the environment regarding to public health.

The exhaust gas treatment section in the incineration process comprises with the pollution control equipment. The main purpose of this section is to limit and eliminate the emission of PCDD/Fs and other typical pollutants. This section including (Antonioni, Guglielmi, Cozzani, Stramigioli, & Corrente, 2014; McKay, 2002);

- Electrostatic precipitator (ESP)
- Fabric filter (FF)
- Dry scrubber (DS)
- Dry sorbent (activated carbon) injection (DSI)
- Wet scrubber (WD) and
- Selective catalytic reactor.



## 2.2 Dioxin

Dioxin is a family name of compound known as chlorinated organic compound, which commonly refers to

- polychlorinated dibenzo-p-dioxins (PCDDs),
- polychlorinated dibenzofurans (PCDFs), and
- polychlorinated biphenyls (PCBs)

The structure of dioxin comprises of two benzene rings connected by either one or two oxygen bridge and contain with four to eight chlorine atoms. The chemical structure of PCDD, PCDF, and PCB are given in Figure 2.5. The difference between congeners of PCDD/Fs is the number and position of chlorine atoms on the molecule. There are possible 75 congeners of PCDD and 135 possible congeners of PCDF as summarized in Table 2.1 (Buser, 1985). The U.S. Environmental Protection Agency (EPA) notes that the most toxic compound of dioxin among the congeners is 2,3,7,8-tetrachloro-dibenzo-p-dioxin (TCDD).

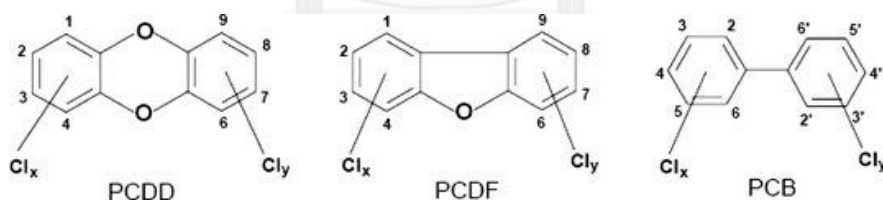


Figure 2. 5 Chemical Structures of PCDD, PCDF, and PCB

In general, the dioxin or dioxin-like compounds (DLCs) mostly exist in the environment as mixtures thus the exposure limits of dioxins and DLCs are reported in terms of TCDD toxicity equivalence concentration (TEQ). The dioxin toxicity can be calculated internationally as the TEQ using the proposed formula provided by the US EPA (2010).

$$TEQ = \sum_{i=1}^n (C_i \times TEF_i) \quad (2.1)$$

Where  $C_i$  is an individual TCDD or DLCs concentration in environmental media and  $TEF_i$  is the toxicity Equivalence Factor assigned for TCDD or the DLCs. In addition, the TEF values of each dioxin congener were evaluated and summarized by WHO in 2005, as shown in Table 2.2 (Van den Berg et al., 2005).

It is well known that incineration plants considered as a primary source of the dioxins and furans emission into the atmosphere. In response with the public concerned about the high toxic potential of each dioxins and furans congener, most of developed countries have been setting the emission standard values expressed as nano-gram per cubic meter of emitted gases ( $\text{ng.I-TEQ}/\text{Nm}^3$ ) as shown in Table 2.3. In Thailand, the standard emission value has set and followed the US EPA criteria, which address as the total emission in both dioxins and furans ( $\text{ng.total}/\text{Nm}^3$ ).

Table 2.1 PCDDs and PCDFs congeners

Homologue Name	Abbreviation	Chlorine Atom	Number of Congener
<b>Dioxins</b>			
Monochlorodibenzo- <i>p</i> -dioxins	MCDD	1	2
Dichlorodibenzo- <i>p</i> -dioxins	DCDD	2	10
Trichlorodibenzo- <i>p</i> -dioxins	TrCDD	3	14
Tetrachlorodibenzo- <i>p</i> -dioxins	TCDD	4	22
Pentachlorodibenzo- <i>p</i> -dioxins	PeCDD	5	14
Hexachlorodibenzo- <i>p</i> -dioxins	HxCDD	6	10
Heptachlorodibenzo- <i>p</i> -dioxins	HpCDD	7	2
Octachlorodibenzo- <i>p</i> -dioxins	OCDD	8	1
			75
<b>Furans</b>			
Monochlorodibenzofurans	MCDF	1	4
Dichlorodibenzofurans	DCDF	2	16
Trichlorodibenzofurans	TrCDF	3	28
Tetrachlorodibenzofurans	TCDF	4	38
Pentachlorodibenzofurans	PeCDF	5	28
Hexachlorodibenzofurans	HxCDF	6	16
Heptachlorodibenzofurans	HpCDF	7	4
Octachlorodibenzofurans	OCDF	8	1
			135

Table 2.2 The 2005 World Health Organization re-evaluation of human and mammalian toxic equivalency factors for dioxins and dioxin-like compounds

Compound	WHO 2005 TEF
<i>Chlorinated dibenzo-p-dioxins</i>	
2,3,7,8-TCDD	1
1,2,3,7,8-PeCDD	1
1,2,3,4,7,8-HxCDD	0.1
1,2,3,6,7,8-HxCDD	0.1
1,2,3,7,8,9-HxCDD	0.1
1,2,3,4,6,7,8-HpCDD	0.01
OCDD	0.0003
<i>Chlorinated dibenzofurans</i>	
2,3,7,8-TCDF	0.1
1,2,3,7,8-PeCDF	0.03
2,3,4,7,8-PeCDF	0.3
1,2,3,4,7,8-HxCDF	0.1
1,2,3,6,7,8-HxCDF	0.1
1,2,3,7,8,9-HxCDF	0.1
2,3,4,6,7,8-HxCDF	0.1
1,2,3,4,6,7,8-HpCDF	0.01
1,2,3,4,7,8,9-HpCDF	0.01
OCDF	0.0003

Table 2.3 Standard Value of PCDDs/PCDFs Emission from Waste Incineration

Country	Standard Value	Note
Austria	0.1 ng.I-TEQ/Nm <sup>3</sup>	All size
Canada	0.1 ng.I-TEQ/Nm <sup>3</sup>	All size
Denmark	0.1 ng.I-TEQ/Nm <sup>3</sup>	All size
European Union	0.1 ng.I-TEQ/Nm <sup>3</sup>	All size
Germany	0.1 ng.I-TEQ/Nm <sup>3</sup>	All size
England	0.1 ng.I-TEQ/Nm <sup>3</sup>	All size
Japan (Existing Incinerator)	0.5 ng.I-TEQ/Nm <sup>3</sup>	Large Size
Japan (Latterly Built Incinerator)	0.1 ng.I-TEQ/Nm <sup>3</sup>	Large Size
Netherlands	0.1 ng.I-TEQ/Nm <sup>3</sup>	All size
Sweden	0.5 ng.I-TEQ/Nm <sup>3</sup>	All size
Switzerland	0.1 ng.I-TEQ/Nm <sup>3</sup>	All size
Taiwan (Existing Incinerator)	1.0 ng.I-TEQ/Nm <sup>3</sup>	All size
Taiwan (Latterly Built Incinerator)	0.1 ng.I-TEQ/Nm <sup>3</sup>	All size
USA (Existing Incinerator)	0.5 ng.I-TEQ/Nm <sup>3</sup>	Large Size
USA (Latterly Built Incinerator)	0.2 ng.I-TEQ/Nm <sup>3</sup>	Large Size
Thailand	0.5 ng.I-TEQ/Nm <sup>3</sup>	MSW 1 ton per day

### 2.3 Dioxins Formation in Combustion process

The presence of dioxins compounds in the environment is mainly produced by incineration process. It is reported in the review that dioxins can be generated predominantly by polyvinyl chloride plastic (PVC) source in waste from several incineration processes (Kulkarni, Crespo, & Afonso, 2008). In Thailand, we can see incineration system for the following purposes;

- Municipal solid waste ,
- Hospital waste,
- Hazardous waste incinerators, and
- Sewage sludge

In addition, a number of studies have reveal evidence that dioxins can be formed during the incineration process by three main mechanisms.

- Reaction between chlorine atoms with aromatic hydrocarbons
- Molecular rearrangement of precursor compounds, and
- De novo synthesis

The following is an introduction and a brief literature which aim to propose on how dioxins compounds can be formed.

#### (2.3.1) Reaction between chlorine atoms with aromatic hydrocarbons

Firstly, the presence of chlorine radicals ( $\text{Cl}\cdot$ ) in waste materials can also lead to the formation of dioxins (Hatanaka, Imagawa, & Takeuchi, 2002). Wang et al. (2003) attempted to investigate the effect of chlorine content from two kinds of waste streams, which were medical waste and municipal solid waste, on the formation of dioxins and furans in the combustion process. The result confirmed that the chlorine content in waste stream showed a significant relationship with PCDDs/Fs formation during the combustion process. Noted that, polyvinylchloride (PVC) in plastic waste was the largest source of dioxin-forming chlorine in

exhaust gas (Joung, Seo, Kim, & Seo, 2006; Wagenaar et al., 1998; Yasuhara, Katami, & Shibamoto, 2006). It is possible to explain this finding that chlorine atoms can be reacted with aromatic hydrocarbon and transformed to the dioxin precursors occurs in various sections of incinerator (Lu et al., 2007).

### **(2.3.2) Molecular rearrangement of precursor compounds**

The second mechanism is the molecular rearrangement of precursor compounds from the thermal breakdown at the low temperatures sector in the combustion chamber (Summoogum, Altarawneh, Mackie, Kennedy, & Dlugogorski, 2012). The precursor compound is defined as the chlorinated aromatic hydrocarbon compounds. Several studies have reported that chlorobenzene and chlorophenol are the dominant precursors for the formation of PCDDs and PCDFs (Kato & Urano, 2001; Lavric, Konnov, & Ruyck, 2005). These precursors derived from incomplete combustion of organic waste in the chamber can lead the PCDDs/Fs formation in the post-combustion regions of incineration process. The process is illustrated in figures, where Figure 2.3 is the formation route of PCDD from 2,4,6-trichlorophenols and Figure 2.4 is the formation pathway of PCDF from chlorobenzene and chlorophenols (Addink & Olie, 1995).

### **(2.3.3) De novo synthesis**

In addition, the other pathway is that a main mechanism for the formation of PCDDs/Fs is called De novo synthesis (Mätzing, 2001). It is noted that De novo synthesis is mainly occurs on the surface of fly ash by the heterogeneous catalyst reaction and the dioxins can be formed in the post-combustion process where the fuel gases are cooled prior being cleaned in the gas treatment section (Huang & Buekens, 1996). The process of De novo synthesis is illustrated in Fig 2.5.

Previous studies have reported and performed a series of experiments to investigate the factors that effect to the formation of dioxins (Everaert et al., 2014; Suzuki, Kasai, Aono, Yamazaki, & Kawamoto, 2004). An interesting of these studies reveals that the dioxins formation by de novo synthesis is mainly related to the low temperature in range between 200°C to 400°C. Moreover, the dioxin formation can be promoted by the presence of HCl in flue gas, which is the major gaseous chlorine sources and transition metals as a catalyst of this pathway.

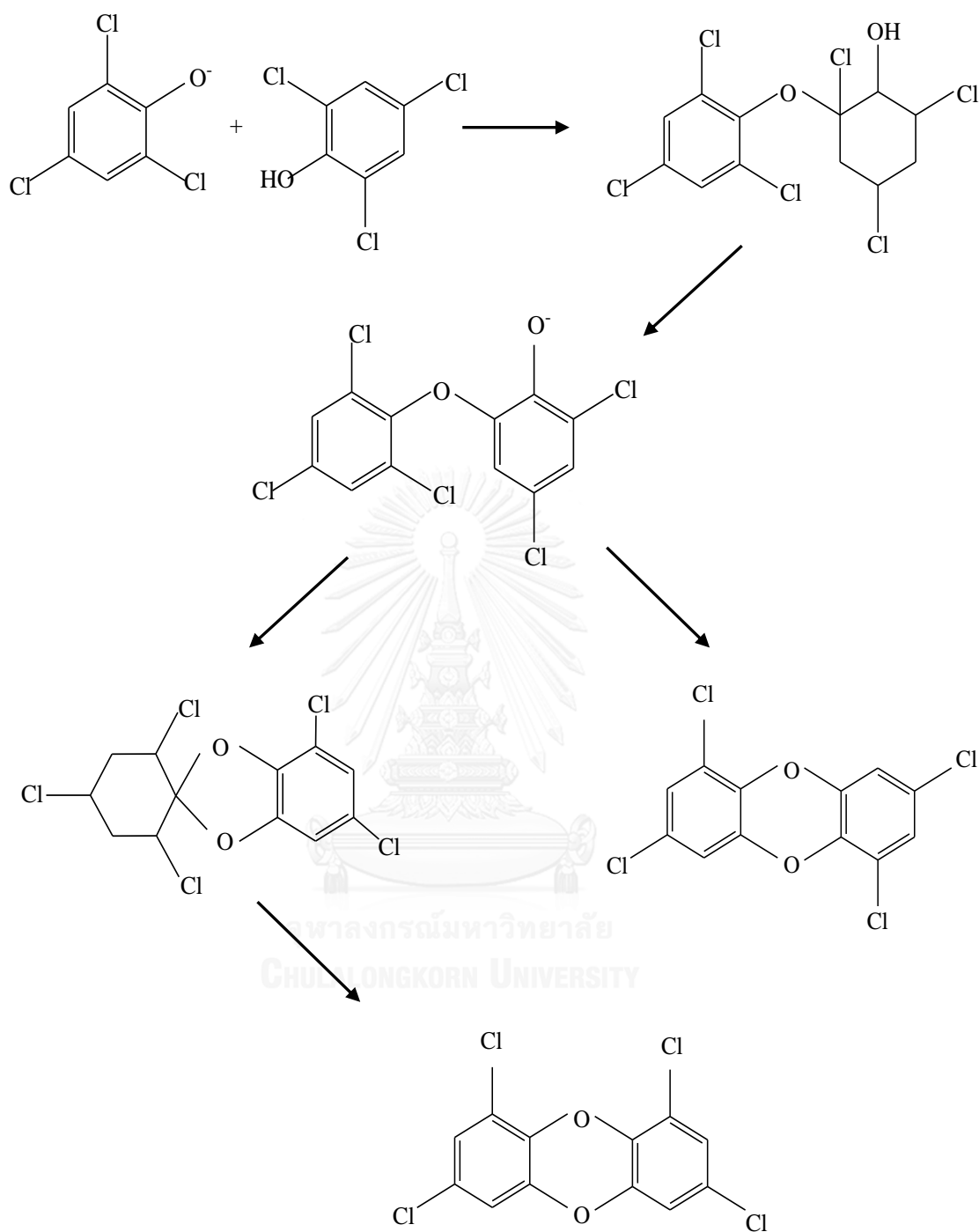


Figure 2.6 Formation route of PCDD from 2,4,6-trichlorophenols.



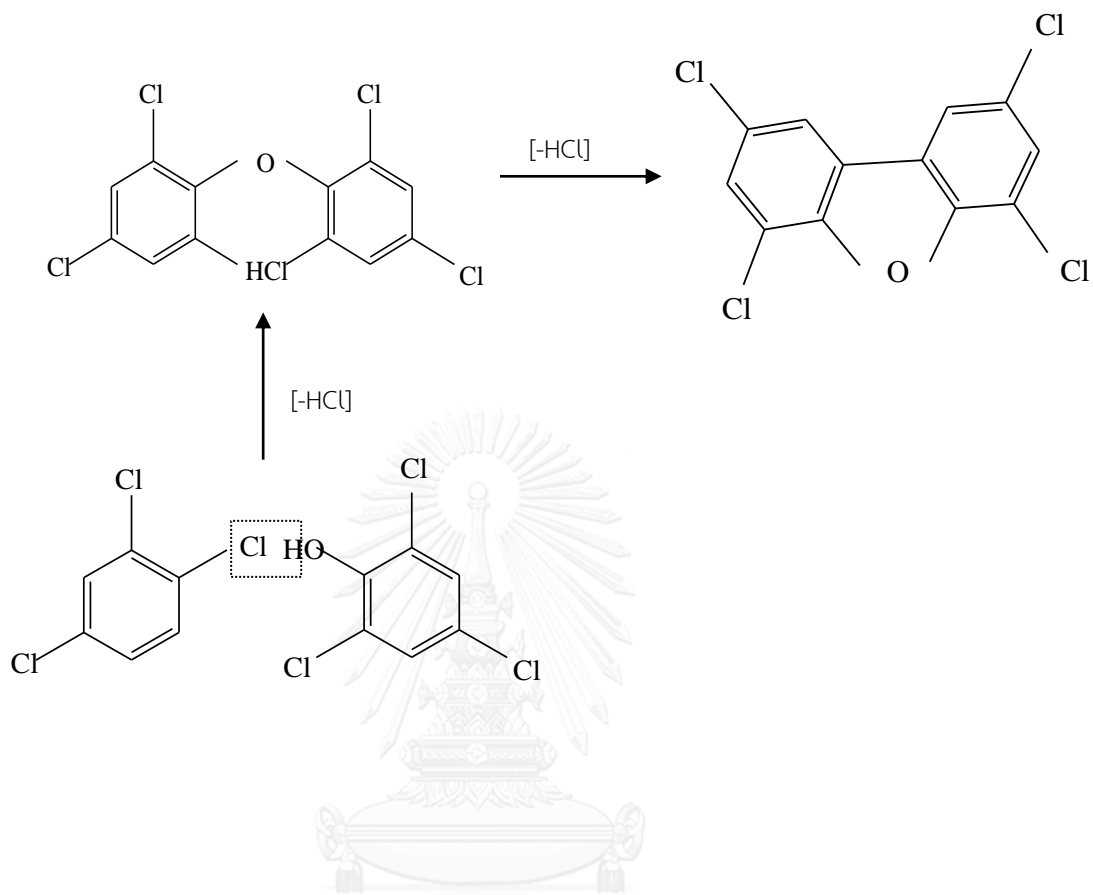


Figure 2.7 Formation route of PCDD/F from chlorobenzenes and chlorophenols

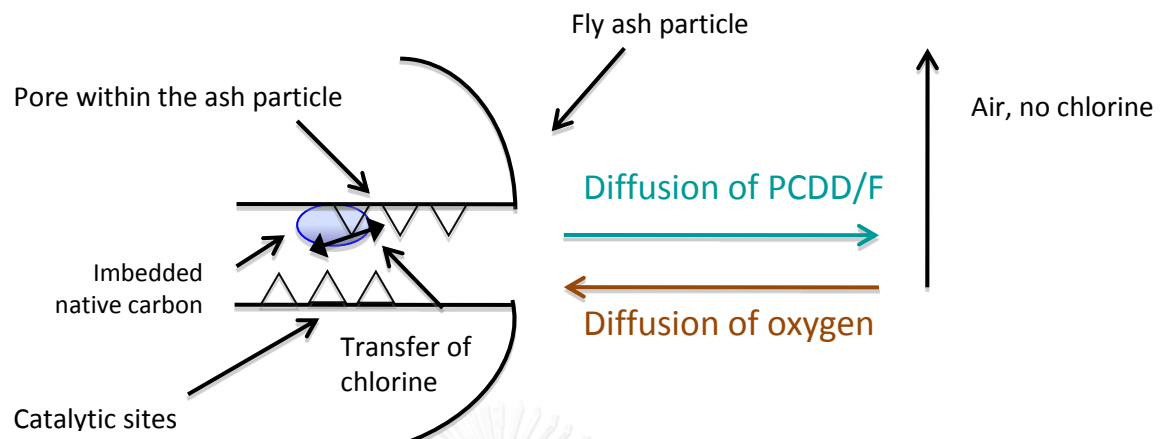


Figure 2.8 Formation route of PCDD/F from by De novo synthesis

## 2.4 Dioxins in Thailand

In an effort to protect human health and the environment from persistent organic pollutants (POPs) exposure from incineration process, the government sectors in Thailand agree to sign and ratify the Stockholm Convention on POPs since 2002. Pollution Control Department, Ministry of Natural Resources and Environment has suggested that the hazardous and hospital/medical/infectious waste incinerators must be applied the Best Available Technology (BAT) in order to prevent and minimize the emission of unintentional hazardous chemicals (such as POPs, dioxins, and furans).

Nowadays, the first Dioxin laboratory is established the Environmental Research and Training Center (ERTC), the Department of Environmental Quality Promotion (DEQP). This project is accomplished by the collaboration among Department of Environmental Quality Promotion (DEQP), Pollution Control Department (PCD), Office of Natural Resources and Environmental Policy and Planning (ONEP), Bangkok Metropolitan Authorities (BMA), Department to Industrial Work (DIW), Department of Industrial Promotion (DIP), and Ministry of Public Health (MOP). The goals of this project are to provide an analytical laboratory for detect and measure PCDDs/Fs and to support the research studies of PCDDs/Fs for reducing their emission in compliance with legal requirements.

## 2.5 An estimation of Dioxin formation by mathematical analysis

Previous researchers have been revealed that combustion conditions may affect the formation of dioxin emission in an incinerator. Several dioxin reduction technologies based on combustion control have been established so far (Buekens & Huang, 1998; Y.-M. Chang et al., 2009; Hung et al., 2011). However, it is worth noting that effective PCDDs emission control strategies should be supported by the accurate prediction of the pollutants (Chang and Chen, 2000). Thus, several research studies have reported the estimation of dioxin emission using mathematical modeling approaches.

Blumenstock et al. (1999) have conducted a study on the estimation of dioxin emission in the fuel and stack gas of a hazardous waste incinerator. This study applied the method of principal component analysis (PCA) and correlation coefficients based on linear regression to find the relationships between the PCDDs emission and potential indicator substances. The study concluded that the chlorinated benzenes can be identified as a good indicator factor for the prediction of PCDDs emission. This finding relied on the result from the regression line and indicated the important factor in the prediction approach.

Choi et al. (2007) applied multi-regression analysis to predict the variations of polychlorinated dibenzofurans (PCDD/Fs), with sampling data sets collected from seven municipal solid waste (MSW) incinerators in Korea. The result indicated that the changes of temperature and dust concentration at the inlets and outlets of wet scrubbers are the important factors (Dong, Jin, & Li, 2003) that affected the PCDD/DF in the flue gas. This prediction is based on empirical data in the study area incinerators. Thus, this discovery might not consistently estimate the levels of PCDD/DF in different incineration plants. However, the most significant parameters (temperatures at wet scrubber and dust concentration) were identified by this study.

Over the past century, ANNs has been widely applied to waste management systems and complex systems. Table 2.4 provides an examples of ANNs used as the prediction model. In brief, ANNs is successfully performed in the estimation of the target data which calculated based on observed historical data. The prediction by ANN provided good accuracy confirmed by previous studies as summarized in the following paragraph.

In 2003, Dong et al. performed a comparative study on the prediction of the calorific value of the municipal solid waste (MSW) in China. The study compared the performance between a feed forward neural network and multiple linear regression models. The physical components of MSW were screened by statistical analysis and used as the predominant factor. This research stated that the neural network provides a more accurate prediction than a traditional model.

Besides, Rene et al. (2011) applied ANN modeling in air pollution control in 2011. The ANN was proposed in order to predict the removal efficiency of gas-phase styrene in biological systems and the results revealed that the ANN model gave high prediction accuracy as well. It is interesting to note that ANN systems perform well and provide satisfactory prediction results. Further study, Qdais et al. (2010) used ANN in the biogas production process for the prediction of methane. The result indicated that ANN shows good performance with tested by  $R^2$  equal to 0.87. In addition, this study also identified the optimal conditions for obtain the maximum methane production by using genetic algorithms (GA) as a helping mathematical tool.

However, it is necessary to point out that there are some drawbacks of using ANNs based predictive model reported by Tu., 1996. One main drawback is that ANN behaves as “black-box” algorithm in nature. Thus, it is difficult to identify which variable is an important predictor. There is no certain rule to show the exact process pattern for obtaining the optimal ANN algorithm.

In addition, the other main drawback is ANN trend to overfitting along the training algorithm (Schittenkopf, Deco, & Brauer, 1997). This is mean that a large number of available data in training step of ANN provides a small value of error but when the new unseen data is applied to the model, a poor performance of ANN occurs. Because the ANN has learned and memorized the most suitable structure from the training data examples, thus, when the new pattern or situation of data used, the higher value of error is unavoidably obtained.

Moreover, overfitting in ANN is generally occurs when a large amount of dependent variables involve in the system (Feng, Zhang, Sun, & Zhang, 2011). The complexity of ANN is related to the number of connection weights among layers and the number of hidden layers that are cause by a variety of predictor variables (Piotrowski, Osuch, Napiorkowski, Rowinski, & Napiorkowski, 2014). The more complex in structure, the more patterns of data require to be

applied in the training step. Thus, the simplest ANN structure could be providing a better performance and the overfitting problem can be reduced.

Schittenkopf et al., (1997) suggests the strategies in order to overcome the overfitting of the training dataset in the feed forward neural network. According this study it can be summarized that the overfitting can be reduced by minimize the redundancy of input patterns by normalization or pre-data treatment. In addition, reduce a number of free parameters was also considered. Note that, dimensionality reduction of the input patterns is accomplished by statistical approach, so called principal component analysis (PCA).

To enhance the performance of ANN, the number of input variables is the important key to achieving an acceptable error. Basically, the patterns between input and output will be recognized through the learning step. Thus, selecting the suitable input variables will enable the learning algorithm to work faster and more effectively (Saxén & Pettersson, 2006) with the help of statistical analyses. Principal component analysis (PCA) is one of the common multivariate statistical techniques that are used to achieve great efficiency of data compression from the original data as well as to indicate natural associations between samples and/or variables (Astel, Tsakovski, Barbieri, & Simeonov, 2007; Wenning & Erickson, 1994) by gaining some information useful in the interpretation of environmental system. PCA consists of diagonalization of the covariance or correlation matrix transforming the original measurements into linear combinations of these measurements, and then explained variance of each principal component can be maximized. It has been widely used to reveal the relationships among variables as well as to classify them into different grouped variable sets, so that some special features inherent in the measured system can be characterized (García Lautre & Abascal Fernández, 2004; Lucas & Jauzein, 2008; Macciotta, Vicario, & Cappio-Borlino, 2006).

Table 2.4 Review of literature data on ANNs-based model application as predicting tool

Authors	Data and accuracy of the model
Dong et al., 2003	<ul style="list-style-type: none"> <li>● Waste Management</li> <li>● Predict heating value of MSW in waste stream for the incineration process</li> <li>● 5 input factors, 1 output factor, 10 data sets</li> <li>● Compare ANN with multiple linear regression model (MLR)</li> <li>● Relative error = 5% for ANN</li> <li>● Relative error = 30% for MLR</li> </ul>
Rene et al., 2011	<ul style="list-style-type: none"> <li>● Biological waste-gas treatment reactor</li> <li>● 4 input factors, 1 output factor, n/a data sets</li> <li>● Predict the removal efficiently of styrene</li> <li>● <math>R^2 = 0.8838</math></li> </ul>
Kurt et al., 2008	<ul style="list-style-type: none"> <li>● Air pollution forecasting</li> <li>● Forecast the air pollution indicators</li> <li>● 7 input factors, 3 output factors</li> <li>● Historical data randomly collected from August 2005 to July 2006</li> <li>● Relative error ranged on acceptable value (not mention the exact value in the article)</li> </ul>
Qdais et al., 2010	<ul style="list-style-type: none"> <li>● Biogas production</li> <li>● Predict the amount of methane production</li> <li>● 4 input factors, 1 output factor, n/a data sets</li> <li>● <math>R^2 = 0.87</math></li> <li>● Identify the key factor for the maximum production using genetic algorithms (GA)</li> </ul>

## 2.6 Dioxin Removal by activated carbon adsorption

The growing concern of the emission of PCDDs/Fs from the combustion process has led many incinerators to consider the technologies for the regulation of emission limit to meet the standard legislation. One of efficient techniques for the removal of PCDDs/Fs is based mainly on the adsorption by carbonaceous materials. Activated carbon is known as an excellent pollutant removal capability. It is certain that the removal of pollutants by activated carbon adsorption is considered as an efficient technology in treatment facilities both contaminated air and water (Brady, Rostam-Abadi, & Rood, 1996; Hale et al., 2012; Meidl, 1997).

Lian et al (2012) revealed comparative adsorption studies on waste-polymer-based, activated carbon, and carbon nanotube for removal of hydrophobic organic compounds. And the study found that activated carbon was provided superior adsorption performance to other adsorbents due to having excellent properties of high surface area, microporous structure, and narrow pore size distribution. Hajizadeh et al (2011) investigated the removal efficiency of dioxin and furan congeners from the incinerator flue gases PCDD/F using 3 types of waste-derived activated carbons: results indicated that the activated carbon containing high surface area and micro-porous would provide high removal efficiency. Hence, it is evident that activated carbon is one of the most promising adsorbent, which is extensively used for PCDD/Fs adsorption.

In most incineration system, the activated carbon is widely applied in the air pollution control devices (APCD) for the removal of PCDDs/Fs from gas stream. Generally, activated carbon adsorption units are usually installed in the incineration system (Hung et al., 2011; Lu et al., 2007) including:

- Fixed-bed adsorption,
- Moving-bed adsorption,
- Entrained flow (activated carbon injection), and
- Wet scrubbers



It should be highlighted that among the dioxin removal technologies, the fixed bed activated carbon adsorption system is considered as a cost-effective and relatively simply to use (Chi, Chang, Huang, Huang, & Chang, 2006). A considerable amount of literature has been published on the application of fixed-bed reactor in the adsorption of PCDD/Fs or dioxin-like compounds using activated carbon, as summarized in Table 2.4.

Table 2.4 provides the previous studies on the removal of PCDD/Fs and dioxin-like compounds using activated carbon derived from various kinds of raw materials. Different types of activated carbon were produced from inexpensive material carbonaceous source materials. Activated carbon with large surface area could provide the high performance of adsorption. Note that, the design of fixed-bed column is preferred to investigate to enhance the adsorption performance in the real situation.



Table 2-5 Review of literature data for the removal of PCDD/Fs and dioxin-like compounds using activated carbon in fixed-bed adsorption reactor

Compound	Activated Carbon (AC)		Adsorption Performance	Reference
	Raw Material	Surface Area (m <sup>2</sup> /g)		
PCDD/Fs	Coconut Shell	555.4	106 ng PCDD/Fs /g-AC	Chi et al., 2006
	Wheat Shell	212.3	108 ng PCDD/Fs /g-AC	
	Rice Shell	62.1	114 ng PCDD/Fs /g-AC	
PCDD/Fs	Coconut Shell	715.8	Removal Efficiency = 89%	Ji et al., 2014
	Lignite	374.9	Removal Efficiency = 95%	
2378-substituted PCDD/Fs	NORIT 80	1,019	Removal Efficiency = 58%	Hajizadeh et al., 2011
	Refuse Derived fuel	333	Removal Efficiency = 57%	
	Textile waste	619	Removal Efficiency = 64%	
	Tyre waste	376	Removal Efficiency = 52%	
1234- tetrachlorobenzene	Palm Shell	1,097	10 mg C <sub>6</sub> H <sub>2</sub> Cl <sub>4</sub> / g- AC	Inoue et al., 2008
	Anthracite	833	8.0 mg C <sub>6</sub> H <sub>2</sub> Cl <sub>4</sub> / g- AC	
	Palm Shell	1,097	2.5 mg C <sub>10</sub> H <sub>8</sub> / g- AC	
Naphthalene	Anthracite	833	2.2 mg C <sub>10</sub> H <sub>8</sub> / g- AC	
	Palm Shell	1,097	55 mg Br <sub>3</sub> C <sub>6</sub> H <sub>2</sub> OH / g- AC	
2,4,6 tribromophenol	Palm Shell	1,097	55 mg Br <sub>3</sub> C <sub>6</sub> H <sub>2</sub> OH / g- AC	
	Anthracite	833	50 mg Br <sub>3</sub> C <sub>6</sub> H <sub>2</sub> OH / g- AC	
Chlorobenzene	n/a	714.2	105.6 mg C <sub>6</sub> H <sub>5</sub> Cl / g-AC	Guo et al., 2014
	AC modified by H <sub>2</sub> O <sub>2</sub>	748.2	120 mg C <sub>6</sub> H <sub>5</sub> Cl / g-AC	

## 2.7 Modeling of breakthrough curve in adsorption process

Due to the highly toxic of PCDD, the incineration plant must be effectively regulated in order to minimize the level of PCDD in flue gas before discharged into the atmosphere. Several incinerators have been employed the activated carbon injection devices coupled with fixed-bed or moving bed adsorption (Hung et al., 2011). According to the dynamic operation, activated carbon injection is hardly to reach to the maximum capacity of adsorbent, causing the utilization of excess amount of activated carbon (Karademir et al., 2004). Spent activated carbon from incineration plant therefore becomes hazardous waste. Thus, a utilization of adsorbent in dynamic process should be modeled and optimized to reduce the operation cost and hazardous waste generation.

The development for the full-scale adsorption process can be accomplished by the simulation process, which performed base on the experimental data (Burkert et al., 2011). In most adsorption process, the dynamic behavior in packed-bed column is generally illustrated as breakthrough curve, which is the plotting between the inlet and outlet concentration ratio versus time in operation (Pan et al., 2005).

In general, the breakthrough point is defined at time that the inlet and outlet concentration of pollutant ratio is equal to 0.05 (depending upon each chemical toxicity level); the adsorbent is no longer use and will be replaced with a new lot. A number of studies have been reported on the adsorption modeling of various pollutants on several adsorbent materials using the correlation between mass or heat transfer equation.

The studies of kinetic and modeling the breakthrough curves for the understanding of adsorption process have been investigated for decades. Richard et al., (2010) performed the adsorption experiment for the removing of complex phenolic compounds by activated carbon in wastewater treatment. The study revealed that the thermodynamic and kinetic parameters are the key component to determine the behavior of the process and these correlations were essentially calculated for the prediction of the critical time (breakthrough point). In another study, Hamdaoui et al., (2007) carried out a number of adsorption experiments on the removal of various organic compounds (phenol and chlorophenols) using activated carbon to determine the thermodynamic factors by adsorption isotherm models.

Hamdaoui (2007) suggests that the adsorption equilibrium isotherm plays as an important tool to investigate the adsorption capacity among the processes and finally the adsorption process can be enhanced and the adsorption process might be efficiently operated. It should be noted that the required crucial factors or thermodynamic correlation for the simulation process were mostly demonstrated such as: energy of adsorption, characteristics of adsorbent, isotherm parameters, material balance, momentum balance, kinetic model, and energy balance (Xiu et al., 2000, Chuang et al., 2003, and Sperlich., 2005).

## 2.8 Aspen Gas Adsorption Simulation Program

Aspen is a promising software package for process simulation that can handle a variety of the complex processes especially in chemical industrial and gas separation. In the Aspen module, the program works based on the mathematical models to estimated or predict the performance in the process. The following diagram illustrates how the Aspen simulation is work and provides the overview process of the second part of this study. Note that, the details in deep will be explained in Chapter 5 further.

As shown in Fig. 2.9, the adsorption experiments will be finished firstly prior start the simulation. The adsorption behavior from the experiment is illustrated as breakthrough curve. From this curve, bed capacity of each experiment can be calculated and considered as an important data to determine the mass transfer coefficient in fixed bed column. The mass transfer coefficient must be set up into the Aspen simulation program. Then, in order to perform the simulation, the appropriate adsorption models with various assumptions need to be selected. It should be highlight that there are several parameters that required be calculating and fulfilling in the program which are depend on the adsorption models. The simulated data from Aspen will be compared with the observed data by the statistic test to obtain the minimum error from the simulation.

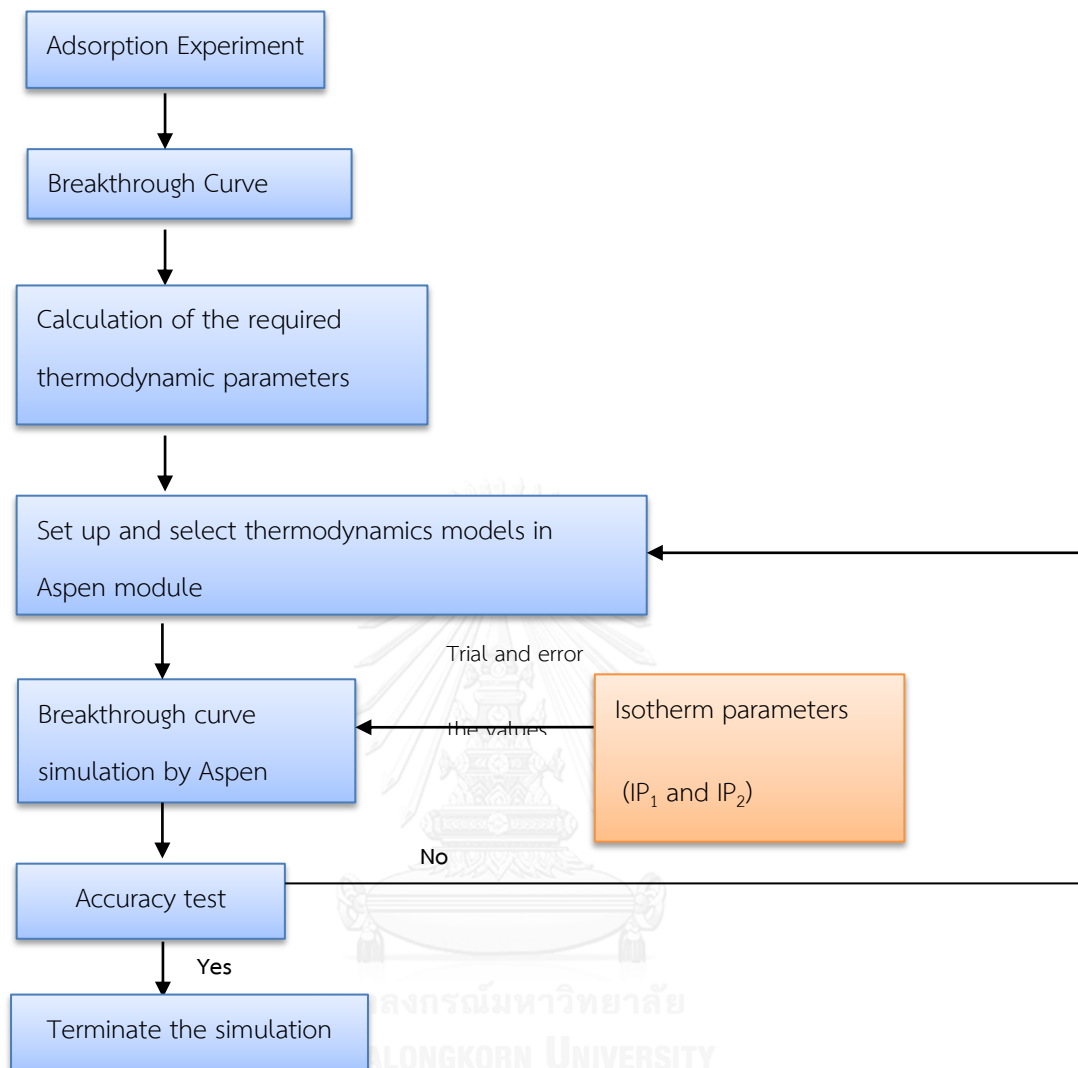


Figure 2.9 Schematic description of experimental procedure

Note that, Aspen contains with a large thermo-physical properties and data for an accurate calculation throughout the process. Hence, a considerable amount of literature has been published on application of Aspen as modeling software to enhance the operation design and find the optimum condition for the process.

Ortiz et al. (2014) have recently developed Aspen Adsorption program to estimate the bed lifetime (breakthrough life) in fixed-bed cylindrical column for biogas (gas mixture) treated in landfill using modified activated carbon as adsorbate. The study was applied linear driving force equation (LDF) with Freundlich isotherm with the following assumptions; mass transfer rate is equivalent to all the points of solid surface (Lumped resistance) and pressure and velocity are constant along the column. The results from the Aspen simulation program provided precise prediction of the breakthrough curves which calculated based on the numeric approaches conduct by Aspen Adsorption program. In addition, Ortiz et al. (2014) concluded that the dynamic simulation for the adsorption process played as a crucial tool for scale-up the system from laboratory scale. So far, time consumed and operation cost can be saved by the advantage of process simulation.

In 2012, Puertolas et al., reported the modeling of breakthrough curves for the adsorption-desorption of propane onto ZSM-5 zeolite in fixed-bed. Puertolas et al. (2012) using the Aspen Adsorption program as a prediction tool. Prior to start the Aspen software, a series of theoretical models and assumptions were selected as following; the effect of pressure drop corresponding to Ergun equation, no radial and axial transfer of heat and mass, constant heat of adsorption, and local thermal equilibrium. Moreover, Langmuir isotherm was considerable to use for the calculation of equilibrium adsorption isotherms. Based on these assumptions, the predicted breakthrough curves obtained from the software were close to the experimental results. In the next section, the fundamental detail of the Aspen Gas Adsorption Simulation Program will be further informed.

### 2.8.1 Introduction to Aspen Gas Adsorption Simulation Program

In the gas adsorption process, mass and energy balance in fixed-bed are the significant topics to concern in order to understand the actual system (Gutsche et al., 2008, Sansalone et al., 2008, and Guerro et al, 2010).

#### (1) Mass balance for gas phase

A general equation for convection and mass transfer from gas to solid phase accounts in a partial differential equation. They are given below in the equation (2.3),

$$\frac{\partial(v_g \rho_g)}{\partial z} + \rho_s \sum_k \frac{\partial w_k}{\partial t} = 0 \quad (2.2)$$

Where  $\frac{\partial(v_g \rho_g)}{\partial z}$  convection term

$\rho_s \sum_k \frac{\partial w_k}{\partial t}$  mass transfer term

In gas phase, the equation for each component is also governed by equation (2.3) with accumulation, axial and dispersion terms (Himmelblau et al., 2003, Smith et al., 2005, and Cussler et al., 2009).

$$-\varepsilon_i E_{zk} \frac{\partial^2 c_k}{\partial z^2} - \varepsilon_i E_{rk} \frac{1}{r} \frac{\partial}{\partial r} \left( r \frac{\partial c_k}{\partial r} \right) + \frac{\partial(v_g c_k)}{\partial z} + \varepsilon_B \frac{\partial c_k}{\partial t} + J_k = 0 \quad (2.3)$$

Where  $-\varepsilon_i E_{zk} \frac{\partial^2 c_k}{\partial z^2}$  axial dispersion term

$-\varepsilon_i E_{rk} \frac{1}{r} \frac{\partial}{\partial r} \left( r \frac{\partial c_k}{\partial r} \right)$  radial dispersion term

$\frac{\partial(v_g c_k)}{\partial z}$  convection term

$$\varepsilon_B \frac{\partial c_k}{\partial t} \quad \text{gas phase accumulation term}$$

$$J_k \text{ rate of flux to solid surface term which is given by } J = -\rho_s \frac{\partial w}{\partial t}$$

(2) Gas phase energy balance

The partial differential equation of gas phase energy balance is given by equation (2.4). It includes thermal conduction, convection of energy, accumulation of heat, compression, heat transfer from gas to solid, heat transfer from gas to the internal wall, and heat of reaction.

$$\begin{aligned} & -k_{ga}\varepsilon_i \frac{\partial^2 T_g}{\partial z^2} + C_{vg}v_g\rho_g \frac{\partial T_g}{\partial z} + \varepsilon_B C_{vg}\rho_g \frac{\partial T_g}{\partial t} + P \frac{\partial v_g}{\partial g} + HTC a_p (T_g - T_s) \\ & + \frac{4H_w}{D_B} (T_g - T_0) + H_r - \varepsilon_i k_{gr} \frac{1}{r} \frac{\partial}{\partial r} \left( r \frac{\partial T_g}{\partial r} \right) + a_{Hx} Q_{Hx} \\ & = 0 \end{aligned} \quad (2.4)$$

Where  $P \frac{\partial v_g}{\partial g}$  effect of compression which indicates the reversible rate

$$C_{vg}v_g\rho_g \frac{\partial T_g}{\partial z} \quad \text{convection term}$$

$$\varepsilon_B C_{vg}\rho_g \frac{\partial T_g}{\partial t} \quad \text{accumulation term which refers to enthalpy accumulation}$$

$$-k_{sa}\varepsilon_i \frac{\partial^2 T_g}{\partial z^2} \quad \text{axial thermal conduction term}$$

$$HTC a_p (T_g - T_s) \quad \text{gas-solid heat transfer and } a_p = (1 - \varepsilon_i) \frac{3}{r_p}$$

$$\frac{4H_w}{D_B} (T_g - T_0) \quad \text{heat exchange between gas and internal wall}$$

$$H_r \quad \text{is rate of heat generation by reaction}$$

$$-\varepsilon_i k_{gr} \frac{1}{r} \frac{\partial}{\partial r} \left( r \frac{\partial T_g}{\partial r} \right) + a_{Hx} \quad \text{axial thermal conduction in gas phase}$$

$$a_{Hx} Q_{Hx} \quad \text{heat exchange between gas and internal heat exchanger}$$



## (3) Solid phase energy balance

The solid phase energy balance includes terms for axial thermal conduction, heat transfer, and chemical reaction which are governed by equation (2.5).

$$\begin{aligned}
 & -k_{sa} \frac{\partial^2 T_s}{\partial z^2} - k_{sr} \frac{1}{r} \frac{\partial}{\partial r} \left( \frac{1}{r} \frac{\partial T_s}{\partial r} \right) + \rho_s C_{ps} \frac{\partial T_s}{\partial t} + \rho_s \sum_{i=1}^n (C_{pai} w_i) \frac{\partial T_s}{\partial t} \\
 & + \rho_s \sum_{i=1}^n \left( \Delta H_i \frac{\partial w_i}{\partial t} \right) - HTC a_p (T_g - T_s) \\
 & = 0
 \end{aligned} \tag{2.5}$$

Where  $\rho_s C_{ps} \frac{\partial T_s}{\partial t}$  accumulation in solid phase

$-k_{sa} \frac{\partial^2 T_s}{\partial z^2}$  axial thermal conductivity in solid phase

$-k_{sr} \frac{1}{r} \frac{\partial}{\partial r} \left( \frac{1}{r} \frac{\partial T_s}{\partial r} \right)$  radial thermal conductivity in solid phase

$HTC a_p (T_g - T_s)$  gas-solid heat transfer

$\rho_s C_{ps} \frac{\partial T_s}{\partial t}$  heat of adsorbed phase

$\Delta H_i \frac{\partial w_i}{\partial t}$  heat of adsorption

## (4) Wall energy balance

The factors that affect the wall energy balance are listed in the equation (2.6). This application is appropriated to use when rigorous model for the heat transfer to the environment is selected. They include axial thermal conduction along the wall, heat accumulation within the wall material, heat transfer from the bed to the inner wall and heat transfer from the outer wall to the environment.

$$\begin{aligned}
 & -k_w \frac{\partial^2 T_w}{\partial z^2} + \rho_w c_{pw} \frac{\partial T_w}{\partial t} - H_w \frac{4D_B}{(D_B + W_T)^2 - D_B^2} (T_g - T_w) \\
 & \quad + H_{amb} \frac{4(D_B + W_T)^2}{(D_B + W_T)^2 - D_B^2} (T_w - T_{amb}) \\
 & = 0 \tag{2.6}
 \end{aligned}$$

Where  $H_w \frac{4D_B}{(D_B + W_T)^2 - D_B^2} (T_g - T_w)$  heat exchange between gas and wall term

$H_{amb} \frac{4(D_B + W_T)^2}{(D_B + W_T)^2 - D_B^2} (T_w - T_{amb})$  heat exchange between wall and environment term

$-k_w \frac{\partial^2 T_w}{\partial z^2}$  axial thermal conductivity along the wall term

$\rho_w c_{pw} \frac{\partial T_w}{\partial t}$  heat content of wall term

## Chapter III

### Methodology: An estimation of Dioxin formation by ANN

The purposes of this study are to apply an artificial neural network to prediction the PCDDs emission from the municipal solid waste incineration and to identify the predominant controlling factors for PCDDs emission from combustion process. The five purposes of this chapter are to (1) explain the data collection, (2) provide an explanation of data pre-treatment, (3) describe the statistical techniques to determine the number of the input variables, (4) describe the procedure of a predicting model and (5) explain the method of sensitivity analysis to identify the key factors.

#### 3.1 Data Collection

An incineration plant located in central Taiwan was selected as the case study of this research. This plant has been in operation at Taichung city since 1995 with an average daily design capacity equal to 900 tons of municipal solid waste. As shown in Fig. 3.1, the incinerator consists of typical components; the furnace for combustion, the heat recovery equipment, and the flue gas treatment section. Various monitoring sites and dioxin sampling points are schematically identified in the Fig. 1 as well.

The sampling method in compliance with the standard sampling method of PCDDs in flue gas exhausted, NIEA A8707.74C, which was issued by Environmental Analysis laboratory EPA, Executive Yuan (ROC). The particles and gaseous are collected by XAD-2 absorbing tube for 8 hours and washed by solvents (acetone, methylene dichloride and toluene). In order to determine the concentration of PCDDs, the samples from MSW incineration will be analyzed by INEA A808.73B method. The collected sampled will be diluted by  $^{13}\text{C}$  isotope dilution following with gas chromatography and high-resolution mass spectrometer. The concentration of dioxin emission standard in discharge flue gas in usually reported as toxicity weight equivalent quantity of 2, 3, 7, 8-tetrachlorinated dibenzo-*p*-dioxin. The calculation is based on non-diluted dry emission volume at temperature of 273 K, pressure of 1 atm and 10% emission oxygen concentration as the reference standard regulated by Taiwan environmental protection

administration (1997). To build the ANN-based prediction model, four-year monitoring data sets are collected, and a systematic flowchart, including data collection; variable reduction; neural network construction, is established as Fig. 3.2.

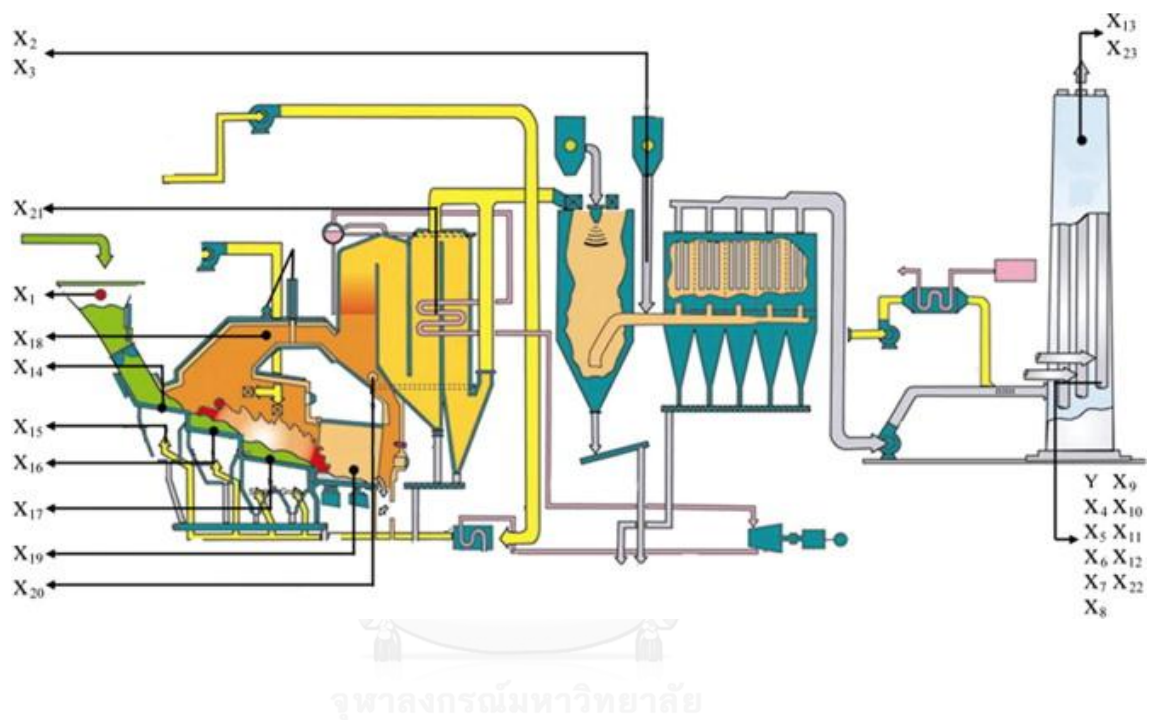


Figure 3.1 The Schematic of Taichung city refuse incineration plant

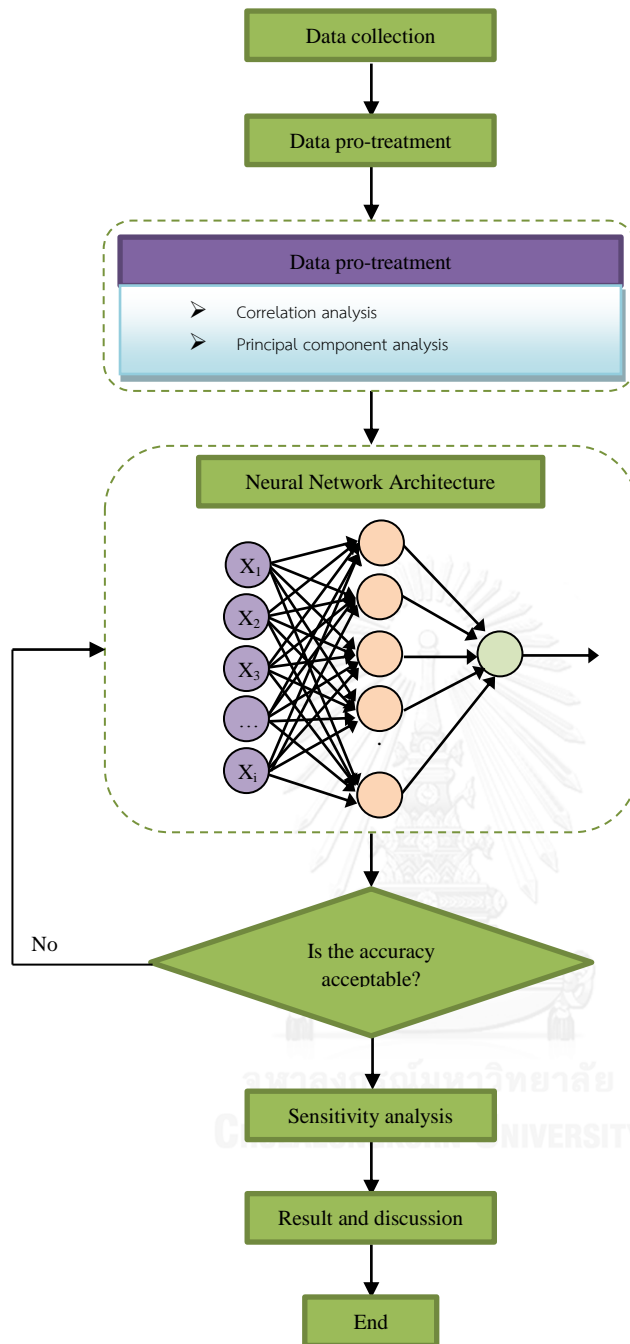


Figure 3.2 Flow chart of the artificial neural network approach for predicting the dioxin emission

Table 3.1 Basic statistical characteristic of variables

Variables	Unit	Max	Min	Mean	Standard Deviation
Waste loading ( $X_1$ )	ton	16.3	3.51	9.13	4.25
Activated carbon injection frequency ( $X_2$ )	Kg/Hr	26.2	14.5	20	2.66
Activated carbon injected ( $X_3$ )	Kg	5.66	3.94	4.63	0.44
Concentration of hydrogen chloride in the flue gas at the stack emission ( $X_4$ )	ppm	34.18	11.11	22.41	5.42
Concentration of carbon monoxide in the flue gas at the stack emission ( $X_5$ )	ppm	21.68	0.87	3.53	4.51
Concentration of nitrogen oxide in the flue gas at the stack emission ( $X_6$ )	ppm	140.46	56.15	98.22	19.40
Concentration of sulfur dioxide in the flue gas at the stack ( $X_7$ )	ppm	8.19	0.22	3.13	2.08
Carbon dioxide at stack emission ( $X_8$ )	%	8.26	4.74	6.86	0.75
Water at stack emission ( $X_9$ )	%	23.44	15.19	20.26	1.84
Oxygen at stack emission ( $X_{10}$ )	%	12.81	8.87	10.64	0.90
Opacity at stack emission ( $X_{11}$ )	%	5.45	0.48	2.2	1.31
Dust at stack emission ( $X_{12}$ )	mg/Nm <sup>3</sup>	4.84	0.48	1.91	1.18
Flue gas flow rate at the chimney final exit ( $X_{13}$ )	Nm <sup>3</sup> /hr	75856.36	42936.28	55811.14	5037.72
Temperature at the 1 <sup>st</sup> furnace room ( $X_{14}$ )	°C	184.98	146.54	167.38	8.97
Temperature at SAH export ( $X_{15}$ )	°C	201	89	155	30.23
Temperature at the 2 <sup>nd</sup> furnace room ( $X_{16}$ )	°C	1069	721	926	65.15
Temperature at burning heart furnace room ( $X_{17}$ )	°C	1176	745	944	109.57
Temperature at vice flue ( $X_{18}$ )	°C	1151	859	1010	60.58
Temperature at rotary kiln exit ( $X_{19}$ )	°C	1136	788	882	61.16
Temperature at mixing chamber ( $X_{20}$ )	°C	1099	916	981	47.52
Temperature at boiler convection zone ( $X_{21}$ )	°C	724	607	667	29.66
Temperature at chimney entrance ( $X_{22}$ )	°C	243	149	167	21.81
Temperature at final fuel gas emission ( $X_{23}$ )	°C	65.28	47.86	55.48	3.93
Dioxin Emission (Y)	ng-TEQ	0.59	0.003	0.15	0.118

### 3.2 Data pre-treatment

For building the prediction model, the operation data sets, consisted of the total numbers of 23 observed and control variables, in selected incinerator plant were gathered at various time points during the 2005-2008. These variables in this research are summarized Table 3.1 and corresponding monitoring sites are leveled in Fig. 3.1. The dioxin was investigated once in a week from the treated exhaust gases with the concentration unit of ng-Toxic Equivalency. Finally, a number of 63 data sets are obtained after screening out some missing or unusable data. To avoid the noise derived from different unit scales, the equation (3.1) is used to normalize the raw data sets.

$$x'_i = \frac{x_i - \text{Min}}{\text{Max} - \text{Min}} \quad (3.1)$$

Where  $x'_i$  is the normalized data,  $x$  is the raw data, Min is the minimum of raw data, and Max is the maximum of raw data. Based on the normalized data; the following statistical analyses can be made.

### 3.3 Statistical analyses

#### 3.3.1 Correlation Analysis

In order to build a simplified and accurate prediction model, an integrated multivariate analysis consisted of correlation analysis and PCA is proposed to pick and select the key variables from massive monitoring variables in an incinerator. Firstly, Pearson's correlation matrix was calculated to present the linear relationship between variables. The mathematical formula for computing the Pearson correlation coefficient ( $R_{\text{pearson}}$ ) in this paper is:

$$r = \frac{\sum_{i=1}^n (x'_i - \bar{x})(y_i - \bar{y})}{(N-1)(s_x)(s_y)}$$

(3.2)

Where  $\bar{x}$ ,  $N$ , and  $s$  are sample mean, sample size, and sample standard deviation, respectively. Normally, Pearson correlation coefficient,  $R_{\text{pearson}}$ , can be ranged from +1 to -1. The closer value of  $r$  to +1 or -1 means the stronger correlation among the variables. On the contrary, if the value of  $r$  is closer to 0 means that variables have a weak strength of correlation and that

variables can be neglected. In this study, the values of  $R_{\text{pearson}}$  which lower than 0.100 were neglected. Thus, from the results of Pearson's correlation, we can exclude some variables with high correlation coefficient from the candidates for building the prediction model. In addition, the software package SPSS® (Version 19.0) for Windows to determine the structure in the relationships between parameters and identify the most important factors contributing to this structure based on the eigen analysis of the correlation matrix.





### 3.3.2 Principal Component Analysis

As stated earlier the relationship between the inputs and the output (dioxin emission) can be identified by the correlation analysis and several factors can be deleted from the system. For the purpose of variables reduction, the principal component analysis was applied in this research. The basis of PCA has been well-explained (Jolliffe, 2002). Briefly, PCA is used for characterizing patterns within large sets of data by re-expressing to a rotated coordinate system in which as much variance as possible is explained by the first few dimensions. In which the eigenvectors of the variance covariance matrix are calculated, so that the principal component score, i.e. the weight of the eigenvector can be obtained. The scores of the original variables, also called principal component loadings (PC loadings), can be used to indicate the relationship between the variable and the principal component. In other word, the variable and the principal component will be stronger related if the PC loading is lager.

By doing this, raw data matrix can be reduced to two or three principal component loadings that account for the majority of the variance. Thus, these factors can be used to account for approximately required information as the original observations do.

### 3.4 Prediction the PCDDs emission by ANNs

The artificial neural network is one of data-derived approaches and widely used to figure out the nonlinear relationships among input and output variables. It imitates the behaviors of nervous system in human brain, being capable of recognize the patterns of a system after experiences learning from a sets of training data. The basic structure of artificial neural network can be determined as consist of three independent layers: input, hidden, and output layer.

The connection between the layers linked with the neural with synaptic weight coefficients ( $w_{ij}$ ). Commonly, when inputs ( $x_i$ ) enter the system, they are multiplied by synaptic weights and summed up at each node ( $\sum(w_{ij})(x_i)$ ). The summed values can be passed throughout the network and activate all hidden nodes until reach the output layer when this values are greater that the threshold values. After the input processed all layers, the errors between the computed and actual output are presented as well.

Notice that synaptic weights and threshold values are uncertainly number. However, the network can adjust these values by applying the example of case into the learning process. The overall of learning process is calculating as a circle until reaches the local error. The hidden nodes are being activated by the sigmoid activation function. When the networks reach output layer, the computed errors are send backward to the first step again for learning the mistake and weight adjustment. The network will recognize the optimal pattern in order to get the target or output with the expectable results. This process of training data is called back-propagation algorithm. The algorithm works as follow (W. C. Chen, Chang, & Chen, 2002; Negnevitsky, 2001; Tsai, Lin, & Shen, 2002; Yetilmezsoy, Fingas, & Fieldhouse, 2011);

(1) Define the input data set for training in neural networks

(2) Calculate the actual outputs at each hidden layer ( $j$ ) by this following mathematical formula, where  $n$  is the number of inputs of neuron  $j$ , and  $\theta_j$  is the threshold value.

$$y_j = f(\sum_{i=1}^n w_{ij}x_i' - \theta_j) \quad (3.3)$$

(3) Transfer the output values ( $y_j$ ) in the hidden layer by using the sigmoid function as shown;

$$f(x) = \frac{1}{(1 - \exp(-y_j))} \quad (3.4)$$

(4) Calculate the actual outputs at the output layer ( $k$ ), where  $m$  is the number of inputs of neuron  $k$ , and transfer  $y_k$  by applying the sigmoid function

$$y_k = f\left(\sum_{j=1}^m w_{jk} x_{jk} - \theta_{jk}\right) \quad (3.5)$$

(5) Calculate the error at the output layer ( $\varepsilon_k$ ), where  $y_{d,k}$  is the desired output of neuron  $k$  at the output layer

$$\varepsilon_k = y_k(1 - y_k)(y_{d,k} - y_k) \quad (3.6)$$

(6) Change the weights at the output layer ( $w_{ij}^*$ ), where  $\eta$  is the constant called learning rate

$$w_{ij}^* = w_{ij} + (\eta)(y_j)(\varepsilon_k) \quad (3.7)$$

(7) Calculate (back-propagate) the error at the hidden layer ( $\varepsilon_j$ ), where  $l$  is the number of outputs of neuron  $k$  at the hidden layer

$$\varepsilon_j = (y_j)(1 - y_j) \sum_{k=1}^l \varepsilon_k w_{jk} \quad (3.8)$$

(8) Change the weights at the hidden neurons ( $w_{ij}^*$ )

$$w_{ij}^* = w_{ij} + (\eta)(x_i)(\varepsilon_j) \quad (3.9)$$

(9) Repeat calculating back through the algorithm and provide the system learn how the error related to the inputs, output, and weights. Finally, the best fit condition among the parameters will be identified.

## Chapter IV

### Result and Discussion: An Estimation of Dioxin Emission by ANN

The aim of this chapter is to reveal the results and discuss the findings in the part of modeling the dioxin emission from municipal solid waste incineration. The content begins with the historical data collection and then screen the obtained data by statistical analyses. Later, the predominant factors that show the highest relative with the dioxin emission will be considered as the input factor for the creating the predicting model. Finally, an artificial neural network will be applied to estimate the dioxin emission from the incinerator. The result from measured and modeled will be compared by root mean square error.

#### 4.1 Basic statistical analysis and variable selection

##### 4.1.1 Correlation analysis

There are 23 variables considered as the candidates for building the ANN-based prediction model. For excluding some redundant variables, correlation analysis and PCA were carried out. Table 4.1 presents the Pearson's coefficients ( $R_{\text{pearson}}$ ) among the 23 variables in this study. It appears from Table 4.1 that the  $R_{\text{pearson}}$  for determine the relationship, revealing that variables are indeed correlated ( $R_{\text{pearson}} > 0.100$ ) with PCDDs emission is highlighted in bold. There is the correlation of PCDDs emission with selected variables including;  $x_3$ ,  $x_4$ ,  $x_5$ ,  $x_6$ ,  $x_8$ ,  $x_{10}$ ,  $x_{11}$ ,  $x_{15}$ ,  $x_{20}$ ,  $x_{21}$ ,  $x_{22}$ ,  $x_{23}$ , and  $x_{24}$ . In contrast, 10 variables including  $x_1$ ,  $x_6$ ,  $x_8$ ,  $x_{11}$ ,  $x_{12}$ ,  $x_{13}$ ,  $x_{15}$ ,  $x_{16}$ ,  $x_{17}$  and  $x_{18}$  are eliminated owing to their low Pearson's coefficient values ( $R_{\text{pearson}} < 0.100$ ) that may indicate there's no relationship with the dioxin emission. Note that, the description of the variables was described in Chapter III, Table 3.1. And then, the other 13 candidates survive into the PCA process.

Table 4.1 Selected variables for building artificial neural network by correlation analysis 48

	Y	X <sub>1</sub>	X <sub>2</sub>	X <sub>3</sub>	X <sub>4</sub>	X <sub>5</sub>	X <sub>6</sub>	X <sub>7</sub>	X <sub>8</sub>	X <sub>9</sub>	X <sub>10</sub>	X <sub>11</sub>	X <sub>12</sub>	X <sub>13</sub>	X <sub>14</sub>	X <sub>15</sub>	X <sub>16</sub>	X <sub>17</sub>	X <sub>18</sub>	X <sub>19</sub>	X <sub>20</sub>	X <sub>21</sub>	X <sub>22</sub>	X <sub>23</sub>	X <sub>24</sub>	X <sub>25</sub>	X <sub>26</sub>					
Y	1.000																															
X <sub>1</sub>	0.2613	1.000																														
X <sub>2</sub>	0.2337	0.2226	1.000																													
X <sub>3</sub>	0.231	0.23	0.4975	1.000																												
X <sub>4</sub>	-0.254 <sup>a</sup>	-0.440	-0.110	-0.135	1.000																											
X <sub>5</sub>	-0.261	0.040	0.071	-0.020	0.130	1.000																										
X <sub>6</sub>	-0.269	0.037	0.041	0.177	0.136	0.250	1.000																									
X <sub>7</sub>	-0.264 <sup>a</sup>	-0.240	-0.26 <sup>a</sup>	-0.240	0.220	0.150	0.170	1.000																								
X <sub>8</sub>	-0.044	0.231	0.121	0.114	0.239	-0.140	-0.022	0.330	1.000																							
X <sub>9</sub>	0.160	0.241	0.172	0.213	-0.010	-0.241	-0.12	0.043	0.422 <sup>a</sup>	1.000																						
X <sub>10</sub>	0.110	0.300	0.209 <sup>a</sup>	0.400 <sup>a</sup>	-0.222	0.285	0.117	-0.243 <sup>a</sup>	-0.171	-0.239	1.000																					
X <sub>11</sub>	0.084	-0.041	0.110	0.020	0.162	0.191	-0.130	0.144	0.110	0.220 <sup>a</sup>	0.220	1.000																				
X <sub>12</sub>	0.08	-0.02	0.115	0.120	0.168	0.200	-0.10 <sup>a</sup>	0.09	0.129	0.12 <sup>a</sup>	0.224	0.160 <sup>a</sup>	1.000																			
X <sub>13</sub>	-0.041	-0.11	-0.110	0.125	0.128	-0.123	0.141	0.14	-0.447 <sup>a</sup>	-0.047	-0.200 <sup>a</sup>	-0.041	-0.012	1.000																		
X <sub>14</sub>	0.101	0.177	0.420 <sup>a</sup>	0.527	-0.300	0.163	0.078	-0.220 <sup>a</sup>	-0.470 <sup>a</sup>	0.122	0.200 <sup>a</sup>	0.077	0.07	0.236	1.000																	
X <sub>15</sub>	-0.09	0.025	0.207 <sup>a</sup>	0.142	-0.110	-0.02	0.044	-0.112	0.300 <sup>a</sup>	0.112	0.148	0.057	0.042	-0.017	-0.072	1.000																
X <sub>16</sub>	0.054	-0.040	0.105	0.020	-0.120	-0.101	0.011	0.100	0.220	0.027	0.190	0.010	0.027	-0.007	0.007 <sup>a</sup>	0.007	1.000															
X <sub>17</sub>	0.011	-0.170	-0.012	0.020	-0.025	-0.144	0.144	0.200 <sup>a</sup>	-0.421	0.029	0.139	0.013	0.002	0.200	-0.020	0.054	0.427 <sup>a</sup>	1.000														
X <sub>18</sub>	0.044	0.041	0.211	0.239	-0.121	-0.162	0.470 <sup>a</sup>	-0.04	0.141	0.129	0.000	-0.042	-0.054	-0.011	0.000	0.007 <sup>a</sup>	0.007 <sup>a</sup>	0.007 <sup>a</sup>	1.000													
X <sub>19</sub>	0.217	-0.174	-0.147	-0.203	0.116	0.103	-0.203	0.207 <sup>a</sup>	-0.02	-0.014	-0.107 <sup>a</sup>	0.086	0.077	0.140 <sup>a</sup>	-0.241 <sup>a</sup>	-0.107 <sup>a</sup>	-0.003	0.000	-0.107 <sup>a</sup>	1.000												
X <sub>20</sub>	-0.182	-0.171	-0.211	-0.110	0.080	-0.207	0.140	0.420 <sup>a</sup>	0.180	-0.121	0.074	0.011	0.011	0.012	-0.241	0.180	0.003	0.007	0.084	0.021	1.000											
X <sub>21</sub>	0.420 <sup>a</sup>	0.071	0.400	0.347	-0.200	-0.00	-0.120	-0.00	-0.00	0.00	0.100	0.140 <sup>a</sup>	0.240 <sup>a</sup>	-0.10	0.220	0.170	0.004	0.040	-0.000	0.071	0.000	1.000										
X <sub>22</sub>	0.147	0.100	0.300	0.440	-0.00	0.271	0.012	-0.300	-0.120 <sup>a</sup>	-0.120	-0.120	0.100	0.200	-0.10	0.440 <sup>a</sup>	0.00	0.027	-0.040	0.171	-0.120 <sup>a</sup>	-0.071	0.100	1.000									
X <sub>23</sub>	0.100	0.100	0.000	0.000	-0.00	0.200	0.000	-0.00	0.00	0.211	0.000	0.211	0.211	0.211	0.211	0.211	0.211	0.211	0.211	0.211	0.211	0.211	1.000									
X <sub>24</sub>																									1.000							
X <sub>25</sub>																										1.000						
X <sub>26</sub>																											1.000					

<sup>a</sup> Correlation is significant at the 0.05 level (2-tailed).

<sup>b</sup> Correlation is significant at the 0.01 level (2-tailed).



#### 4.1.2 Principal component analysis (PCA)

After the correlated data were identified by correlation analysis, PCA was performed to reduce dimensionality of data by divided the data into principal components (PC). The number of PCs that should be extracted was sorted by the plot between number of components versus eigenvalue as displayed as scree plot (Fig. 4.1). In general, at the point in scree plot which shows the eigenvalues higher than one (or the point turns from steep into a flat line), the possible PCs can be obtained (Segreto, Simeone, & Teti, 2014). Looking at the plot in Fig 4.1, five PCs were identified in accordance with the eigenvalue larger than one. Noted that, in this study, the analysis is based on orthogonal transformation method with varimax rotation and retention of PC which eigenvalues were larger than one.

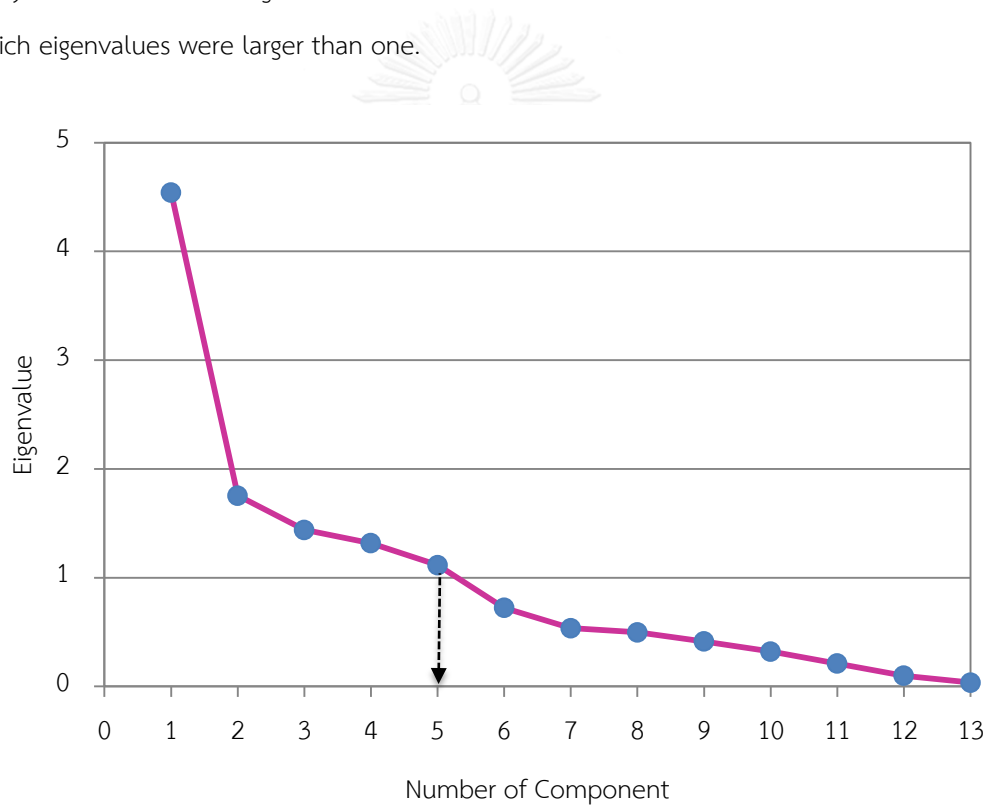


Figure 4.1 Scree Plot for determine the principal components (PC)

The result obtained from the PCA analysis can be summarized in Table 4.2. Note that the abbreviations are detailed in the former chapter. As shown in Table 4.2, a five-factor model was determined by PCA, in which their percentage of variance and cumulative percentage of variance explained 75.78% of the total variance in the dataset. For each factor the PC loadings were 33.00%, 12.65%, 11.01%, 10.47% and 8.91% of the variance. The factor loadings in Table 4.2 show the correlation between the principal components with the variables. The higher value of factor loading represents the strong correlation. Therefore, 5 variables were chosen with loading values over 0.8. These are considered to be the input variables for building the dioxin emission prediction model. The input variables consist of activated carbon injection ( $x_2$  and  $x_3$ ), concentration of hydrogen chloride in the flue gas at the stack emission ( $x_4$ ), temperature at the mixing chamber ( $x_{20}$ ), and temperature of final fuel gas emission ( $x_{23}$ ).

Table 4.2 Selected variables for building artificial neural network by principal component analysis

Variable	Principal Component				
	PC1	PC2	PC3	PC4	PC5
$X_3$	<b>0.945</b>	-0.125	-	-	-
$X_2$	<b>0.923</b>	-	-	-	0.148
$X_{23}$	<b>0.913</b>	-0.116	-	-	-0.214
$X_4$	-	<b>0.851</b>	-	-	-0.139
$X_7$	-0.223	0.790	-	0.295	0.243
$X_{14}$	0.485	-0.539	0.410	-0.120	-0.120
$X_9$	0.301	-	-0.764	-0.126	-
$X_{22}$	0.408	-0.275	0.652	-	-0.135
$X_5$	-	0.349	0.598	-0.525	0.147

$X_{10}$	0.490	-0.205	0.589	-	-0.216
$X_{20}$	-0.147	0.229	-	<b>0.881</b>	-
$X_{19}$	-0.256	0.144	-0.142	-0.156	0.747
$X_{21}$	0.422	-0.238	0.105	0.354	0.647
% of Variance	32.995	12.651	11.011	10.471	8.651

---





A strong relationship between PCDDs emission and operation temperature has been reported in the literature. In a typical incineration process, MSW are successfully burned in a furnace with the series of grate rods while the PCDDs can be formed in the temperature range of 400–800 °C (Altarawneh, Dlugogorski, Kennedy, & Mackie, 2009). The reduction of PCDDs emission will occur with temperature greater than 900 °C (McKay, 2002). The finding from the correlation analysis in this research is similar to the earlier work that can be stated as “when the temperature increases the PCDDs emission should decrease.” Thus, the temperature at the mixing chamber ( $x_{20}$ ) can be noted as the key factor for the dioxin emission as well.

Normally, activated carbon has been applied as the adsorbent for removal of unwanted gases in the waste incinerator gas stream. Moreover, there are several kinds of gases that might be adsorbed in the activated carbon such as  $HCl$ ,  $SO_x$ ,  $NO_x$ ,  $CO_2$  and/or volatile organic compounds. In this study, the results also accord with the earlier studies, which stated that activated carbon injection is widely used in waste incinerators as the major air pollution control device for control of the PCDDs emission (Chi et al., 2006; Hsi et al., 2007). Therefore, the frequency of activated carbon injection is closely related to the PCDDs emission factors in incineration plants.

From the previous studies about the PCDDs emission from incinerators, the mechanism of PCDDs formation can occur with the presence of hydrogen chlorine during the burning process (Ruokojarvi, Asikainen, Tuppurainen, & Ruuskanen, 2004). The possible explanation for this is that hydrogen chloride can react with oxygen that provides chlorine (Deacon Reaction). Therefore, chlorine is a key component for the formation of PCDDs precursors when chlorine reacts with organic compounds (Kilgroe, 1996; Thomas & McCreight, 2008).

## 4.2 The estimation of dioxin emission using ANN

After a series of testing, an optimized frame of ANN is obtained, where one input layer, one hidden layer with 8 hidden nodes, and one output layer are constructed. Amount of activated carbon injection ( $kg$ ), activated carbon injection rate ( $kg\ hr^{-1}$ ), concentration of  $HCl$  in the fuel gas at the stack emission, temperature at mixing chamber ( $^{\circ}C$ ), and temperature at fuel gas excretion ( $^{\circ}C$ ) were taken as the input while Dioxin emission at stack gas was the output parameter as shown in Fig. 4.2. The properties of ANN model for the prediction of Dioxin are given in Table 4.3.

The normalized raw data sets were randomly separated into training and testing by 70% and 30% of the data set, respectively. The maximum number of iterations for the training step was set as 100 (number of epochs). The back propagation algorithm was used as the supervised training for weight adjustment. In order to minimize the prediction error in the network, weights and biases values were modified by learning rate. The training process will be completed when the predicted values was nearest to the actual vales.

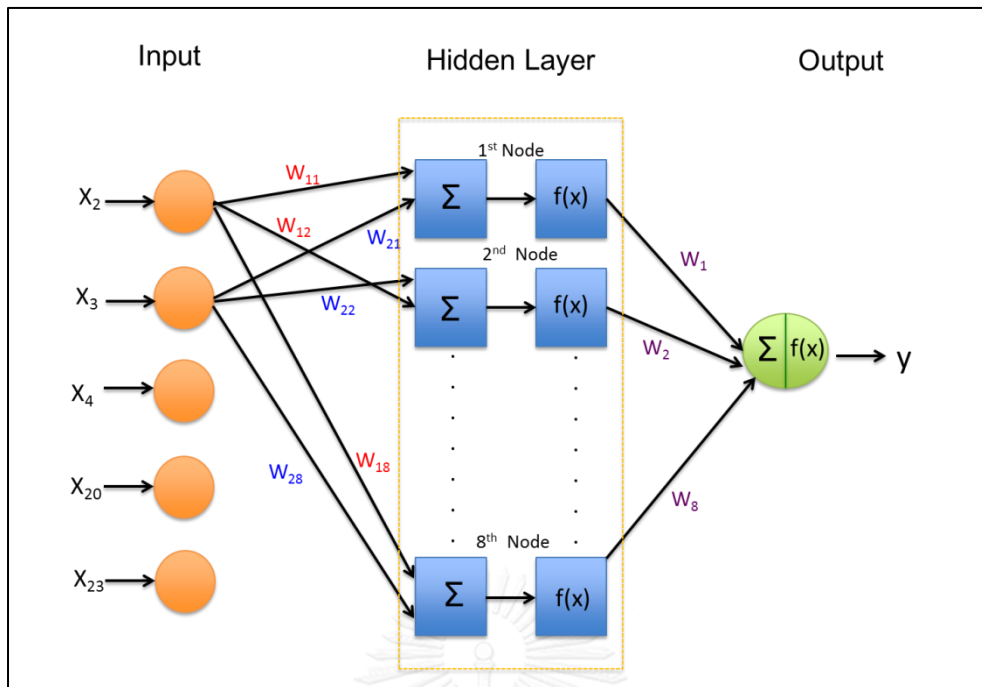


Figure 4.2 The structure of ANN model for the Dioxin emission prediction

Table 4.3 Properties of the ANN model for the Dioxin emission prediction

Structure	Property
Algorithm	Back propagation
Learning Rate	0.1
Number of Epochs	10
Transfer Function	Sigmoid
Data Type	Normalized data
Number of Inputs	5
Network Structure	From 5 to 30 neurons step by step

Figs. 4.3 presents the comparisons observed and predicted values in training and testing steps, respectively. It is apparent from these figures that the ANN model with the back-propagation learning algorithm provides high performance in the prediction of PCDDs emission ( $R^2$  equal to 0.998). The low variance shown in Figs. 4.3 and 4.4 indicates that the total random error is almost equal to zero. However, a systematic error happened in the training and testing steps. In the testing step, the predicted values are systematically larger than observed data. Fortunately, such errors can be revised by curve translation.

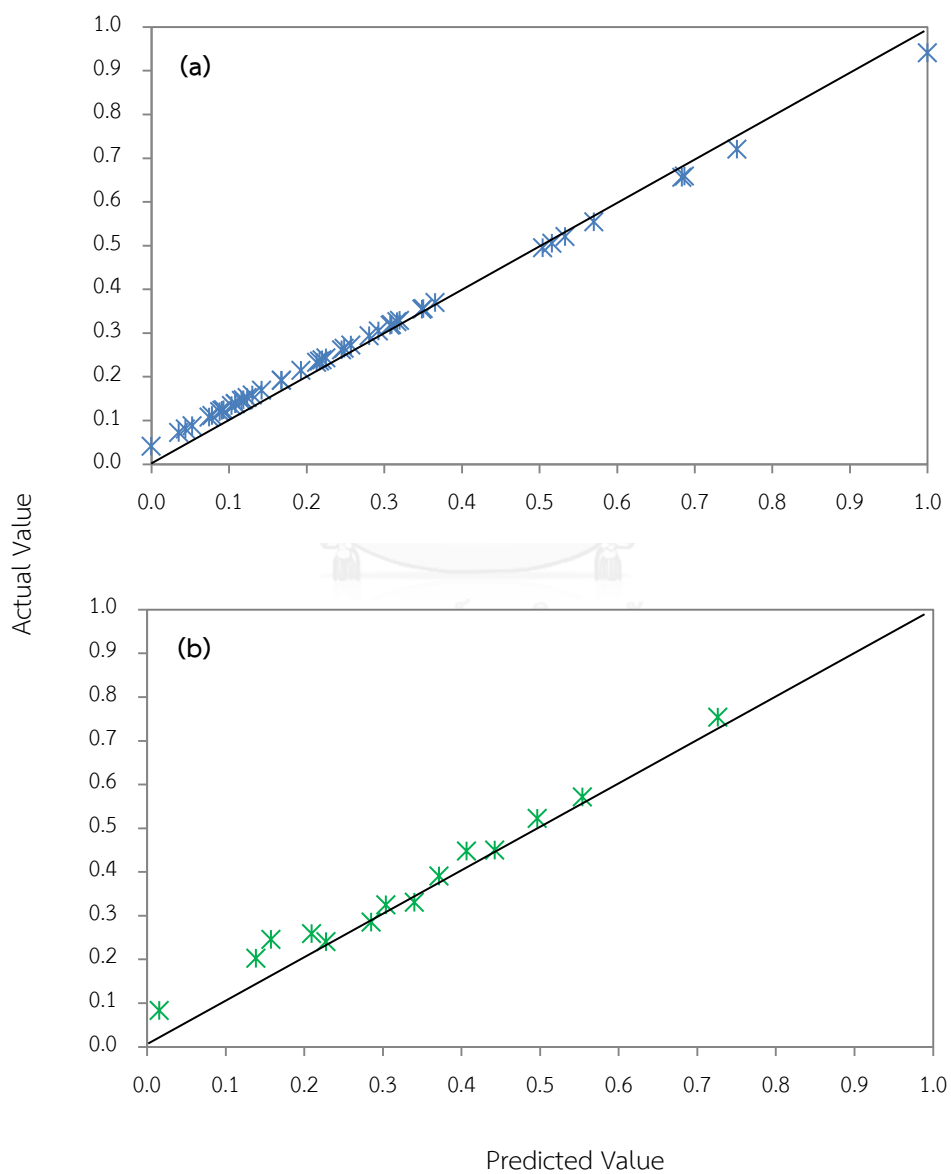


Figure 4.3 The dioxin emission predicted value versus target value (a) training step

and (b) testing step.



### 4.3 Sensitivity analysis

Sensitivity analysis can be applied to investigate the relative importance among the various input factors on PCDDs emission by means of the weights method proposed by Gevrey et al. (2003). To assess the relative importance approach, the connection weights between input layer, hidden layer, and output layer were carried out to identify which input factor plays the most important role in the dioxin emission. The calculation details were summarized in Appendix A. The five input factors considered were: the frequency of activated carbon injection, the amount of activated carbon injection, the concentration of hydrogen chloride, the temperature at the mixing chamber, and the temperature at the flue excretion. Fig.4.4 indicates the resulting relative importance between the factors. The result can be summarized as showing that the frequency of activated carbon injection ( $\text{kg h}^{-1}$ ) is the most significant factor for the PCDDs emission, followed by the concentration of hydrogen chloride and the temperature at the mixing chamber.

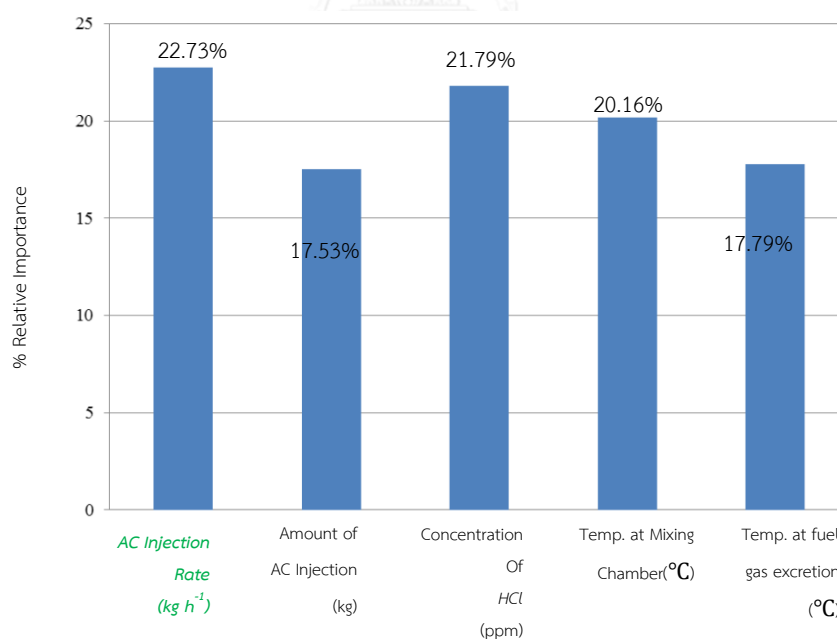


Figure 4.4 The result of sensitivity analysis from weights method

## Chapter V

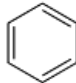
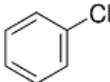
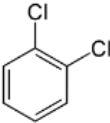
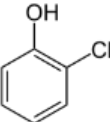
### Experimental procedures: Adsorption of dioxin derivatives

The adsorption of derivative of PCDDs compounds onto activated carbon has been provoked as crucial information for the incineration. The adsorption in our study will be carried out on both laboratory and simulation patterns.

#### 5.1 Chemicals and Materials

Chlorobenzene ( $C_6H_5Cl$ ), Ortho-dichlorobenzene ( $C_6H_4Cl_2$ ), Ortho-chlorophenol ( $C_6H_5ClO$ ), and Benzene ( $C_6H_6$ ) were used as the derivatives of dioxin compounds. The chemicals properties are shown in Table 5.1. Four different types of commercial activated carbon were used as adsorbents. All activated carbon adsorbents were sieved to a size range from 1.0 to 2.0 mm and preheated at  $100^\circ C$  overnight to remove moisture and other impurities, prior to use. Granular activated carbons (GACs) were kindly supplied by CarbokarnCo.,Ltd and NoriCo.,Ltd.

Table 5.1 Chemical properties.

Chemical Structure	Chemical name	Molecular Formula	Molecular Weight (g/mol)
	Benzene	$C_6H_6$	78.11
	Chlorobenzene	$C_6H_5Cl$	112.56
	Dichlorobenzene	$C_6H_4Cl_2$	147.01
	O-Chlorophenol	$C_6H_5ClO$	128.56

## 5.2 Adsorption Experimental

The adsorption experiment of derivatives of dioxin compounds from gas phase on GACs has been designed and set up. The system primarily consists of the following components: refrigeration unit, a series of saturators for pollutant generation in gas phase, a gas flow controller, packed bed column, 1/8" outer diameter stainless steel tube, and a gas chromatography (GC) apparatus. In summary, these components can be grouped into three main parts: refrigeration unit, adsorption column, and gas sampling equipment.

The series of saturators were placed in refrigeration unit. The 1<sup>st</sup> saturator was filled with the chemical and connected with the 2<sup>nd</sup> saturator that filled with full length of glass bead. At last, the blank saturator was used as the 3<sup>rd</sup> one for mixing the evaporated chemical and balanced nitrogen until the system reached the complete saturation. When the initial concentration of chemical was stable (checked by GC), the desired concentration was fed into the system for the starting of the adsorption operation. Be noted, the series of saturators were submerged in the water and kept inside a refrigeration unit, hence, the concentration of dioxin liked-structure compounds were regulated by adjusting the temperature in a refrigeration unit. The schematic diagram of the experimental system is visualized in the Figure 5.2. The initial concentration in this study was set at 1,800 ppm in entire experiments and the preparation of initial was detailed in Appendix B.

In order to investigate the derivatives of dioxin compounds adsorption on GACs, four types of dioxin precursors were chosen as pollutants in this research. The adsorbents were sieved to desired mesh size and dried overnight. Afterwards, the adsorbent was packed in a vertical borosilicate glass tube, which was used as the adsorption column. The column was packed with 20 mm of glass wool at the bottom followed by 60 mm of activated carbon and covered with 10 mm of glass bead and 20 mm of glass wool on the top layer (detailed in Fig 5.2).

The pollutant vapor was fed into the packed bed column through wire with an inner diameter of 10 mm coupled to the gas chromatography technique. For the purpose of sample analysis, GC equipped with flame ionization detector was used as gas sampling equipment. The analytical GC column was a DR-WAX capillary column of 30m x 0.53mm with 3  $\mu$ m film thickness. The inlet pressure of pure helium carrier gas (99.99%) was set at 1 kg/cm<sup>2</sup>. The oven



temperatures were programmed from 50 to 120°C at 8°C /min. The injection port and FID temperature were set at 250°C. The samples were injected by split mode with the ration 1:40.

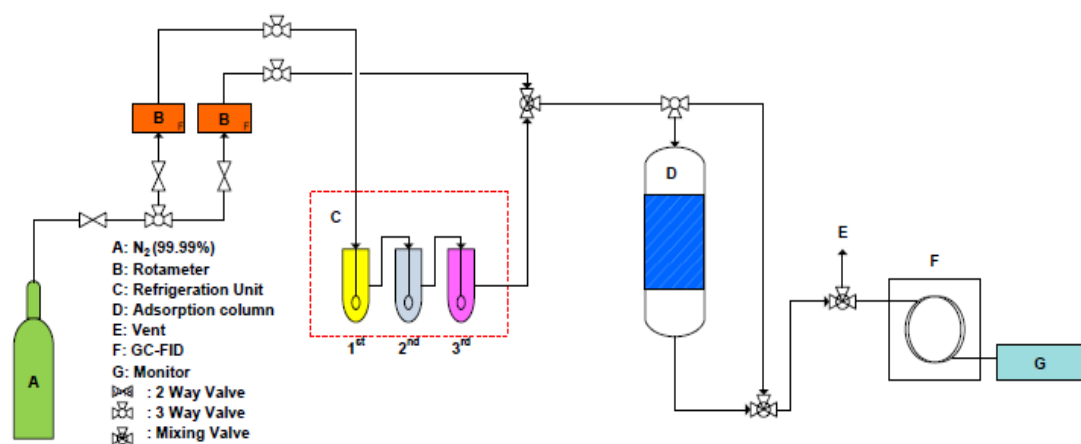


Figure 5.1 Schematic diagram of adsorption experimental

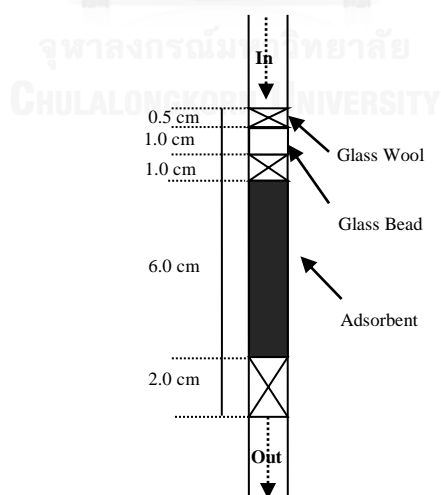


Figure 5.2 Schematic diagram of packed bed column

### 5.3 Derivatives of Dioxin Compounds Calibration

According to the adsorption experiments, the concentrations of adsorbates were measured using gas chromatography technique. In order to determine the concentration, the calibration curves were essentially to be established. In this study, the gas sampling bulb with 125 mL was used as a container coupled with an injection ports. Note that, the gas sampling bulb was contained with a certain amount of adsorbate. Procedure could be extracted as follows;

- Firstly, nitrogen gas (99.99%) was introduced to the gas sampling bulb to eliminated contaminants and vacuumed.
- Secondly, the pressures between outside and inside gas sampling bulb were equalized at 1 atm.
- Finally, the completely evaporation of adsorbate will be done after 15 minutes and the gas phase of adsorbate was injected with 0.5 mL to gas chromatography to analyze the concentration which visualized as the peak area in chromatogram.

The volume of adsorbate was converted to concentration in ppm as detailed in Appendix B. The calibration curve was plotted between the adsorbate concentrations in ppm versus the peak areas. The detection limits of adsorbates under GC-FID condition in this study were: benzene (10 ppm), chlorobenzene (17 ppm), di-chlorobenzene (20 ppm), and 0-chlorophenol (25 ppm). The calibrations of the dioxin derivatives are displayed in Figure 5.3. The correlation coefficients for each adsorbate are in satisfactory as tabulated in Table 5.2.

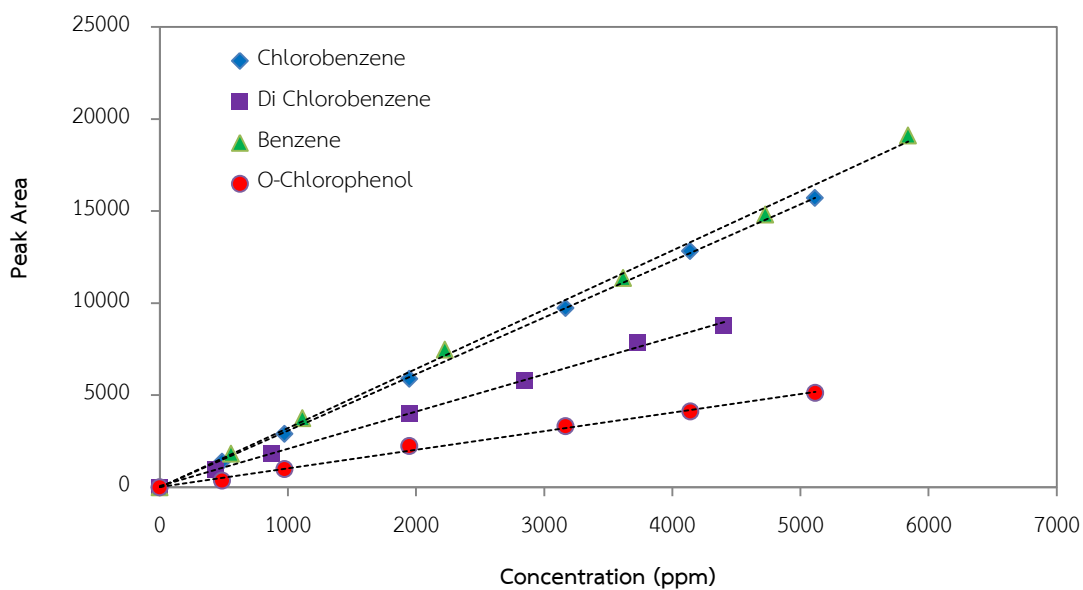


Figure 5.3 Calibration graph of peak area versus concentration

Table 5.2 Liner equation and  $R^2$  of the derivatives of dioxin compounds

Chemical	Equation	$R^2$
Benzene	$y=3.2146x$	0.998
Chlorobenzene	$y=3.0746x$	0.999
Di-Chlorobenzene	$y=2.0431x$	0.998
O-Chlorophenol	$y=1.0153x$	0.995

## 5.4 Adsorption Behavior

The thermal gravimetric analyzer (TGA) was performed to investigate the activation energy for desorption of the derivatives of dioxin compounds on activated carbons. Prior to the commencing this study, the activated carbons were heated overnight at 100°C to remove the moisture content from the particles. Prior to the commencing this study, the activated carbon was weighted in 1 g and placed in the desiccant that has 10 ml of derivatives of dioxin compounds. The adsorption was taken place in the normal condition about 1 week to ensure that the system has reached the equilibrium. Then, samples were saturated with vapor of chemicals were evaluated the weight loss regarding to temperature increases. Four different heating rates of 3, 5, 12 and 20°C min<sup>-1</sup> were used in this study.

## 5.5 Activated Carbon Characterization by N<sub>2</sub> Adsorption Isotherms and BET Surface Area

The pore structure of the activated carbons were examined through nitrogen isotherms at -196°C and relative pressure ( $P/P_0$ ) range of 0.01-0.99 with the use of a Micromeritics ASAP 2010. Meanwhile, Barret-Joyner-Halenda (BJH) analysis was applied to measure pore area and specific pore volume using adsorption and desorption techniques. The surface area evaluation of activated carbon can be also determined by Brunauer-Emmet-Teller (BET) analysis. Prior to the characterization, the activated carbons were dried overnight and placed in desiccator.

## 5.6 Aspen Gas Adsorption Simulation Program

### 5.6.1 Empirical equations of mass transfer

In this part of work, Aspen Gas Adsorption Simulation package will be considered as a major tool for the modeling of breakthrough curve. The fundamental kinetic parameters and mass-transfer coefficient ( $k_p$ ) are required in the adsorption simulation process. In this study, the Wakao and Funakvi correlation (Wakao & Funazkri, 1978) was used to obtain mass transfer coefficient in packed bed column based on the experiment data. The calculation will be performed using the relationship between Sherwood, Schmitt, and Reynolds number expressed as,

$$Sh = 2 + 1.1Sc^{0.33}Re^{0.60} \quad (5.1)$$

$$\frac{k_f d_p}{D_e} = 2 + 1.1 \left( \frac{\mu}{\rho D_e} \right)^{0.33} \left( \frac{d_p V_p}{\mu} \right)^{0.60} \quad (5.2)$$

Where  $d_p$  is particle size (mm),  $u_s$  is velocity (m/s),  $\rho$  is gas density ( $\text{kg/m}^3$ ),  $\mu$  gas viscosity (kg/m-s),  $k_f$  fluid mass transfer coefficient (m/s), and  $D_e$  is effective diffusivity ( $\text{m}^2/\text{s}$ ). In addition, the effective diffusivity can be calculated with the following equation:

$$D_e = \frac{\tau_p}{D_m} + \frac{1}{\frac{D_k}{\tau_p} + \left( \frac{1-\varepsilon_p}{\varepsilon_p} \right) \left( \frac{D_s}{\tau_p} \right) (K)} \quad (5.3)$$

and

$$K = \frac{w \rho_{ap,s}}{C_0} \quad (5.4)$$

Where  $\tau_p$  is pore tortuosity,  $\varepsilon_p$  is intraparticle porosity,  $K$  is equilibrium constant which can be obtained from eq.(4). When  $w$  is equilibrium adsorption capacity ( $\text{g}_{\text{adsorbate}}/\text{g}_{\text{adsorbent}}$ ),  $\rho_{ap,s}$  is apparent density of adsorbent ( $\text{kg/m}^3$ ), and  $C_0$  is initial concentration (ppm).  $D_m$  is molecular diffusivity,  $D_s$  is surface diffusivity, and  $D_k$  is Knudsen diffusivity. These parameters can be calculated as following relationship respectively:

$$D_m = \frac{0.01498T^{1.81} \cdot (1/M_a + 1/M_g)^{0.5}}{P \cdot (T_{c,g} \cdot T_{c,a})^{0.1405} \cdot (V_{c,a}^{0.4} + V_{c,g}^{0.4})^{0.2}} \quad (5.5)$$

Where  $T$  is temperature (K),  $M_a$  is molecular weight of the adsorbate,  $M_g$  is molecular weight of the adsorbent,  $V_c$  is critical volume ( $\text{m}^3/\text{mol}$ )

$$D_k = \frac{2}{3} \sqrt{\frac{RT}{\pi M}} \cdot R_p = 9700 R_p \left(\frac{T}{M}\right)^{1/2} \quad (5.6)$$

Where  $R_p$  is mean pore radius (m)

$$D_s = \frac{0.016}{\tau_p} \exp\left(\frac{-0.45\Delta H_{ads}}{RT}\right) \quad (5.7)$$

Consequently, mass-transfer coefficient ( $k_p$ ) can be calculated as following equation:

$$\frac{1}{k_p} = \frac{d_p}{6 \times k_f} + \frac{d_p^2}{4 \cdot 15 \cdot \varepsilon_p D_e} \cdot K \quad (5.8)$$

Where  $d_p$  is particle diameter (m),  $\varepsilon_p$  is intraparticle porosity.

In this study, Langmuir isotherm was selected to describe the adsorption behavior of the derivative of PCDDs compounds onto activated carbons in gas phase. The equation is written to express to adsorption capacity as a function of equilibrium concentration:

$$q_e = \frac{Q_m b c_e}{1 + b c_e} \quad (5.9)$$

Where  $q_e$  is loading of adsorbent (mg adsorbate/g adsorbent),  $Q_m$  is maximum loading adsorbate (mg adsorbate/ g adsorbent),  $b$  is Langmuir constant (L/g adsorbent), and  $c_e$  is equilibrium concentration (mg adsorbate/L). The adsorption isotherm parameters in Aspen Gas Adsorption Simulation program can be expressed in terms of constant factors, which is define as follow;

$$W_i = \frac{IP_1 P_i}{1 + IP_2 P_i} \quad (5.10)$$

Following this, the thermodynamic parameters were compute and the requirement of Aspen Adsorption module in the program can be accomplished by these calculated values. In the model simulation,  $IP_1$  and  $IP_2$  were randomly selected to account for the breakthrough curve which is provided a nearest curve-fitting to the experimental data. Consequently, the data from

simulated of the breakthrough curves can be provided useful data to determine the breakpoint time or the time to replace a new adsorbent in the adsorption column of incineration process. And finally, the air polluted from combustion process will be managed properly to ensure the level of air emission is safe for human health.

### 5.6.2 Model selection for Aspen Gas Adsorption Simulation Program

In order to simulate the adsorption behavior between gas and solid in the system, mass and energy balance must be considered as mentioned in Chapter II. Aspen Gas simulation Program contains with several assumptions that need to be set prior to start the simulation, here are the topics as summarized in table below.



Table 5.3 Required information in Aspen Gas Adsorption Simulation Program

Topic	Availabilities of assumption	Assumption detail
Material balance	Convection only	There is no effect of dispersion, the model would act as like as plug flow reactor.
	Convection with constant dispersion	There is the effect of convection and dispersion, it allows to supply the dispersion coefficient for all components.
	Convection with estimated dispersion	<p>It has the same assumption as convection with constant dispersion but there is no need to fill the dispersion coefficient. It can be estimated by equation (2.8).</p> $E_{zk} = 0.73D_{mk} + \frac{v_g r_p}{\varepsilon_i \left(1 + 9.49 \frac{\varepsilon_i D_{mk}}{2v_g r_p}\right)} \quad (5.11)$



Table 5.4 Required information in Aspen Gas Adsorption Simulation Program (Continue)

Topic	Availabilities of assumption	Assumption detail
Momentum balance	Burke-Plummer	<p>The velocity and pressure gradients relate to Burke-Plummer equation as stated in equation (5.12).</p> $\frac{\partial P}{\partial z} = -1.75 \times 10^{-5} \frac{M\rho_g(1 - \varepsilon_i)}{2r_p\psi\varepsilon_i^3} v_g^2 \quad (5.12)$
	Constant pressure and velocity	<p>The velocity and pressure are constant along the bed.</p>
	Constant pressure with varying velocity	<p>The pressure does not change in axial direction but the superficial velocity varies due to the adsorption rate.</p>
	Darcy's law	<p>This is the optional selection for linear relationship between superficial velocity and pressure gradient at particular point as illustrated in equation (5.13).</p> $\frac{\partial P}{\partial z} = -K_p v_g \quad (5.13)$
	Ergun equation	<p>This option describes the pressure drop in laminar and turbulent flow as demonstrated in equation (5.14).</p> $\frac{\partial P}{\partial z} = - \left( \frac{1.5 \times 10^{-3}(1 - \varepsilon_i)^2}{(2r_p\psi)^2 \varepsilon_i^3} \mu v_g + 1.75 \times 10^{-5} M\rho_g \frac{(1 - \varepsilon_i)}{(2r_p\psi)^2 \varepsilon_i^3} v_g^2 \right) \quad (5.14)$

Table 5.5 Required information in Aspen Gas Adsorption Simulation Program (Continue)

Topic	Availabilities of assumption	Assumption detail
Kinetic model	Lump resistance	Mass transfer rate is equivalent to all the points of solid surface.
	Micropore and macropore effect	There is the effect of diffusion rate within the pores of the solid and the void spaces between particles.
	Particle MB	This assumption can determine the loading and gas phase concentration profiles inside an adsorbent. To satisfy this assumption, the structure of adsorbent must be uniform and diffusion parameters are also required such as Knudsen, molecular, and effective diffusivity.
	Particle MB2	This assumption is the same as Particle MB but material flux ( $J_i$ ) is the additional parameter that needs to be considered.
Isotherm assumption	Langmuir	Langmuir isotherm can be used when the adsorption of monolayer occurs. $w_i = \frac{IP_1P_i}{1+IP_2P_i} \quad (5.15)$
	Langmuir 2	This isotherm is the function of temperature and one partial pressure. $w_i = \frac{IP_1e^{IP_2/T_s}P_i}{1+IP_3e^{IP_4/T_s}P_i} \quad (5.16)$

Table 5.6 Required information in Aspen Gas Adsorption Simulation Program (Continue)

Topic	Availabilities of assumption	Assumption detail
Energy balance	Isothermal	The energy balance is completely ignored because the temperatures of gas and solid are constant
	Non-isothermal	There are the options for non-isothermal such as no conduction, gas conduction, solid conduction, and both gas and solid conduction.
Reaction	None	There is no reaction take place in the adsorption process.
	Homogeneous	The occurrence of reaction is only in the gas phase.
	Heterogenous	There is the solid reaction takes place.
	Homogeneous and heterogenous	Both assumptions from homogeneous and heterogeneous are valid.

## 5.7 General function in Aspen

In general, Aspen adsorption program is operating in coupled with Aspen properties and Aspen Reaction Modeler. However, there is no reaction occurs in this study. Thus, an Aspen property is considered as the parallel program and Aspen Reaction Modeler is neglected.

The properties of chemicals in the design process need to be fulfilled in the program through the Aspen properties module. The set-up of the chemical properties can be set by following step as displayed in Fig 5.4

Component List >> Configure >> Use Aspen properties system >> Edit Aspen properties

as

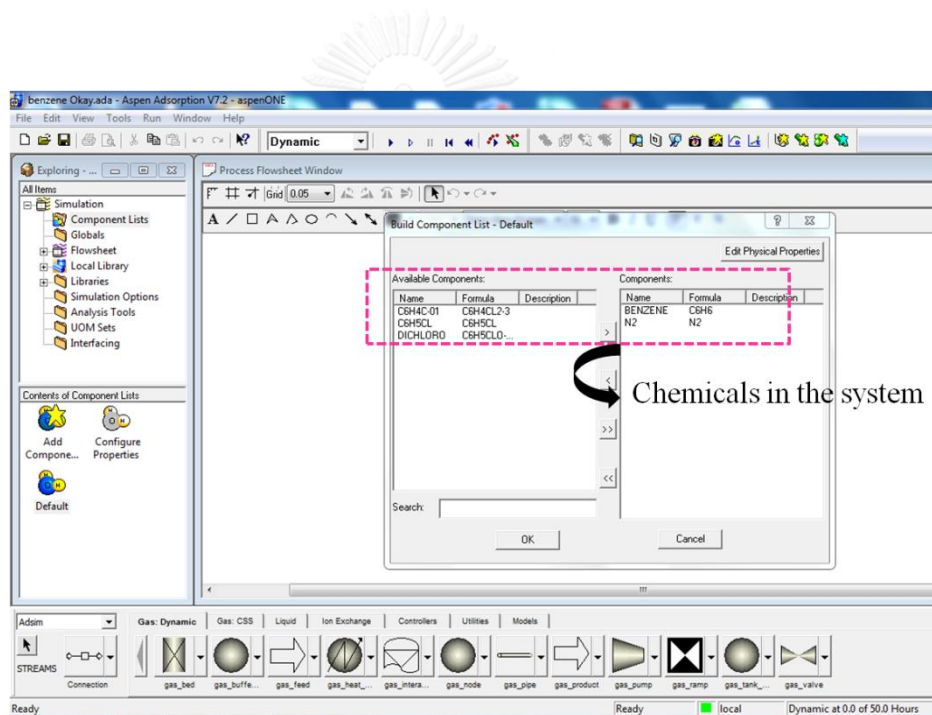


Figure 5.4 Chemicals properties adding in the Aspen program

After the chemicals properties are set, the next step is to draw the flow sheet by selecting the configurations as provided in the program (model libraries). The system consists of three main parts, including, input feed, adsorbed column, and product. In this study, packed bed column is used as the adsorbed column. In addition, the details experimental condition must be fulfilled in the modules. Figure 5.5 shows the flow sheet in this study.

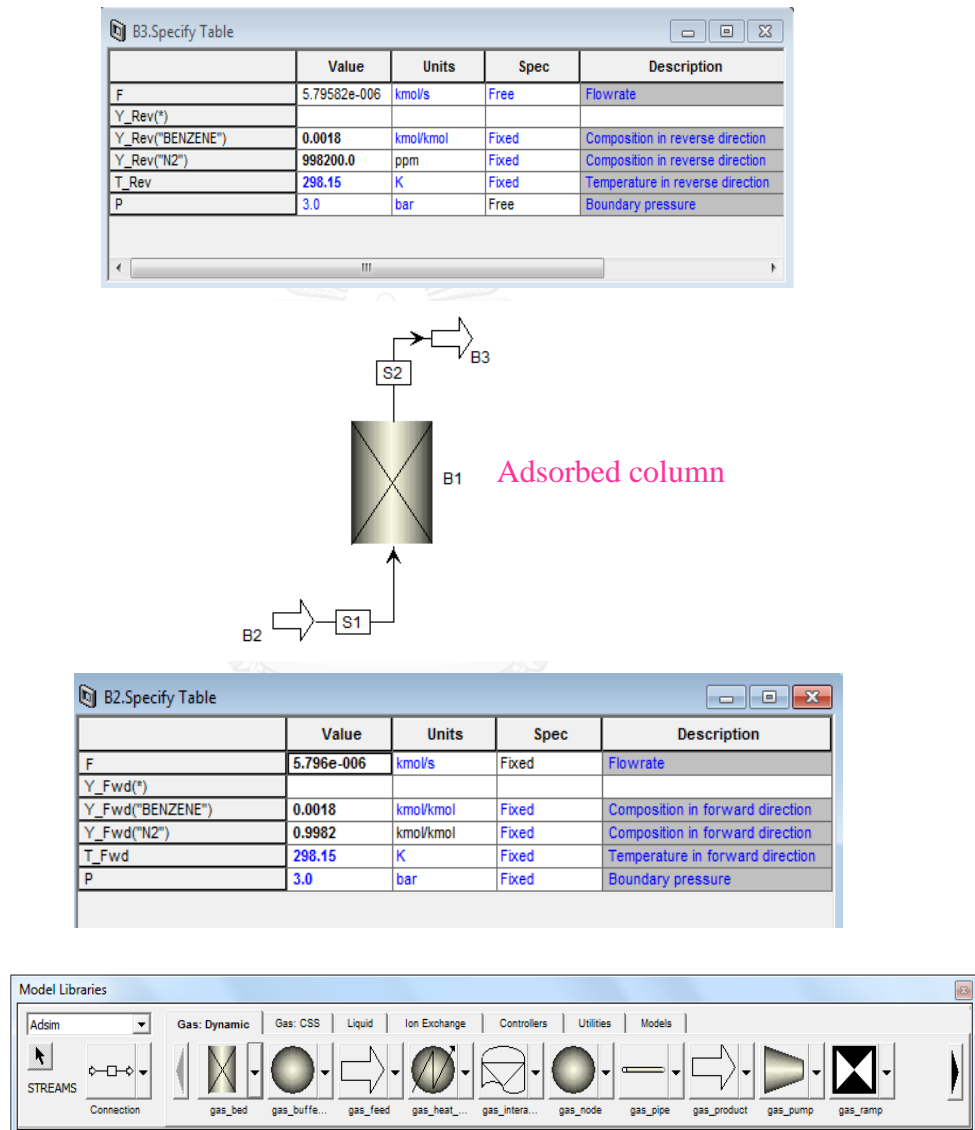


Figure 5.5 Flow sheet set up

In the last step, the column conditions, thermodynamic, and isotherm parameters are essentially to be addressed (Fig. 5.6). As shown in the figure below (Fig. 5.7), the program provides various types of thermodynamic models for the user usage. It is important to highlight that the accurate modeling of thermodynamic properties is crucial for the prediction of adsorption process illustrate as the breakthrough curve. In the data browser, the user is required to select the appropriate one for starting the simulation. Consequently, all required parameters and models should now complete. The simulation can be started and the simulated breakthrough curve will be compared to the actual value from experimental and accuracy test will be considered.

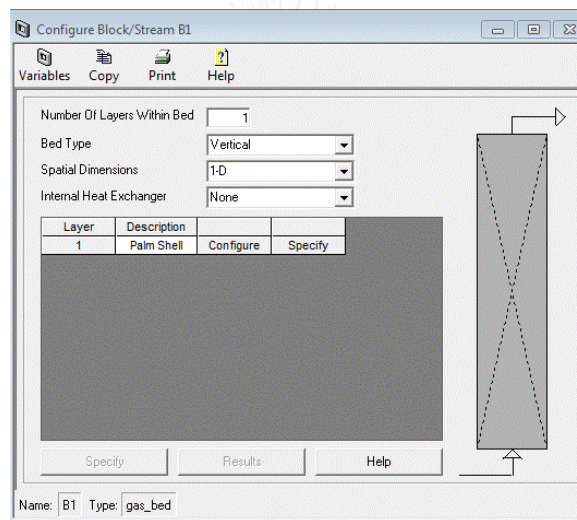


Figure 5.6 Required components in the simulation

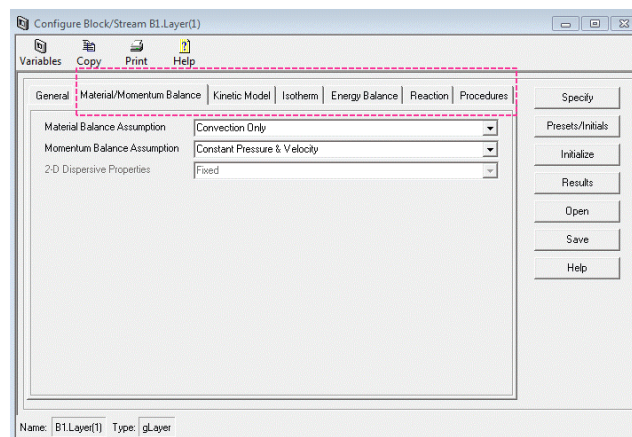


Figure 5.7 Model selection

## Chapter VI

### Results and discussion: Adsorption of dioxin derivatives

This chapter presents experimental and numerical modeling results for the adsorption of the derivatives of dioxin compounds onto activated carbons. The results from the experimental of the adsorptions are presented as the breakthrough curves and discussed. The results from the breakthrough curves simulation by Aspen Gas Adsorption program are summarized. Finally, the adsorption behavior of the adsorption, including adsorption isotherm and thermodynamic parameters are also presented.

#### 6.1 Characterization of Activated Carbon

The  $N_2$  isotherm curve is a plot between relative pressures with amount of adsorbate volume in pore and usually exhibits a hysteresis loop. Theoretically, the adsorption isotherms are classified into six categories by IUPAC (Ryu, Zheng, Wang, & Zhang, 1999; Yu-Chun Chiang, Pen-Chi Chiang, & Chang, 2001). Type I isotherm describe adsorbent is a typical microporous adsorbent (Langmuir equation), the next two isotherms (Type II and III) describe adsorption on macroporous adsorbent, Type IV and V isotherms are characteristic of mesoporous adsorbent, and finally type VI is stepped isotherm and nonporous material (Fig.6.1).

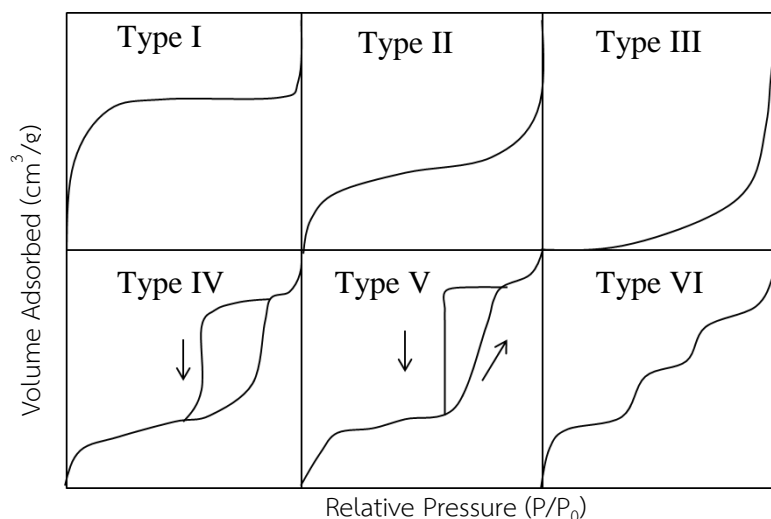


Figure 6.1 The classification of adsorption isotherms defined by IUPAC

The adsorption-desorption isotherms of activated carbon adsorbents used in this study are illustrated in Fig. 6.1. The four activated carbons were prepared from bituminous coal (ACB), coconut shell (ACC), palm shell (ACP), and anthracite (ACA). As shown in Fig. 6.1, the result indicates that isotherm type I is predominantly present in all adsorbents. The major structure of adsorbent was micro pores and it can be assumed that the sorption is localized as a monolayer.

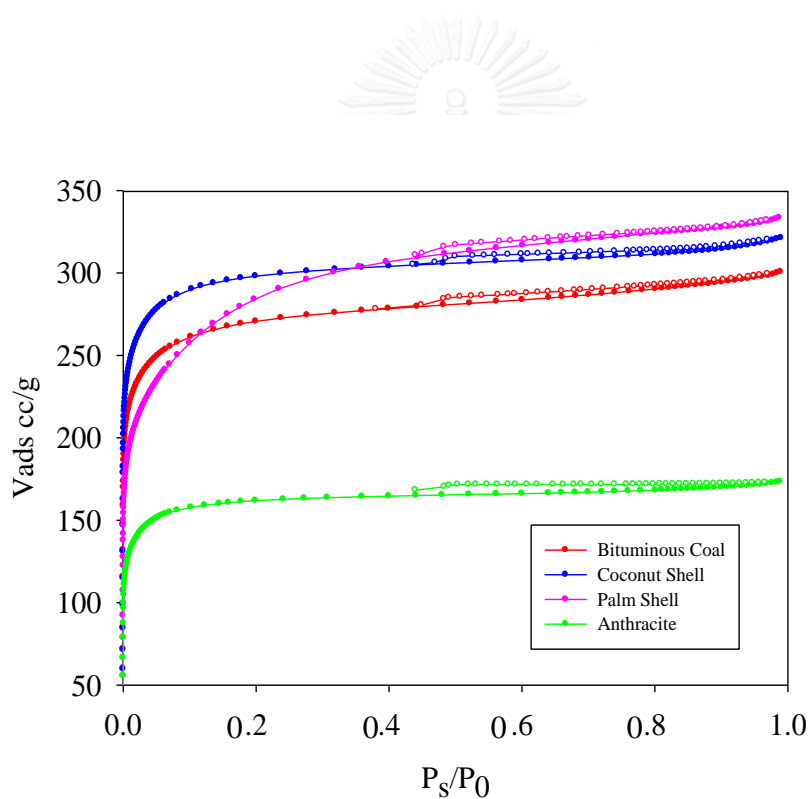


Figure 6.2  $N_2$  adsorption/desorption isotherms of the adsorbents



High surface area and appropriate pore size are primary requirement to use in the VOC adsorption. Table 6.1 presents the specific surface area ( $S_{\text{BET}}$ ) and average pore size. The results indicate that all adsorbents derived from bituminous coal (ACB), coconut shell (ACC), and palm shell (ACP) possess in similar range of surface area (ca.  $900 \text{ m}^2/\text{g}$ ) as well as average pore size (1.2 nm). In contrast with adsorbent derived from anthracite (ACA) has the lowest surface area (ca.  $558 \text{ m}^2/\text{g}$ , 1.195 nm in pore size). According to  $\text{N}_2$  adsorption-desorption isotherms, they showed isotherm type I (not shown). This implied that the major structure of the adsorbents was micropores.



Table 6.1 Porous structure of activated carbons

Adsorbent	Surface area (m <sup>2</sup> /g)
ACC	1029
ACP	1012
ACB	935
ACA	559

## 6.2 Adsorption of the derivatives of dioxin compounds

In order to investigate the adsorption performance, the area under the breakthrough curves were integrated for the calculation of adsorption capacity. Normally, breakthrough curve is displayed as s-shaped and gives a plot of outlet to inlet concentration ( $C/C_0$ ) versus time (t) in different operations. The performance of adsorbent can be determined from the area above the breakthrough curve according to the equations 6.1-6.3. Where  $F_A$  is a pollutant feed rate (g/cm<sup>2</sup> h),  $W_b$  is the adsorbate loading at breakthrough (g adsorbent/ g adsorbate), and  $W_{sat}$  is the adsorbate loading at saturation (g adsorbent/ g adsorbate).

In this study, the adsorptions of the derivative of dioxin compounds on the different types of activated carbons were carried out in the fixed-bed column with the similar flow rate at 50 m min<sup>-1</sup>, diameter of column is 10 mm, and particle size is 1-2 mm. The initial concentration ( $C_0$ ) was fixed at 1,800 ppm and the break point time ( $t_b$ ) where the relative concentration ( $C/C_0$ ) was considered at 0.05 in all experiment.

$$\text{Area above the graph} = \int_0^t \left(1 - \frac{c}{c_0}\right) dt \quad (6.1)$$

$$W_b = \frac{(F_A)(\text{Area above the curve at } \frac{c}{c_0}=0.05)}{\text{Mass of adsorbent per unit cross sectional area of bed}} \quad (6.2)$$

$$W_{sat} = \frac{(F_A)(\text{Area above the curve at } \frac{c}{c_0}=1.0)}{\text{Mass of adsorbent per unit cross sectional area of bed}} \quad (6.3)$$

$$\text{Bed capacity} = \frac{w_b}{w_{sat}} \quad (6.4)$$

Adsorption performances for each VOC and adsorbent were carried out in the dynamic system, ultimately providing the breakthrough curves. Figure 6.3-6.6 shows the breakthrough curves on four kinds of studied activated carbons of O-chlorophenol, di-chlorobenzene, chlorobenzene, and benzene, respectively. The VOC uptake on each adsorbent can be evaluated by the area above breakthrough curve. Table 6.2 includes adsorption capacities at breakthrough points and saturated points as well as the bed capacities for each VOC and adsorbent testing.

The observation found that ACA gave the breakthrough time fastest compared to other activated adsorbents in all studied chemicals. This would due to activated carbon derived from anthracite have the lowest surface area compared to others. The surface area of the adsorbents is evidently affected to the adsorption process. It is apparent that the adsorbents with a larger surface area provide a longer time to reach the saturation.

Considering chlorinated hydrocarbons (such as O-chlorophenol, di-chlorobenzene and chlorobenzene excepting benzene), activated carbons derived from bituminous coal, coconut shell and palm shell could adsorb those chemicals in the same patterns. The adsorption capacity could be ranked from high-to-low as follows; O-chlorophenol, dichlorobenzene and chlorobenzene, respectively.

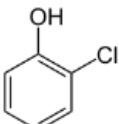
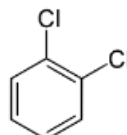
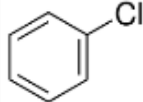
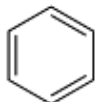
Generally, the different in bed capacity value from various kinds of adsorbents might be explained by the pore characteristics (interparticle region) along the column. As mentioned earlier that the adsorbents in this study were pulverized and sieved to 1-2 mm in particle size. Thus, the physical structures of the adsorbents were effect by this step. It is possible that in the columns which the adsorbents were packed uniformly with sphere-shaped, the flow pattern as plug flow might be achieved. Thus, the systems could provide the adsorption capacity higher

than others. In the meantime, the columns filled with non-uniform adsorbent with various particle sizes and shapes can sometimes cause voidage in a packed bed; hence, the bed capacity is reduced leading to the channeling or wall effect in this manner.

In conclusion, adsorption capacities of all VOCs over ACC and ACP adsorbents provide higher values than other adsorbents. To understand what behaviors of those adsorptions are, thermal desorption technique is then used to examine the adsorption energy of the adsorption.



Table 6.2 Bed capacity of derivatives of dioxin compounds adsorbed onto various activated carbons at  $WHSV=1.2 \text{ m}^3/\text{kg-hr}$

Adsorbate	Adsorbent	$W_{sat}$ $\left(\frac{g_{adsorbate}}{g_{adsorbent}}\right)$	$W_b$ $\left(\frac{g_{adsorbate}}{g_{adsorbent}}\right)$	Bed capacity
	ACC	0.467	0.458	<b>0.981</b>
	ACP	0.456	0.445	0.976
	ACB	0.498	0.476	0.956
	ACA	0.294	0.286	0.973
	ACC	0.224	0.222	<b>0.991</b>
	ACP	0.228	0.225	0.987
	ACB	0.154	0.145	0.941
	ACA	0.235	0.140	0.596
	ACC	0.233	0.230	<b>0.990</b>
	ACP	0.221	0.218	0.986
	ACB	0.145	0.139	0.960
	ACA	0.145	0.142	0.979
	ACC	0.166	0.152	<b>0.916</b>
	ACP	0.276	0.24	0.871
	ACB	0.250	0.2	0.799
	ACA	0.135	0.115	0.857

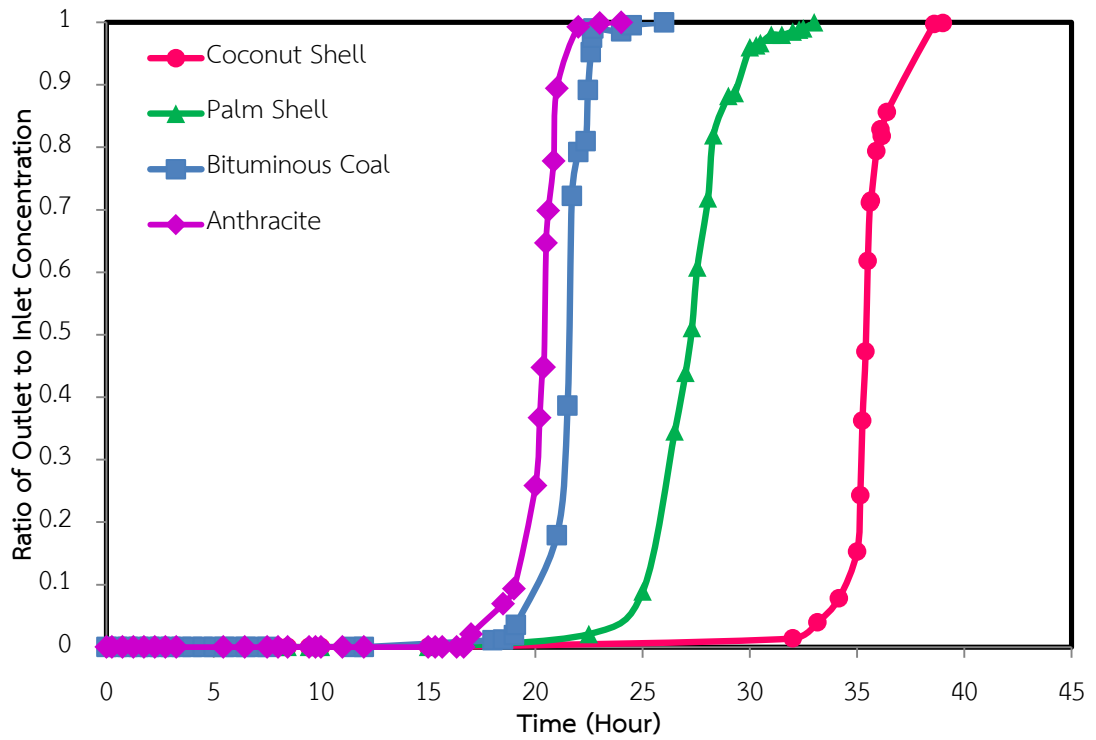


Figure 6.3 Breakthrough curve for Benzene adsorption by various activated carbons

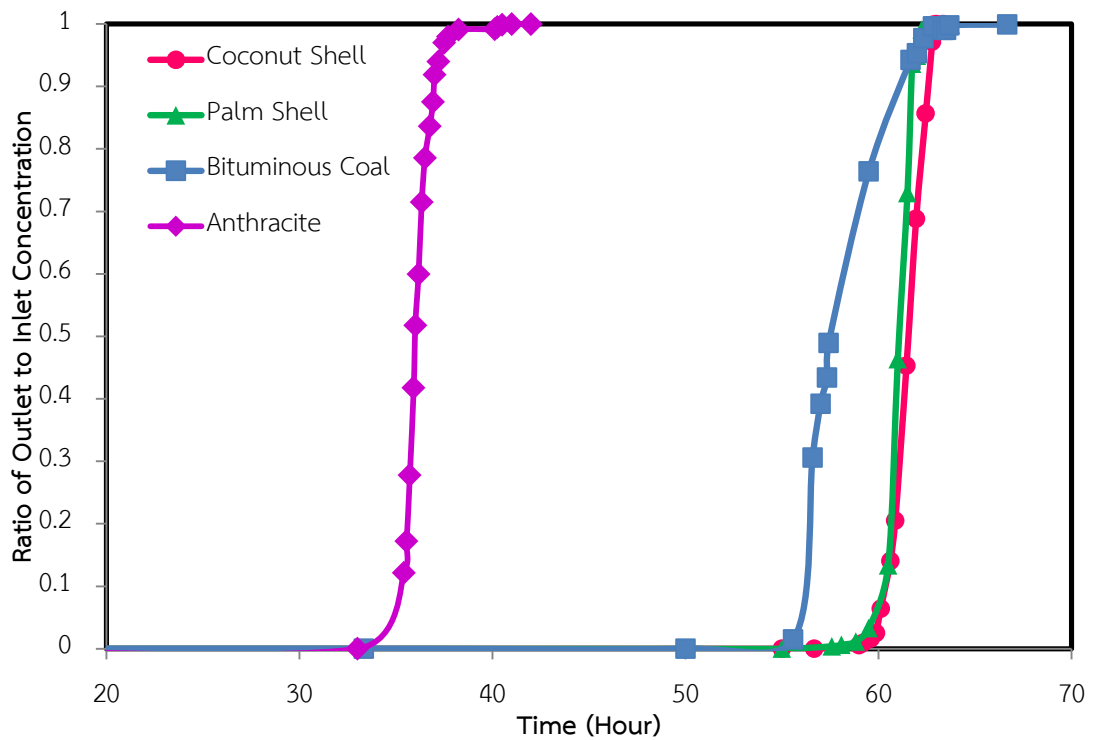


Figure 6.4 Breakthrough curve for Chlorobenzene adsorption by various activated carbons

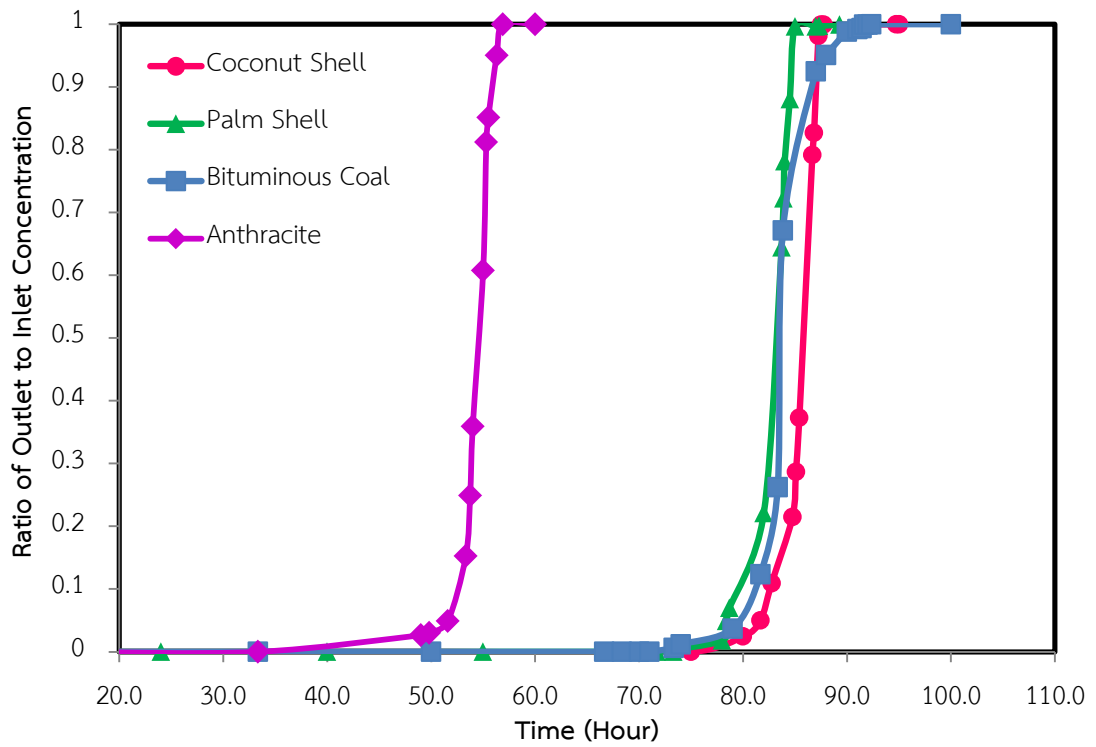


Figure 6.5 Breakthrough curve for Di-chlorobenzene adsorption by various activated carbons

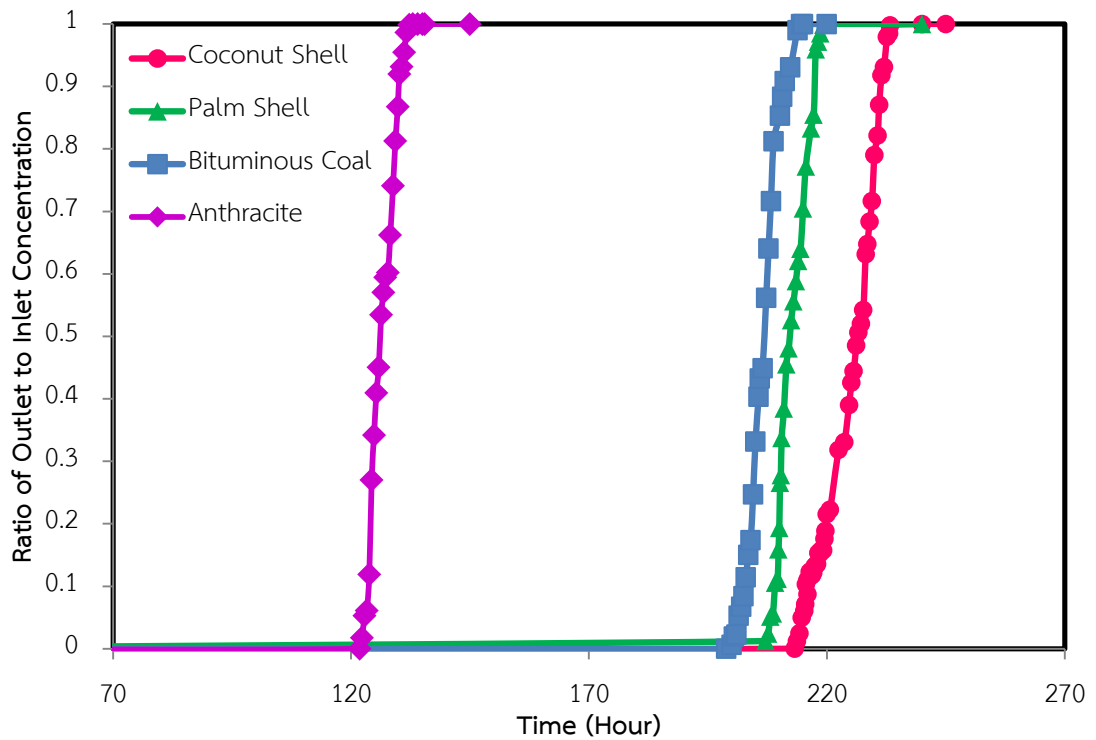


Figure 6.6 Breakthrough curve for O-chlorophenol adsorption by various activated carbons

### 6.3 Adsorption Behavior

Physical and chemical adsorption behaviors are classified based on the adsorption energy between adsorbate and adsorbent. To determine the adsorption energy, weight loss with temperature dependency has been preliminarily determined, according to equation (6.4). Where parameter  $\Theta$  is the surface coverage at time  $t=0$  and  $t$ ,  $A$  is the pre-exponential factor,  $B$  is a heating rate ( $\text{K min}^{-1}$ ),  $R$  is a gas constant,  $T$  is temperature weight loss (K) and  $E_d$  is the activation energy for desorption.

$$\int_{\Theta_0}^{\Theta_t} \frac{d\Theta}{\Theta} = \frac{A}{B} \int_{T_0}^{T_t} \exp\left(-\frac{E_d}{RT}\right) dT \quad (6.4)$$

The inverse-derivatives of desorption ( $-dm/dT$ ) from temperature programmed desorption of the derivative of dioxin compounds with the various heating rates are plotted as shown in Figure 6.7. Further, the linearized form of equation (6.4) could be arranged as equation (6.5). The adsorption energy was obtained by the slope from the plotting between  $2 \ln T_m - \ln B$  and  $1000/T_m$ . The maximum peaks of each heating rate will be plotted in the form of natural log value versus reversed maximum peaks ( $T_m$ ) as the following equation

$$2 \ln T_m - \ln B = \frac{E_d}{RT_m} + \frac{E_d}{AR} \quad (6.5)$$

From the slope of these lines in Figure 6.8 the activation energy ( $E_d$ ) can be determined. The calculation results revealed that the  $E_d$  of benzene listed as the lowest one (42 kJ/mol), followed by chlorobenzene (55 kJ/mol), dichlorobenzene (102 kJ/mol), and ortho-chlorophenol (107 kJ/mol).

As the results, it can be concluded that the strong interaction bonding between adsorbent and adsorbates in this study was mostly occupied by chemisorption owing to the activation energy for desorption is higher than 40 kJ/mol (Berger & Bhowan, 2011; Tunali, Ozcan, Ozcan, & Gedikbey, 2006). Furthermore, the adhesions of dioxin derivatives onto ACC surface were localized as monolayer. Consequently, Langmuir adsorption isotherm best describes in this process (Boparai, Joseph, & O'Carroll, 2011).



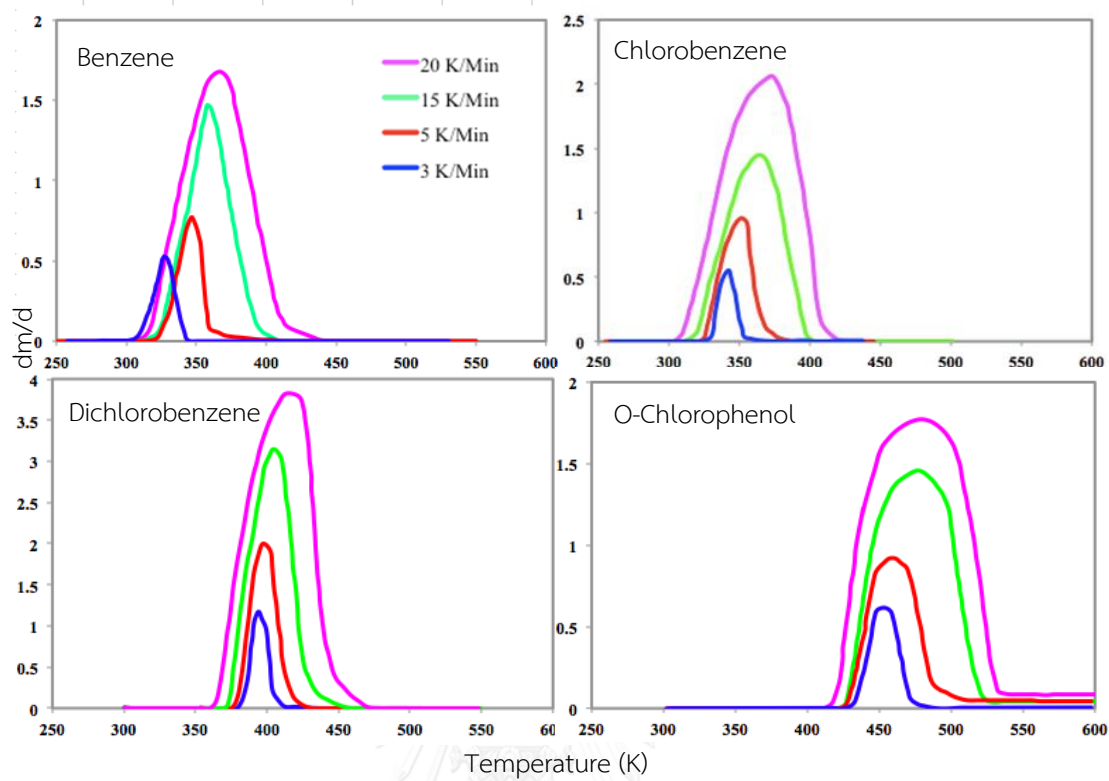


Figure 6.7 TPD profiles of dioxin derivatives from activated carbon derived from coconut shell at various heating rates.

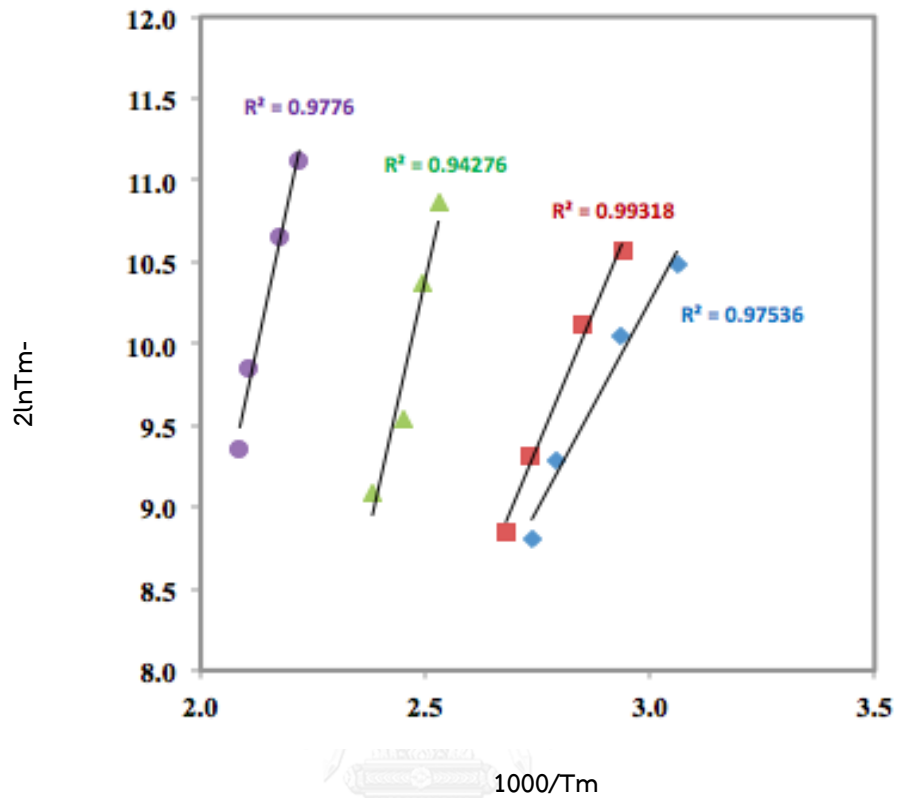


Figure 6.8

Plot of  $2\ln T_m - \ln B$  value as a function of  $1000/T_m$  of the derivatives of dioxin compounds adsorb onto activated carbon derived from coconut shell

#### 6.4 Modeling of the breakthrough curves by Aspen Gas simulation Program

The adsorption module from Aspen simulation software was applied to model the adsorption behavior of the derivative of dioxin compounds. The software was utilized under a number of assumptions. The adsorbent which has the highest bed capacity in each pollutant were selected for the breakthrough curves simulation in this study. Additionally, the simulation was based on the assumptions as follow:

Table 6.3 Assumptions for the simulation in Aspen Gas Adsorption Program

Topic	Assumption	Description
Material balance	Convection only	There is no effect of dispersion, the model would act as like as plug flow reactor.
Momentum balance	Constant pressure and velocity	The velocity and pressure are constant along the bed.
Kinetic model	Lump resistance	Mass transfer rate is equivalent to all the points of solid surface.
Isotherm assumption	Langmuir	Langmuir isotherm can be used when the adsorption of monolayer occurs.
Energy balance	Isothermal	There is no reaction take place in the adsorption process
Reaction	None	There is no reaction

Since, Langmuir isotherm equation in Aspen software is provided as

$$w_i = \frac{IP_1P_i}{1+IP_2P_i} \quad (6.7)$$

In the comparison with the Langmuir isotherm equation, the general equation is

$$q_e = \frac{Q_m b C_e}{1+bC_e} \quad (6.8)$$

Where  $q_e$  is loading of adsorbent (mg adsorbate/ g adsorbent),  $Q_m$  is maximum loading adsorbate (mg adsorbate/g adsorbent),  $b$  is Langmuir constant (L/g adsorbent), and  $C_e$  is equilibrium concentration (mg adsorbate/L). Finally,  $IP_1$  is referring to  $Q_m b$  and  $IP_2$  referring to  $b$ . Finally, the adsorption isotherm will be determined and the breakthrough curve based on the experimental data can be established using the software and applied in operating procedures under various conditions.

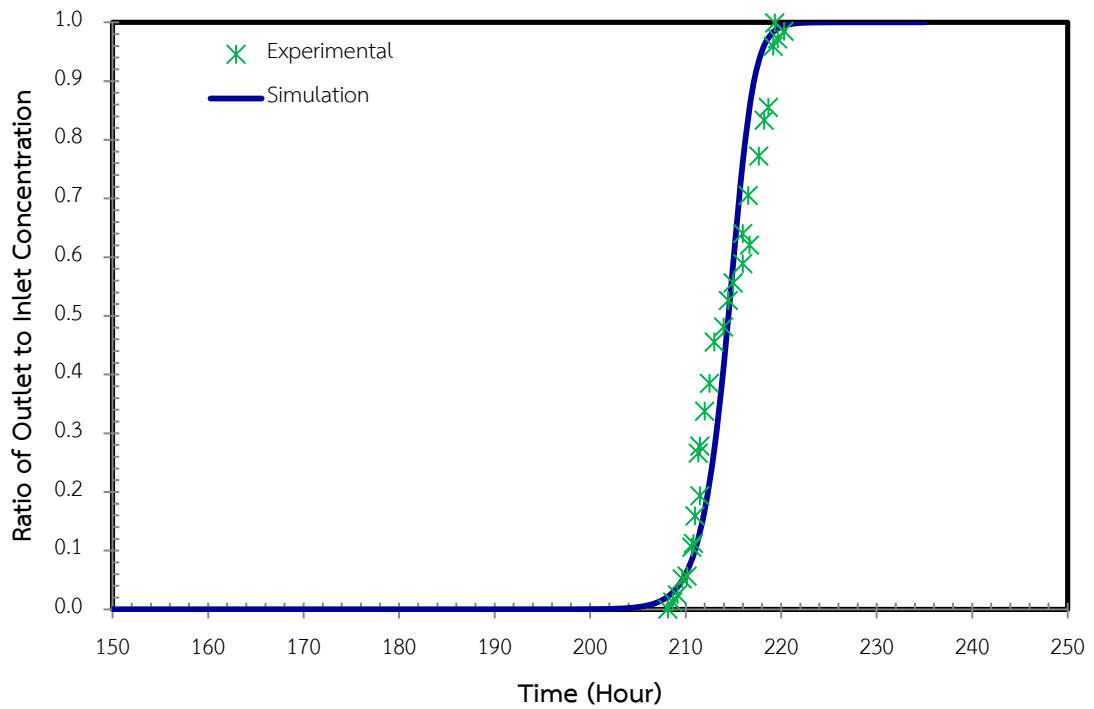


Figure 6.9 The comparison between the simulations (strength line) and experimental (points) for **O-chlorophenol** adsorbed onto ACC

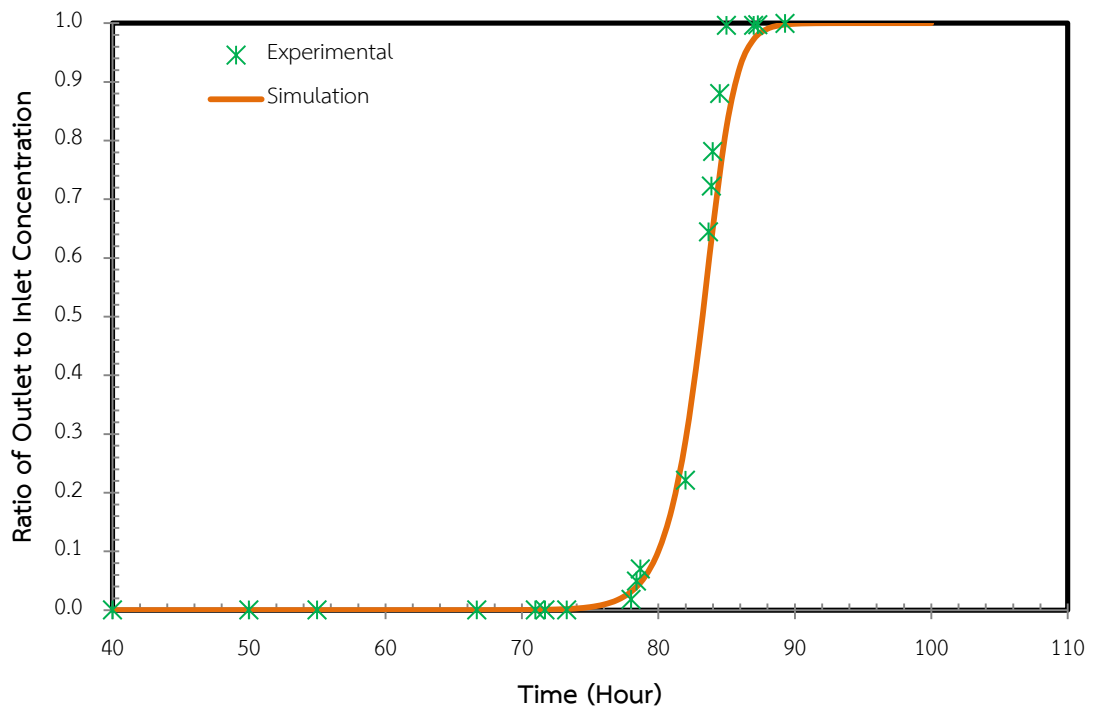


Figure 6.10 The comparison between the simulations (strength line) and experimental (points) for **Dichlorobenzene** adsorbed onto ACC

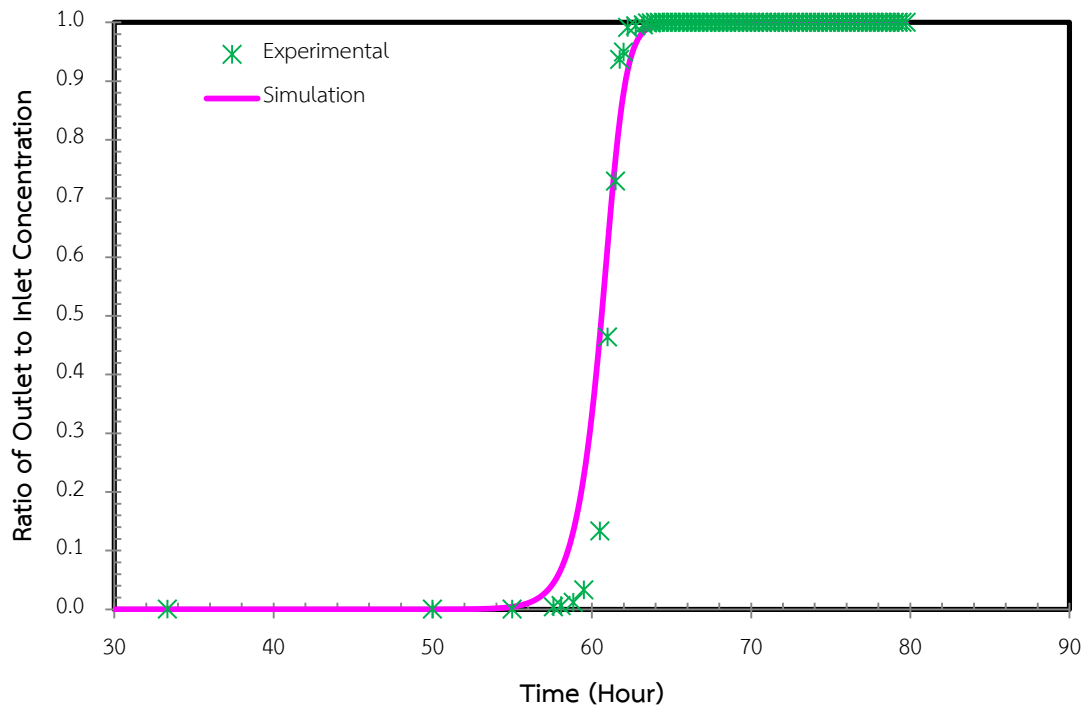


Figure 6.11 The comparison between the simulations (strength line) and experimental (points) for **Chlorobenzene** adsorbed onto ACC

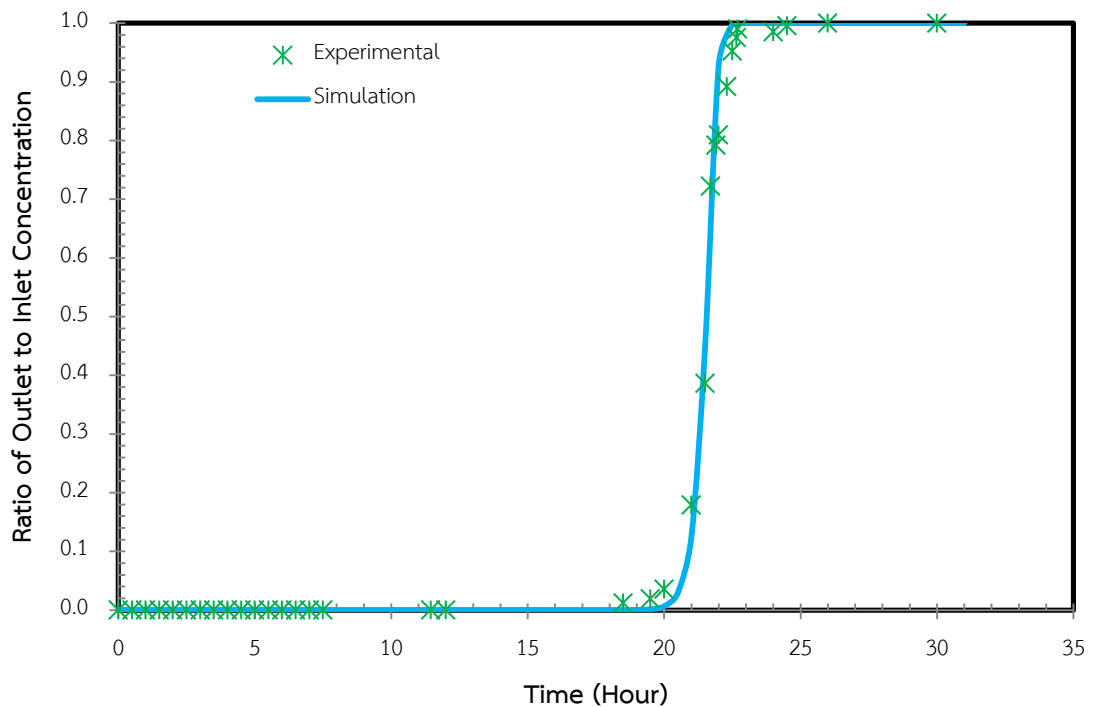


Figure 6.12 The comparison between the simulations (strength line) and experimental (points) for **Benzene** adsorbed onto ACC

Table 6.4 Isotherm parameters obtained by Aspen Gas Adsorption Simulation program

Derivative of Dioxin Compounds	IP <sub>1</sub> (mg/g adsorbent)	IP <sub>2</sub> (b) (L/ml)	Q <sub>m</sub> (mg/g adsorbent)	Q <sub>m</sub> (g/g adsorbent)	SSE
Benzene	204	1.20	170.00	0.17	1.47x10 <sup>-4</sup>
Chlorobenzene	358	1.46	245.21	0.25	2.20x10 <sup>-4</sup>
Dichlorobenzene	349	1.51	231.13	0.23	1.63x10 <sup>-4</sup>
O-dichlorophenol	603	1.28	471.09	0.47	1.59x10 <sup>-4</sup>

Interestingly, the simulated data was able to closely predict the breakthrough time when compared with the experimental data (Fig. 6.9-12). The results, the isotherm parameters from the simulation were found and summarized in Table 6.2. Further, the sum of square error (SSE) was applied to compare the different between the experimental and simulation result. The equation is stated as followed,

$$SSE = \sum_{i=1}^N \frac{(r_{im} - r_{ic})^2}{N-K} \quad (6.9)$$

Where  $r_{im}$  is experimental result,  $r_{ic}$  is simulation result, N is a number of collection data (equal to 100), and K is considerable parameters. In this study, IP<sub>1</sub> and IP<sub>2</sub> are mainly parameters; therefore K is equal to 2. The lowest SSE values were summarized and displayed in Table 6.3.

## Chapter VII

### Conclusions and recommendations

Dioxin emission from incinerators attracts much attention from the public owing to their high health risk. In this research, the ANN-based model was used for the predicting dioxin emission from the selected incinerator. Moreover, the removal of dioxin derivatives using activated carbon was further conducted. Outcomes could be expressed as follows;

1. ANN-based prediction model can successfully estimate the PCDDs emission in an selected incinerator with  $R^2$  equal to 0.998.

2. A sensitivity analysis indicated that the activated carbon adsorption injection unit played an important role in the dioxin emission.

3. The interaction energy of dioxin derivatives was confirmed by selected activated carbon (coconut shell-based) by TGA, chemisorption ( $E_d > 40$  KJ/mol) were predominantly occupied, Langmuir adsorption isotherm was therefore best representing adsorption behavior.

4. The Aspen Gas Adsorption Simulation Program, provided a high accuracy performance in predicting the adsorption behavior illustrated as the breakthrough curves with following assumption; the convection and diffusion took place based on Langmuir assumption, the system operated at constant pressure, velocity and temperature, and there was no chemical reaction.

5. Adsorption isotherms ( $IP_1$  and  $IP_2$ ) based Langmuir between dioxin derivatives and ACC were predicted by Aspen Gas Adsorption Simulation Program, the results can be listed as follow; Benzene:  $IP_1 = 204$  mg/g adsorbent,  $IP_2 = 1.20$  L/ml, Chlorobenzene  $IP_1 = 358$  mg/g adsorbent,  $IP_2 = 1.46$  L/ml, Dichlorobenzene  $IP_1 = 349$  mg/g adsorbent,  $IP_2 = 1.51$  L/ml, and O-chlorophenol  $IP_1 = 603$  mg/g adsorbent,  $IP_2 = 1.28$  L/ml.

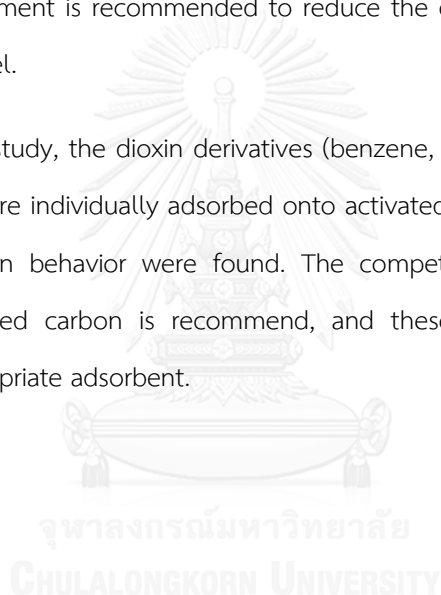


## Recommendations

1. The research was carried out based on the data collection in Taiwan, which most data has been available for some period of time. It is interesting to use the same technique to implement such a similar incineration system in Thailand. In case of that a lot of data should be lacked. This will provide a systematic collecting data in our country to fulfill the prediction.

2. It should be highlight that the input data for building ANN-based prediction model is an important point which should be concerned. Mostly, the operation data in incineration come out with a wide range of numerical numbers according to their different units. Thus, the data pre-treatment is recommended to reduce the complexity among the input data prior construct the model.

3. In this study, the dioxin derivatives (benzene, chlorobenzene, dichlorobenzene, and O-chlorophenol) were individually adsorbed onto activated carbon in fixed-bed column and the favorable adsorption behavior were found. The competitive study of dioxin derivatives adsorption onto activated carbon is recommend, and these results will contribute to the investigation of an appropriate adsorbent.



## REFERENCES

- Abu Qdais, H., Bani Hani, K., & Shatnawi, N. (2010). Modeling and optimization of biogas production from a waste digester using artificial neural network and genetic algorithm. *Resources, Conservation and Recycling*, 54(6), 359-363.
- Addink, R., & Olie, K. (1995). Mechanisms of Formation and Destruction of Polychlorinated Dibenzo-p-dioxins and Dibenzofurans in Heterogeneous Systems. *Environ Sci Technol*, 29(6), 1425-1435.
- Altarawneh, M., Dlugogorski, B. Z., Kennedy, E. M., & Mackie, J. C. (2009). Mechanisms for formation, chlorination, dechlorination and destruction of polychlorinated dibenzo-p-dioxins and dibenzofurans (PCDD/Fs). *Progress in Energy and Combustion Science*, 35(3), 245-274.
- Altwicker, E. R. (1996). Relative rates of formation of polychlorinated dioxins and furans from precursor and de novo reactions. *Chemosphere*, 33(10), 1897-1904.
- Antonioni, G., Guglielmi, D., Cozzani, V., Stramigioli, C., & Corrente, D. (2014). Modelling and simulation of an existing MSWI flue gas two-stage dry treatment. *Process Safety and Environmental Protection* 92(3), 242-250.
- Astel, A., Tsakovski, S., Barbieri, P., & Simeonov, V. (2007). Comparison of self-organizing maps classification approach with cluster and principal components analysis for large environmental data sets. *Water Res*, 41(19), 4566-4578.
- Berger, A. H., & Bhowan, A. S. (2011). Comparing physisorption and chemisorption solid sorbents for use separating CO<sub>2</sub> from flue gas using temperature swing adsorption. *Energy Procedia*, 4, 562-567.
- Blumenstock, M., Zimmermann, R., Schramm, K. W., Kaune, A., Nikolai, U., Lenoir, D., & Kettrup, A. (1999). Estimation of the dioxin emission (PCDD/FI-TEQ) from the concentration of low chlorinated aromatic compounds in the flue and stack

- gas of a hazardous waste incinerator. *Journal of Analytical and Applied Pyrolysis*, 49(1–2), 179-190.
- Bonte, J. L., Fritsky, K. J., Plinke, M. A., & Wilken, M. (2002). Catalytic destruction of PCDD/F in a fabric filter: experience at a municipal waste incinerator in Belgium. *Waste Manag*, 22(4), 421-426.
- Boparai, H. K., Joseph, M., & O'Carroll, D. M. (2011). Kinetics and thermodynamics of cadmium ion removal by adsorption onto nano zerovalent iron particles. *J Hazard Mater*, 186(1), 458-465.
- Brady, T. A., Rostam-Abadi, M., & Rood, M. J. (1996). Applications for activated carbons from waste tires: natural gas storage and air pollution control. *Gas Separation & Purification*, 10(2), 97-102.
- Buekens, A., & Huang, H. (1998). Comparative evaluation of techniques for controlling the formation and emission of chlorinated dioxins/furans in municipal waste incineration. *J Hazard Mater*, 62(1), 1-33.
- Burkert, C. A. V., Barbosa, G. N. O., Mazutti, M. A., & Maugeri, F. (2011). Mathematical modeling and experimental breakthrough curves of cephalosporin C adsorption in a fixed-bed column. *Process Biochemistry*, 46(6), 1270-1277.
- Buser, H. R. (1985). Formation, occurrence and analysis of polychlorinated dibenzofurans, dioxins and related compounds. *Environ Health Perspect*, 60, 259–267.
- Caneghem, J. V., Brems, A., Lievens, P., Block, C., Billen, P., Vermeulen, I., Vandecasteele, C. (2012). Fluidized bed waste incinerators: Design, operational and environmental issues. *Progress in Energy and Combustion Science*, 38(4), 551–582.
- Chang, Y.-H., Chen, W. C., & Chang, N.-B. (1998). Comparative evaluation of RDF and MSW incineration. *J Hazard Mater*, 58(1–3), 33-45.
- Chang, Y.-M., Hun, C.-Y., Che, J.-H., Chan, C.-T., & Chen, C.-H. (2009). Minimum feeding rate of activated carbon to control dioxin emissions from a large-scale municipal solid waste incinerator. *J Hazard Mater*, 161(2-3), 1436–1443.

- Chen, C. K., Lin, C., Wang, L. C., & Chang-Chien, G. P. (2006). The size distribution of polychlorinated dibenzo-p-dioxins and dibenzofurans in the bottom ash of municipal solid waste incinerators. *Chemosphere*, *65*(3), 514-520.
- Chen, W. C., Chang, N.-B., & Chen, J.-C. (2002). GA-based fuzzy neural controller design for municipal incinerators. *Fuzzy Sets and Systems*, *129*(3), 343-369.
- Chen, W. S., Lin, C. W., Chang, F. C., Lee, W. J., & Wu, J. L. (2012). Utilization of spent activated carbon to enhance the combustion efficiency of organic sludge derived fuel. *Bioresource Technology*, *113*, 73-77.
- Cheng, T., Jiang, Y., Zhang, Y., & Liu, S. (2004). Prediction of breakthrough curves for adsorption on activated carbon fibers in a fixed bed. *carbon*, *42*(15), 3081-3085.
- Chi, K. H., Chang, S. H., Huang, C. H., Huang, H. C., & Chang, M. B. (2006). Partitioning and removal of dioxin-like congeners in flue gases treated with activated carbon adsorption. *Chemosphere*, *64*(9), 1489-1498.
- Choi, K. I., Lee, D. H., Osako, M., & Kim, S. C. (2007). The prediction of PCDD/DF levels in wet scrubbers associated with waste incinerators. *Chemosphere*, *66*(6), 1131-1137. doi: 10.1016/j.chemosphere.2006.06.019
- Chuang, C. L., Chuang, P. C., & Chang, E. E. (2003). Modeling VOCs adsorption onto activated carbon. *Chemosphere*, *53*(1), 17-27.
- Cunliffe, A. M., & Williams, P. T. (2009). De-novo formation of dioxins and furans and the memory effect in waste incineration flue gases. *Waste Manag*, *29*(2), 739-748.
- Dong, C., Jin, B., & Li, D. (2003). Predicting the heating value of MSW with a feed forward neural network. *Waste Manag*, *23*(2), 103-106.
- Everaert, G., De Laender, F., Deneudt, K., Roose, P., Mees, J., Goethals, P. L. M., & Janssen, C. R. (2014). Additive modelling reveals spatiotemporal PCBs trends in marine sediments. *Marine Pollution Bulletin*, *79*(1-2), 47-53.
- Feng, Y., Zhang, W., Sun, D., & Zhang, L. (2011). Ozone concentration forecast method based on genetic algorithm optimized back propagation neural networks and support vector machine data classification. *Atmospheric Environment*, *45*(11), 1979-1985.

- García Lautre, I., & Abascal Fernández, E. (2004). A methodology for measuring latent variables based on multiple factor analysis. *Computational Statistics & Data Analysis*, 45(3), 505-517.
- Gevrey, M., Dimopoulos, I., & Lek, S. (2003). Review and comparison of methods to study the contribution of variables in artificial neural network models. *Ecological Modelling*, 160(3), 249-264.
- Hajizadeh, Y., Onwudili, J. A., & Williams, P. T. (2011). Removal potential of toxic 2378-substituted PCDD/F from incinerator flue gases by waste-derived activated carbons. *Waste Manag*, 31(6), 1194-1201.
- Hale, S. E., Elmquist, M., Brandli, R., Hartnik, T., Jakob, L., Henriksen, T., . . . Cornelissen, G. (2012). Activated carbon amendment to sequester PAHs in contaminated soil: a lysimeter field trial. *Chemosphere*, 87(2), 177-184.
- Hartenstein, H.-U., & Horvay, M. (1996). Overview of municipal waste incineration industry in west Europe (based on the German experience). *J Hazard Mater*, 47(1-3), 19-30.
- Hatanaka, T., Imagawa, T., & Takeuchi, M. (2002). Effects of copper chloride on formation of polychlorinated dibenzofurans in model waste incineration in a laboratory-scale fluidized-bed reactor. *Chemosphere*, 46(3), 393-399.
- Hsi, H. C., Wang, L. C., & Yu, T. H. (2007). Effects of injected activated carbon and solidification treatment on the leachability of polychlorinated dibenzo-p-dioxins and dibenzofurans from air pollution control residues of municipal waste incineration. *Chemosphere*, 67(7), 1394-1402.
- Huang, H., & Buekens, A. (1996). De novo synthesis of polychlorinated dibenzo-p-dioxins and dibenzofurans Proposal of a mechanistic scheme. *Science of The Total Environment*, 193(2), 121-141.
- Hung, P. C., Lo, W. C., Chi, K. H., Chang, S. H., & Chang, M. B. (2011). Reduction of dioxin emission by a multi-layer reactor with bead-shaped activated carbon in simulated gas stream and real flue gas of a sinter plant. *Chemosphere*, 82(1), 72-77.

- Ishikawa, R., Buekens, A., Huang, H., & Watanabe, K. (1997). Influence of combustion conditions on dioxin in an industrial-scale fluidized-bed incinerator: experimental study and statistical modelling. *Chemosphere*, *35*(3), 465-477.
- Jolliffe, I. T. (2002). *Principal Component Analysis*: Springer Series in Statistics.
- Joung, H.-T., Seo, Y.-C., Kim, K.-H., & Seo, Y.-C. (2006). Effects of oxygen, catalyst and PVC on the formation of PCDDs, PCDFs and dioxin-like PCBs in pyrolysis products of automobile residues. *Chemosphere*, *65*(9), 1481-1489.
- Karademir, A., Bakoglu, M., Taspinar, F., & Ayberk, S. (2004). Removal of PCDD/Fs from flue gas by a fixed-bed activated carbon filter in a hazardous waste incinerator. *Environ Sci Technol*, *38*(4), 1201-1207.
- Kato, M., & Urano, K. (2001). A measuring method of chlorobenzenes as a convenient substitute index of dioxins in stack gas from waste incineration facilities. *Waste Manag*, *21*(1), 63-68.
- Kilgroe, J. D. (1996). Control of dioxin, furan, and mercury emissions from municipal waste combustors. *J Hazard Mater*, *47*(1-3), 163-194.
- Kim, S. C., Song, G. J., Seok, K. S., Ko, Y. H., & Hunsinger, H. (2013). Enrichment of PCDDs/PCDFs in peripheral utilities of the municipal solid waste incineration facility. *Waste Manag*, *33*(5), 1158-1164.
- Kulkarni, P. S., Crespo, J. G., & Afonso, C. A. M. (2008). Dioxins sources and current remediation technologies — A review. *Environment International*, *34*(1), 139-153.
- Lavric, E. D., Konnov, A. A., & Ruyck, J. D. (2005). Surrogate compounds for dioxins in incineration. A review. *Waste Manag*, *25*(7), 755-765.



## APPENDIX A

### Sensitivity Analysis

The sensitivity analysis is aim to identified an important factors that effect to the dioxin emission. In this study, 5 input factors were concerned in the dioxin emission prediction. The input consists of activated carbon injection (*Input 1* and *Input 2*), concentration of hydrogen chloride in the flue gas at the stack emission (*Input 3*), temperature at the mixing chamber (*Input 4*), and temperature of final fuel gas emission (*Input 5*). The weights method was applied in this study, and this method is basically based on the weights connection between input-hidden-output at each neuron in an artificial neural network system. To calculate the relative importance among the factors, the process presents as follow (Gevrey et al., 2003);

From the structure of ANN in Fig A.1, the values of weight connection and threshold between input and output node were summarized in Table A.1. And take the absolute value in each value, the results are shown in Table A.2. Multiply  $W_{ij}$  in Table 2 by the absolute vale of threshold value. The products named as  $P_{ij}$ , and then sum up the value ( $\sum P_{ij}$ ), the results are shown in Table A.3. For each  $P_{ij}$ , divided by  $\sum P_{ij}$  to obtain  $Q_{ij}$  as shown in Table A.4. In each input neuron, sum the products of  $Q_{ij}$  in the previous step and name the product as  $S_{ij}$ . Finally, the relative important (%) can be obtained from the equation in Table A.4.



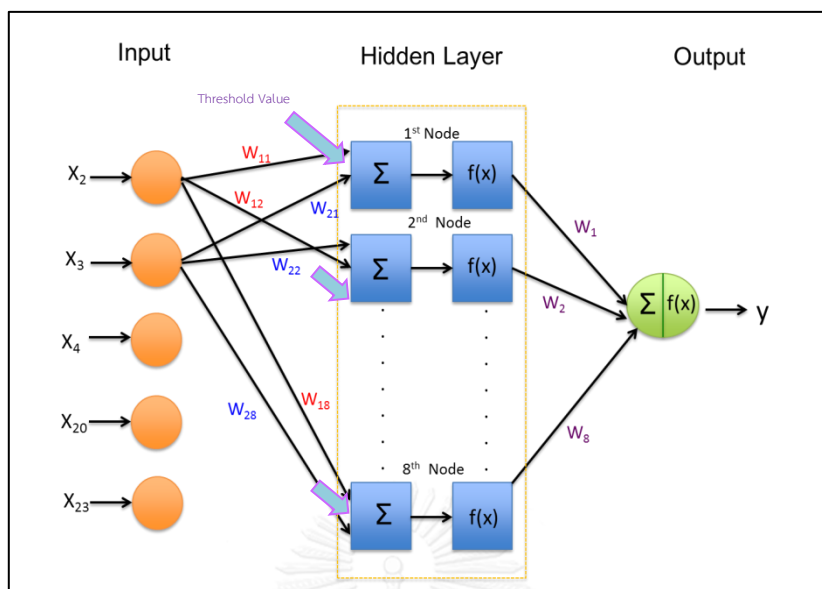


Figure A. 1 The structure of ANN model for the Dioxin emission prediction

Table A1 Weight and Threshold Values

Hidden Neurons	Weights Connection between Input and Hidden node					Threshold value ( $\theta$ )
	Input 1	Input 2	Input 3	Input 4	Input 5	
<i>N1</i>	-0.397	0.5703	0.6945	0.0296	-0.5101	0.2852
<i>N2</i>	-2.5563	0.3442	-0.6629	2.9694	1.3001	1.0646
<i>N3</i>	2.0836	0.8403	-1.6282	-1.1567	1.175	-0.292
<i>N4</i>	-3.9759	-0.0239	-0.6963	2.8501	2.7502	-1.4618
<i>N5</i>	0.5253	-1.3113	-0.5825	1.567	1.9673	0.5639
<i>N6</i>	1.727	-3.0103	2.2957	-0.0197	1.4739	-0.8162
<i>N7</i>	1.334	1.1425	-0.2856	1.3442	-0.7573	-0.9466
<i>N8</i>	-0.0984	0.1122	1.7114	-2.0093	0.0932	1.1832

Table A.2 Absolute Value

Hidden Neurons	Weights Connection between Input and Hidden node ( $W_{ij}$ )					Absolute Threshold value ( $\theta$ )
	<i>Input 1</i>	<i>Input 2</i>	<i>Input 3</i>	<i>Input 4</i>	<i>Input 5</i>	
<i>N1</i>	$W_{11}=0.397$	$W_{12}=0.570$	$W_{13}=0.695$	$W_{14}=0.029$	$W_{15}=0.510$	0.2852
<i>N2</i>	$W_{21}=2.556$	$W_{22}=0.344$	$W_{23}=0.663$	$W_{24}=2.969$	$W_{25}=1.300$	1.0646
<i>N3</i>	$W_{31}=2.083$	$W_{32}=0.840$	$W_{33}=1.628$	$W_{34}=1.157$	$W_{35}=1.175$	0.292
<i>N4</i>	$W_{41}=3.976$	$W_{42}=0.023$	$W_{43}=0.696$	$W_{44}=2.850$	$W_{45}=2.750$	1.4618
<i>N5</i>	$W_{51}=0.525$	$W_{52}=1.311$	$W_{53}=0.583$	$W_{54}=1.567$	$W_{55}=1.967$	0.5639
<i>N6</i>	$W_{61}=1.727$	$W_{62}=3.010$	$W_{63}=2.296$	$W_{64}=0.020$	$W_{65}=1.474$	0.8162
<i>N7</i>	$W_{71}=1.334$	$W_{72}=1.143$	$W_{73}=0.286$	$W_{74}=1.344$	$W_{75}=0.757$	0.9466
<i>N8</i>	$W_{81}=0.098$	$W_{82}=0.112$	$W_{83}=1.711$	$W_{84}=2.009$	$W_{85}=0.093$	1.1832

Table A.3  $P_{ij}$  values

Hidden Neurons	$P_{ij} = W_{ij} \times \text{Absolute value of } \theta$					Absolute Threshold value ( $\theta$ )	$\sum P_{ij}$
	Input 1	Input 2	Input 3	Input 4	Input 5		
N1	$P_{11}=0.113$	$P_{12}=0.163$	$P_{13}=0.198$	$P_{14}=0.008$	$P_{15}=0.145$	0.2852	0.63
N2	$P_{21}=2.721$	$P_{22}=0.366$	$P_{23}=0.706$	$P_{24}=3.161$	$P_{25}=1.384$	1.0646	8.34
N3	$P_{31}=0.608$	$P_{32}=0.245$	$P_{33}=0.475$	$P_{34}=0.338$	$P_{35}=0.343$	0.292	2.01
N4	$P_{41}=5.812$	$P_{42}=0.035$	$P_{43}=1.018$	$P_{44}=4.166$	$P_{45}=4.020$	1.4618	15.0
N5	$P_{51}=0.296$	$P_{52}=0.739$	$P_{53}=0.328$	$P_{54}=0.884$	$P_{55}=1.109$	0.5639	3.36
N6	$P_{61}=1.410$	$P_{62}=2.457$	$P_{63}=1.874$	$P_{64}=0.016$	$P_{65}=1.203$	0.8162	6.96
N7	$P_{71}=1.263$	$P_{72}=1.081$	$P_{73}=0.270$	$P_{74}=1.272$	$P_{75}=0.717$	0.9466	4.60
N8	$P_{81}=0.116$	$P_{82}=0.133$	$P_{83}=2.025$	$P_{84}=2.377$	$P_{85}=0.110$	1.1832	4.76

Table A.4  $Q_{ij}$  values

Hidden Neurons	$Q_{ij} = \frac{P_{ij}}{\sum P_{ij}}$				
	Input 1	Input 2	Input 3	Input 4	Input 5
N1	$Q_{11}=0.180$	$Q_{12}=0.259$	$Q_{13}=0.315$	$Q_{14}=0.013$	$Q_{15}=0.232$
N2	$Q_{21}=0.326$	$Q_{22}=0.044$	$Q_{23}=0.085$	$Q_{24}=0.379$	$Q_{25}=0.166$
N3	$Q_{31}=0.303$	$Q_{32}=0.122$	$Q_{33}=0.237$	$Q_{34}=0.168$	$Q_{35}=0.171$
N4	$Q_{41}=0.386$	$Q_{42}=0.002$	$Q_{43}=0.068$	$Q_{44}=0.277$	$Q_{45}=0.267$
N5	$Q_{51}=0.036$	$Q_{52}=0.089$	$Q_{53}=0.039$	$Q_{54}=0.106$	$Q_{55}=0.133$
N6	$Q_{61}=0.420$	$Q_{62}=0.732$	$Q_{63}=0.558$	$Q_{64}=0.005$	$Q_{65}=0.358$
N7	$Q_{71}=0.181$	$Q_{72}=0.155$	$Q_{73}=0.039$	$Q_{74}=0.183$	$Q_{75}=0.103$
N8	$Q_{81}=0.025$	$Q_{82}=0.029$	$Q_{83}=0.440$	$Q_{84}=0.516$	$Q_{85}=0.024$
$S_j = \sum Q_{ij}$	1.858 ( $S_1$ )	1.432 ( $S_1$ )	1.780 ( $S_1$ )	1.647 ( $S_1$ )	1.454 ( $S_1$ )
$\sum S_j$	1.858+1.432+1.780+1.647+1.454 = <b>8.171</b>				
<i>Relative Important</i>					
$RI (\%)$ $= \frac{S_j \times 100}{\sum S_j}$	22.733	17.527	21.789	20.160	17.791

## APPENDIX B

## Calculation to convert volume to concentration

For converting 2  $\mu\text{l}$  of ortho-chlorophenol to concentration in ppm the calculation below will be used in all adsorbates.

2  $\mu\text{l}$  of ortho-dichlorobenzene is equal to 0.0002 mL

At Standard Temperature Pressure (STP), 1 mol of ortho-chlorophenol gas has a volume equal to 24.79 L.

Therefore, 0.0002 mL of ortho-chlorophenol in 125 mL of gas sampling bulb

$$\frac{0.002}{125} \text{ mL} \times 1.2643 \frac{\text{g}}{\text{mL}} \times \frac{1 \text{ mol}}{147.01 \text{ g}} \times \frac{24.79 \text{ L}}{1 \text{ mol}} = \frac{4.26 \times 10^{-5} \text{ L}}{125 \text{ mL}}$$

∴ In 125 mL of gas container, it has a volume of ortho-chlorophenol equal to

$$4.26 \times 10^{-2} \text{ mL in gas phase.}$$

Therefore, the concentration of ortho-chlorophenol in ppm is equal to

$$\frac{4.26 \times 10^{-2} \times 10^6}{125} = 341 \text{ ppm}$$

**APPENDIX C**  
**Breakthrough curve data**

Table C.1 Breakthrough curve for benzene

Coconut shell		Palm Shell		Coal		Anthracite	
Time (Hr.)	C/C0	Time (Hr.)	C/C0	Time (Hr.)	C/C0	Time (Hr.)	C/C0
0	0	0	0	0	0	0	0
0.25	0	0.25	0	0.5	0	0.25	0
0.75	0	0.75	0	1	0	0.75	0
1.25	0	1.25	0	1.5	0	1.25	0
1.75	0	1.75	0	2	0	1.75	0
2.25	0	2.25	0	2.5	0	2.25	0
2.75	0	2.75	0	3	0	2.75	0
3.25	0	3.25	0	3.5	0	3.25	0
5.45	0	5.45	0	4.00	0	5.45	0
6.45	0	6.45	0	4.50	0	6.45	0
7.5	0	7.5	0	5	0	7.5	0
8	0	8	0	5.5	0	8	0
8.45	0	8.45	0	6.00	0	8.45	0
9.45	0	9.45	0	6.50	0	9.45	0
9.75	0	9.75	0	7	0	9.75	0
10	0	10	0	7.5	0	10	0
11.45	0	11.45	0	11.45	0	11	0
12	0	12	0	12.00	0	12	0
15	0	15	0	18.00	0.011	15	0
32	0.014	22.5	0.021	18.50	0.012	15.333	0
33.15	0.040	25	0.089	19.00	0.019	15.667	0
34.15	0.078	26.5	0.345	19.10	0.035	16.333	0
35	0.153	27	0.438	21.00	0.179	16.667	0
35.15	0.243	27.3	0.510	21.50	0.386	17	0.021
35.25	0.363	27.55	0.607	21.70	0.722	18.5	0.069

Table C.2 Breakthrough curve for benzene (continue)

Coconut shell		Palm Shell		Coal		Anthracite	
Time (Hr.)	C/C0	Time (Hr.)	C/C0	Time (Hr.)	C/C0	Time (Hr.)	C/C0
35.4	0.473	28.05	0.718	22.00	0.792	19	0.093
35.5	0.618	28.3	0.819	22.35	0.809	20	0.258
35.6	0.711	29	0.882	22.45	0.892	20.2	0.367
35.65	0.714	29.3	0.887	22.59	0.952	20.33	0.447
35.9	0.794	30	0.960	22.65	0.975	20.4	0.448
36.1	0.829	30.3	0.963	22.70	0.990	20.5	0.647
36.15	0.818	30.5	0.967	24.00	0.985	20.6	0.699
36.4	0.856	31	0.980	24.50	0.995	20.85	0.778
38.6	0.997	31.5	0.980	26.00	1.000	21	0.894
39	0.999	32	0.985	30.00	1	22	0.992
-	-	32.3	0.988	35.00	1	23	0.999
-	-	32.5	0.990	40.00	1	24	1.000
-	-	33	1.000	45.00	1	-	-

Table C.3 Breakthrough curve for chlorobenzene

Coconut shell		Palm Shell		Coal		Anthracite	
Time (Hr.)	C/C0	Time (Hr.)	C/C0	Time (Hr.)	C/C0	Time (Hr.)	C/C0
0	0	0	0	0	0	0	0
0.25	0	0.25	0	0.25	0	0.25	0
0.75	0	0.75	0	0.75	0	0.75	0
1.25	0	1.25	0	1.25	0	1.25	0
1.75	0	1.75	0	1.75	0	1.75	0
2.25	0	2.25	0	2.25	0	2.25	0
2.75	0	2.75	0	2.75	0	2.75	0
3.25	0	3.25	0	3.25	0	3.25	0
5.42	0	5.42	0	5.417	0	5.417	0
6.33	0	6.33	0	6.333	0	6.333	0
7.5	0	7.5	0	7.5	0	7.5	0
8	0	8	0	8	0	8	0
8.33	0	8.33	0	8.333	0	8.333	0
8.67	0	8.67	0	8.667	0	8.667	0
9.75	0	9.75	0	9.75	0	25	0
10	0	10	0	10	0	33	0
11.67	0	11.67	0	11.667	0	35.417	0.122
13.33	0	13.33	0	13.333	0	35.55	0.172
15	0	15	0	15	0	35.717	0.278
33.33	0	33.33	0	33.333	0	35.917	0.418
50	0	50	0	50	0	36	0.518
55	0	55	0	55.583	0.015	36.167	0.600
56.67	0	57.58	0.004	56.583	0.306	36.333	0.715
59	0.006	58.08	0.006	57	0.392	36.5	0.786
59.2	0.010	58.83	0.011	57.333	0.434	36.75	0.836
59.62	0.017	59.5	0.033	57.417	0.489	36.917	0.875
59.87	0.025	60.5	0.133	59.5	0.764	37	0.919
60.12	0.064	61	0.463	61.667	0.943	37.2	0.94



Table C.4 Breakthrough curve for chlorobenzene (continue)

Coconut shell		Palm Shell		Coal		Anthracite	
Time (Hr.)	C/C0	Time (Hr.)	C/C0	Time (Hr.)	C/C0	Time (Hr.)	C/C0
60.62	0.141	61.5	0.729	62	0.953	37.5	0.97
60.87	0.205	61.75	0.936	62.333	0.977	37.7	0.98
61.45	0.453	62	0.949	62.833	0.996	38.25	0.991
61.95	0.688	62.25	0.991	63.333	0.990	40.12	0.992
62.45	0.857	62.75	0.994	63.500	0.991	40.25	0.995
62.78	0.972	63.25	0.995	63.667	0.998	40.5	0.999
62.83	0.999	63.5	0.999	66.667	0.999	41	1.000
63.00	1.000	63.75	0.999	-	-	42	1.000
63.33	1.000	-	-	-	-	-	-



Table C.5 Breakthrough curve for dichlorobenzene

Coconut shell		Palm Shell		Coal		Anthracite	
Time (Hr.)	C/C0	Time (Hr.)	C/C0	Time (Hr.)	C/C0	Time (Hr.)	C/C0
0.0	0	0	0	0.0	0	0.0	0
1.7	0	1.7	0	1.7	0	1.7	0
3.3	0	3.3	0	3.3	0	3.3	0
5.0	0	5	0	5.0	0	5.0	0
6.3	0	6.3	0	6.3	0	6.3	0
6.7	0	6.7	0	6.7	0	6.7	0
8.3	0	8.3	0	8.3	0	8.3	0
10.0	0	10	0	10.0	0	10.0	0
11.7	0	11.7	0	11.7	0	11.7	0
13.3	0	13.3	0	13.3	0	13.3	0
15.0	0	15	0	15.0	0	15.0	0
33.3	0	24	0	33.3	0	33.3	0
50.0	0	33.3	0	50.0	0	49.0	0.026
75.0	0	40	0	66.7	0	49.8	0.030
80.0	0.024	50	0	68.3	0	51.6	0.049
81.7	0.050	55	0	70.0	0	53.3	0.153
82.8	0.109	66.7	0	71.0	0	53.8	0.249
84.8	0.215	73.3	0	73.3	0.006	54.0	0.359
85.1	0.286	71	0	74.0	0.012	55.0	0.607
85.4	0.373	71.7	0	79.0	0.037	55.3	0.812
86.7	0.792	78	0.018	81.7	0.123	55.5	0.851
86.8	0.827	78.4	0.049	83.3	0.262	56.3	0.950
87.3	0.981	78.7	0.070	83.8	0.671	56.9	1.000
87.5	0.999	82	0.221	87.0	0.925	60.0	1.000
87.8	0.999	83.7	0.644	88.0	0.951	-	-
94.8	0.999	83.9	0.722	90.0	0.988	-	-
95.0	0.999	84	0.781	91.0	0.992	-	-
-	-	84.5	0.880	91.4	0.994	-	-

Table C.6 Breakthrough curve for dichlorobenzene (continue)

Coconut shell		Palm Shell		Coal		Anthracite	
Time (Hr.)	C/C0	Time (Hr.)	C/C0	Time (Hr.)	C/C0	Time (Hr.)	C/C0
-	-	85	0.996	91.7	0.999	-	-
-	-	87	0.996	92.0	0.999	-	-
-	-	87.3	0.997	92.3	1.000	-	-
-	-	89.3	0.999	100.0	1.000	-	-



Table C.7 Breakthrough curve for O-chlorophenol

Coconut shell		Palm Shell		Coal		Anthracite	
Time (Hr.)	C/C0	Time (Hr.)	C/C0	Time (Hr.)	C/C0	Time (Hr.)	C/C0
0	0	0	0	0	0	0	0
200	0	207.17	0.012	198.83	0	121.83	0
213.75	0.012	207.67	0.024	200	0.006	122.33	0.0173
214.25	0.025	208.17	0.051	200.5	0.019	122.83	0.0531
214.75	0.050	208.67	0.057	201	0.023	123.33	0.0612
215.25	0.061	209.17	0.106	201.5	0.053	123.83	0.1192
215.5	0.071	209.67	0.112	202	0.067	124.33	0.2703
215.92	0.087	209.83	0.159	202.5	0.084	124.83	0.3418
215.58	0.103	210	0.193	203	0.115	125.33	0.4095
215.92	0.110	210.17	0.266	203.5	0.150	125.83	0.4506
216.42	0.123	210.33	0.278	204	0.174	126.33	0.5346
216.92	0.117	210.5	0.337	204.5	0.247	126.83	0.5703
217.17	0.122	211	0.385	205	0.331	127.25	0.5947
217.42	0.132	211.5	0.455	205.67	0.403	127.75	0.6023
217.75	0.135	212	0.481	205.92	0.432	128.25	0.6619
218	0.136	212.5	0.526	206.5	0.449	128.83	0.7409
218.25	0.153	213	0.556	207.25	0.562	129.33	0.8130
218.5	0.152	213.5	0.588	207.75	0.641	129.83	0.8677
218.75	0.157	214	0.620	208.25	0.716	130.17	0.9197
219.25	0.157	214.5	0.640	208.83	0.812	130.67	0.9316
219.5	0.176	215	0.705	210.17	0.853	131.17	0.9549
219.75	0.189	215.58	0.772	210.67	0.883	131.67	0.9863
220	0.215	216.67	0.833	211.17	0.908	132.25	0.9988
220.67	0.223	217.25	0.855	212.33	0.931	133	1
222.5	0.318	217.67	0.959	213.83	0.990	-	-

Table C.8 Breakthrough curve for O-chlorophenol (continue)

Coconut shell	Palm Shell	Coal	Anthracite	Coconut shell	Palm Shell	Coal	Anthracite
Time (Hr.)	C/C0	Time (Hr.)	C/C0	Time (Hr.)	C/C0	Time (Hr.)	C/C0
223.67	0.331	218.17	0.971	214.58	1.000	-	-
224.67	0.390	218.67	0.985	214.6	1	-	-
225.17	0.426	219.33	0.999	215	1	-	-
225.67	0.444	220	1	220	1	-	-
226.17	0.485	240	1	-	-	-	-
226.67	0.506	-	-	-	-	-	-
227.17	0.520	-	-	-	-	-	-
227.67	0.542	-	-	-	-	-	-
228.17	0.631	-	-	-	-	-	-
228.5	0.648	-	-	-	-	-	-
229	0.684	-	-	-	-	-	-
229.5	0.717	-	-	-	-	-	-
233.08	0.985	-	-	-	-	-	-
233.33	0.998	-	-	-	-	-	-
240	1.000	-	-	-	-	-	-
245	1.000	-	-	-	-	-	-

## VITA

The author was born in Bangkok, Thailand on July 19th, 1985. She received her bachelor's degree in Chemical Engineering from Thammasat University, Thailand. Then she continued her studies at Chulalongkorn University and obtained her Master's degree in Chemical Engineering. In 2009, she enrolled the Doctoral degree in the Center of Excellence on Hazardous Substance Management.

